

Copyright  
by  
Daniel J. Hochman  
2012


**The Dissertation Committee for Daniel Jason Hochman Certifies that this is the  
approved version of the following dissertation:**

**Airway Inflammatory States in Response to Environmental Pollutants and the  
Influence of Oxidative Balance**

**Committee:**



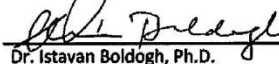
Dr. Edward Brooks, M.D., Chair



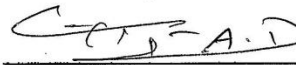
Dr. William Argeredes, Ph.D., Co-Chair



Dr. Roberto Garofalo, M.D.



Dr. Istavan Boldogh, Ph.D.



Dr. Azzeddine Dakhama, Ph.D.

---

Dean, Graduate School

**Airway Inflammatory States in Response to Environmental Pollutants and the  
Influence of Oxidative Balance**

**by**

**Daniel Jason Hochman, B.B.A., B.S., M.S., M.Ed.**

**Dissertation**

Presented to the Faculty of the Graduate School of

The University of Texas Medical Branch

in Partial Fulfillment

of the Requirements

for the Degree of

**Doctor of Philosophy**

**The University of Texas Medical Branch**

**December, 2012**

## **Dedication**

This body of work is dedicated to my loving and supportive parents Laurie and Dr. Robert Hochman who have guided me and supported me, through thick and thin, as I struggled and triumphed, to Dr. Edward Brooks for his limitless patience and guidance and to my daughter Abby Hochman, whose unconditional love has saved me countless times.

## **Acknowledgements**

I would like to extend my sincerest thanks to Dr. Edward Brooks (UTHSCSA) and Dr. Bill Ameredes (UTMB) for their undying support, advice, and scientific expertise throughout the course of this study. Dr. Brooks and Dr. Ameredes continued their support, despite what seemed like insurmountable odds. Dr. Dorian Coppenhaver, Senior Associate Dean of Student Affairs, GSBS (UTMB) never gave up on me and gave me every opportunity possible to complete this degree. To Dr. Antonella Casola for believing in me at the last possible minute and providing me much needed support.

My gratitude also goes out to Dr. Roberto Garofalo, Dr. Istvan Boldogh, and Dr. Azzeddine Dakhma for serving on my committee for so many years. Dr. Mary Moslen supported my entry into the graduate program and provided me support through the NIEHS T32 Toxicology training grant. She provided valuable insights and guidance throughout the process of my graduate training. She also helped me become involved in the training of high school and undergraduate students through the Bromberg Fellows and SURP programs and introduced me to the Society of Toxicology which has provided me with wonderful opportunities over the years.

Special thanks go out to Dr. Lance Hallberg for teaching me how to operate the inhalation facility that was vital to my research. I would also like to recognize the many dedicated hours of the students who worked with me through the SURP and Bench Tutorial programs and Laura Teed for her never ending assistance navigating the waters.

Thanks to the GSBS and UTMB for the opportunity to prove myself a worthy student in the doctoral program.

# **Airway Inflammatory States in Response to Environmental Pollutants and the Influence of Oxidative Balance**

Daniel Jason Hochman, Ph.D.

The University of Texas Medical Branch, 2012

Supervisor: Edward Brooks, Bill Ameredes

Abstract: Asthma continues to grow as a major health issue worldwide. Epidemiologic evidence points to a link between urban air pollution and exacerbation of asthma cases. The pathophysiology of airway inflammation and hyperresponsiveness in relation to air pollution is not well understood. Based upon previous experiments, this study hypothesized that key components of air pollution, specifically sulfates and aldehydes, enhance allergic sensitization, thus triggering inflammatory processes in airways. Further, it was hypothesized that oxidative stress plays a role in the aforementioned inflammatory enhancement. Sulfite and acrolein were utilized *in vitro* to test the ability of pollutants generate reactive oxygen species and initiate allergic inflammation in mast cells. Sulfur dioxide was then employed to translate the *in vitro* findings into a whole animal model. Oxidative pathways were examined *in vivo* through the use of apocynin, a NAD(P)H oxidase inhibitor and 1[2-Cyano-3,12-dioxooleana-1,9(11)-dien-28-oyl]imidazole (CDDO) a triterpenoid mimetic of the Nrf2 anti-oxidant DNA binding element. Data obtained confirmed the hypothesis that both acrolein and sulfite induced ROS in mast cells and enhanced degranulation of inflammatory mediators *in vitro*. Treatment of cells with anti-oxidants ameliorated the effects of the exogenous pollutant stimulation of mast cells. The *in vivo* model was more complex, however,

sulfur dioxide exposure did enhance allergic sensitization in a mixed inflammatory state. Type I (IL-6, IL-12, IFN- $\gamma$ ) and type II (IL-13, IL-4, IL-5) inflammatory cytokines were enhanced by exposure of mice to sulfur dioxide. T-cell proliferation was enhanced by exposure to SO<sub>2</sub>. IgE was actually reduced by SO<sub>2</sub> exposure, but IgG<sub>1</sub> was heightened. Measures of oxidative stress such as glutathione, NOx, and heme oxygenase-1 confirmed that the oxidative balance was shifted to a pro-oxidative status both in ovalbumin (OVA) sensitized mice and in those exposed to SO<sub>2</sub> in combination with OVA. Treatment with anti-oxidants presented a complex picture of systems biology. Apocynin treatment ameliorated the effects of SO<sub>2</sub> exposure, however, in animals that were not both allergic sensitized and SO<sub>2</sub> exposed, apocynin had an opposite effect on oxidative balance and enhanced inflammatory reactivity. Alternatively, CDDO, operating through the Nrf2 pathway, displayed anti-inflammatory and anti-hyperresponsive properties, shifting the balance of oxidative state towards an enhanced anti-oxidant capacity.

## Table of Contents

<b>List of Figures .....</b>	<b>viii</b>
<b>Chapter 1. Introduction .....</b>	<b>1</b>
<b>Chapter 2. Effect of Sodium Sulfite on Mast Cell Degranulation and Oxidant Stress .....</b>	<b>7</b>
<b>Chapter 3. Acrolein Induced Oxidative Stress and Allergic Inflammation in Mast Cells .....</b>	<b>24</b>
<b>Chapter 4. Effects of Sulfur Dioxide Exposure in an Animal Model of Asthma .....</b>	<b>45</b>
<b>Chapter 5. Amiloratation of Airway yperresponsiveness by Activation of Antioxidant Responses .....</b>	<b>78</b>
<b>Chapter 6. Conclusion.....</b>	<b>92</b>
<b>Reference List.....</b>	<b>97</b>
<b>Vita .....</b>	<b>110</b>



## List of Figures

<b>Figure 1.</b> Summary of particulate induced lung inflammation model.....	6
<b>Figure 2.</b> $\beta$ -hexosaminidase assay demonstrating sodium sulfite induced degranulation .....	18
<b>Figure 3.</b> Propidium iodide staining to assess cell viability.....	19
<b>Figure 4.</b> Sulfite induced degranulation is unaffected by extracellular calcium depletion .....	20
<b>Figure 5.</b> Sodium sulfite induces ROS formation.....	20
<b>Figure 6a.</b> Intracellular ROS generated by sulfite exposure is inhibited by antioxidants TMTU .....	21
<b>Figure 6b.</b> Intracellular ROS generated by sulfite exposure is inhibited by antioxidants NAC .....	21
<b>Figure 7.</b> Inhibition of sulfite induced degranulation by TMTU.....	22
<b>Figure 8.</b> Inhibition of cellular flavoenzymes inhibits sulfite induced ROS generation .....	22
<b>Figure 9.</b> Inhibition of sulfite induced degranulation by DPI.....	23
<b>Figure 10.</b> Sulfite induced histamine release from PBL.....	23
<b>Figure 11.</b> Degranulation of RBL-2H3 upon exposure to acrolein or acrolein with DNP/anti-DNP IgE cross-linking .....	38
<b>Figure 12.</b> Degranulation of RBL-2H3 cells in response to treatment with acetaldehyde or formaldehyde .....	39
<b>Figure 13.</b> Detection of release of intracellular $\text{Ca}^{2+}$ .....	39
<b>Figure 14.</b> Effect of $\text{Ca}^{2+}$ depletion on acrolein induced degranulation.....	40
<b>Figure 15.</b> Reactive oxygen species as measured by DCFH-DA fluorescence..	40
<b>Figure 16a.</b> Acrolein induced degranulation in RBL-2H3 cells.....	41
<b>Figure 16b.</b> Acrolein induced ROS generation in RBL-2H3 cells.....	41
<b>Figure 17a.</b> TNF- $\alpha$ mRNA expression as measured by RNase protection assay .....	42

<b>Figure 17b.</b> IL-4 mRNA expression as measured by RNase protection assay.....	42
<b>Figure 18.</b> Cytokine production in RBL-2H3 cells exposed to acrolein.....	43
<b>Figure 19.</b> Leukotriene C <sub>4</sub> release from RBL-2H3 cells.....	43
<b>Figure 20.</b> MTT assay assessing cell mitochondrial viability in RBL-2H3 ..... cells treated with increasing concentrations of acrolein	44
<b>Figure 21.</b> Flow cytometry of RBL-2H3 cells exposed to increasing ..... doses of acrolein and stained with propidium iodide to examine cell toxicity	44
<b>Figure 22.</b> JAM Assay, RBL-2H3 cells.....	45
<b>Figure 23.</b> JAM Assay, Human lung epithelial A549 cells.....	45
<b>Figure 24a.</b> Whole animal plethysmography 24 hours ..... post-OVA challenge, SO <sub>2</sub>	64
<b>Figure 24b.</b> Whole animal plethysmography 24 hours ..... post-OVA challenge, w/Apocynin	65
<b>Figure 25a.</b> Whole animal plethysmography 48 hours ..... post-OVA challenge, SO <sub>2</sub>	65
<b>Figure 25b.</b> Whole animal plethysmography 48 hours ..... post-OVA challenge, w/Apocynin	66
<b>Figure 26a.</b> Whole animal plethysmography 24 hours ..... post-OVA challenge, OVA	66
<b>Figure 26b.</b> Whole animal plethysmography 48 hours ..... post-OVA challenge, OVA	67
<b>Figure 27a.</b> Trachea Ring Assay measuring smooth muscle contractility.....	67
<b>Figure 27b.</b> Trachea Ring Assay measuring smooth muscle..... contractility, w/Apocynin	68
<b>Figure 27c.</b> Trachea Ring Assay measuring smooth muscle ..... contractility, controls	68
<b>Figure 28a.</b> Average number of mast cells per millimeter of murine airway.....	69

<b>Figure 28b.</b> Average number of mast cells per histologic location in murine airway	69
<b>Figure 29.</b> Differential cell counts in treated mice	70
<b>Figure 30.</b> T cell proliferation in treated mice	70
<b>Figure 31.</b> IgE Measured by ELISA in serum obtained from cardiac puncture	71
<b>Figure 32.</b> IgG1a Measured by ELISA in serum obtained from cardiac puncture	71
<b>Figure 33a.</b> IL-13 measured in BAL	72
<b>Figure 33b.</b> IL-4 measured in BAL	72
<b>Figure 33c.</b> IL-5 measured in BAL	73
<b>Figure 33d.</b> IFN- $\gamma$ measured in BAL	73
<b>Figure 33e.</b> IL-1a measured in BAL	74
<b>Figure 33f.</b> IL-6 measured in BAL	74
<b>Figure 33g.</b> IL-12 measured in BAL	75
<b>Figure 33h.</b> RANTES measured in BAL	75
<b>Figure 34.</b> Total Glutathione measured by ELISA in whole lung homogenate	76
<b>Figure 35.</b> Heme Oxygenase measured in whole lung homogenate by ELISA	76
<b>Figure 36.</b> Total nitric oxides measured in BAL by ELISA	77
<b>Figure 37a.</b> Whole body plethysmography in C57Bl/6	88
<b>Figure 37b.</b> Whole body plethysmography Balb/c	88
<b>Figure 38.</b> Tracheal ring contractility	89
<b>Figure 39.</b> Bronchoalveolar lavage inflammatory cells	89
<b>Figure 40a.</b> OVA-specific IgE immune responses	90
<b>Figure 40b.</b> OVA-specific T-cell immune responses	90
<b>Figure 41a.</b> Pro-oxidant/antioxidant balance	90
<b>Figure 41b.</b> Total hydroperoxides (dRom assay)	90

<b>Figure 41c.</b> Antioxidant capacity.....	90
<b>Figure 42.</b> Glutathione with CDDO.....	91
<b>Figure 43.</b> Heme-oxygenase with CDDO.....	91

## **Chapter 1. INTRODUCTION**

Asthma is an increasing epidemic. It is projected that by 2020 9% of the U.S. population will suffer from asthma: roughly 30 million Americans. Asthma-related costs ranked number one world-wide among childhood diseases, and the socio-economic burden of the disorder is increasing in all age brackets [1].

Asthma is marked by a chronic state of inflammation combined with hypersensitive and hyperresponsive airway bronchoconstriction [2]. Mast cells and basophils play a major role in asthma pathogenesis, and increased numbers of these inflammatory cells are detected in the airways of patients with asthma [3]. Airway mast cells release inflammatory mediators, such as histamine, cytokines and leukotrienes, responsible, in part, for the initiation of allergic inflammation [4]. During the process of allergic sensitization, inflammatory cytokines initiate the humoral immune response for allergen specific IgE production and signal to granulocytes such as basophils and resident mast cells to express IgE receptors on the membrane surface. Secondary exposure to the allergen will then lead to IgE crosslinking and the initiation of inflammatory mediator release through granule exocytosis [5]. These inflammatory mediators signal, in part, through the mitogen activated protein kinase (MAP Kinase) pathway for the upregulation of cytokine expression and proliferation of inflammatory cells, thus enhancing the adaptive immune inflammatory response in a cyclic fashion [6]. Mediators released by mast cells have been shown to play a major role in airway hyperresponsiveness [3]. The worldwide increase in asthma may be linked to increased urban air pollution. Environmental insult from pollutant particles may initiate release of the aforementioned inflammatory mediators either directly or through enhanced allergic sensitization through IgE binding pathways [7]. Those possible mechanisms were examined in this study.

Increased global urbanization has been epidemiologically associated with amplified levels of respiratory distress. “The World Health Organization (WHO) also found that the air quality in large cities in many developing countries is remarkably poor and that very large numbers of people in those countries are exposed to ambient concentrations of air pollutants well above the WHO guidelines for air quality [8].” Epidemiologic studies have repeatedly indicated an association between air pollution levels and increased hospitalizations, lost days of school and work and development of chronic airway disorders such as asthma and chronic obstructive pulmonary disease (COPD) [9-18]. D’amato et al, in a series of studies, show that increased populations and industrialization in urban settings is naturally associated with increased air pollution. Air pollution is, in turn, associated with increased morbidity worldwide with respect to episodic respiratory disease. Additionally D’amato shows climate change due to greenhouse gas emissions plays a role in the availability of air pollution components to human airways as a result of trapped air inversions [19-23].

Urban settings are inevitably associated with higher levels of photochemical air pollutants resulting from anthropomorphic activities such as motor vehicle usage and heavy industrial effluent [24]. A major component of these pollutants is particulate matter [25]. Particulate matter is described in terms of its size. Typically, particulate matter  $\leq 10$  micrometers in size is known as PM 10, particulates between 5 micrometers and 10 micrometers is labeled PM 5, and particles  $\leq 2.5$  micrometers is known as PM 2.5. It has been shown in epidemiologic and empirical studies that the smaller the particles, the more dangerous they may be in terms of causing respiratory illness [26]. Smaller particles have a greater surface area to biochemically with pleural tissues [27].

Additionally, the smaller particle is able to evade typical biomechanical defenses and reach deeper into the alveolar spaces, leading to immune responses in the lower airway through expression of proinflammatory cytokines and alteration of the mucosal barrier to interstitial cellular insult [27-30].

There has been considerable debate as whether the physiologic effects of PM 2.5 should be examined as a whole particle, or if the individual chemical components of the particle should be examined. It has been shown that the components comprising these pollutants vary highly from region to region, and even within a single city, the constituents of PM 2.5 will shift depending on proximity to manufacturing, roadway, or agricultural land usage [31-34]. It is therefore increasingly difficult to describe a single mechanism of action for the respiratory disease development associated with particulate air pollution. One approach, then, is to look at the individual components of PM 2.5 and find more universal descriptions of disease processes based on each major chemical portion of the particulate air pollutant [32;35-40].

One of the aforementioned groups of chemicals typically associated with PM 2.5 during combustion processes are the aldehydes, such as acrolein, formaldehyde and acetaldehyde. Often released as a result of industrial processes, aldehydes are highly susceptible to photochemical reactivity. As such, they are often transformed in the air to more reactive states. Acrolein is one such aldehyde. Acrolein is the simplest unsaturated aldehyde ( $C_3H_3O$ ) and known carcinogen. It has an acrid odor and is a product of incomplete combustion. In industrial applications, acrolein is sometimes used as a biocide and is a precursor to other chemical formulations. It is a major component in

diesel and gasoline exhaust and cigarette smoke, and is formed in the atmosphere as a result of photochemical transformation of industrial effluent [41-45].

Sulfates have also been shown to make up a considerable portion of PM 2.5 around the globe [25;46-48]. The largest source of SO<sub>2</sub> is auto and diesel exhaust [49-51]. Diesel exhaust particles are an important source of particulate matter less than 2.5 µm in diameter. In situ mass spectrometric analysis of diesel exhaust particles reveals that sulfur oxides dominate the particle composition when the engine that generates the particle is under a higher load [52]. There has been strong epidemiological evidence showing links with increased urbanization and higher levels of ambient SO<sub>2</sub> [53]. Additionally, the increased SO<sub>2</sub> has been associated with exacerbations of airway hypersensitivity [16;25;54-58]. Diaz-Sanchez et al documented the role of diesel exhaust particles in augmenting allergen-induced mast cell degranulation [59;60].

While the epidemiological evidence is abundant, there is a dearth of information explaining the relationship between particulate component exposure and the development of airway disease. In studies of other particle like exposures such as pollen [61-66] and respiratory syncytial virus (RSV), there is an associated burst reactive oxygen species (ROS) [67;68]. ROS are known to act as signaling molecules for pro-inflammatory pathways as a part of mounting cellular defense. It is thought that their production is a function of NADPH oxidase in the cell membrane. Oxidative anions are also produced as part of the mitochondrial electron transport chain during cellular metabolism [61]. There is a delicate balance, however, between expression of ROS and the cellular anti-oxidant enzymes such as catalase, glutathione peroxidase (GSH) and superoxide dismutase (SOD). Production of these anti-oxidant enzymes is associated with the Nrf2



signaling pathway. Nrf2 is a regulator of anti-oxidant enzyme gene expression. When more ROS is produced than can be scavenged by anti-oxidant enzymes, or the Nrf2 pathway is damaged or interrupted, a state of oxidative stress is reached. Oxidative stress, in turn, can lead to cellular damage via lipid peroxidation that may lead to disease states of chronic inflammation such as asthma or COPD. In some cases, the balance can be restored by treatment of cells with anti-oxidant scavengers or anti-oxidant enzyme mimetics. It follows, then, that airway inflammation and hypersensitivity may be ameliorated by treatment with anti-oxidants.

In order to establish that both aldehydes and SO<sub>2</sub> can lead to chronic inflammatory states via an imbalance in oxidative stress, we employed an *in vitro* model in airway mast cells utilizing the RBL-2H3 cell line for both acrolein and SO<sub>2</sub>. The cellular model was then followed by *in vivo* modeling in mice to translate the cellular model to whole animal airway response. Additionally, we utilized treatment of mice with an Nrf2 pathway mimetic (CDDO) to examine the ability of said anti-oxidant enzyme precursor to ameliorate the imbalance initiated in a classic allergic inflammatory state (Figure 1). We have shown in our studies presented herewith that exposure of airway to foreign particles triggers an inflammatory response associated with the generation of reactive oxygen species that leads to the release of inflammatory mediators and that response can be reduced by treatment with anti-oxidants.

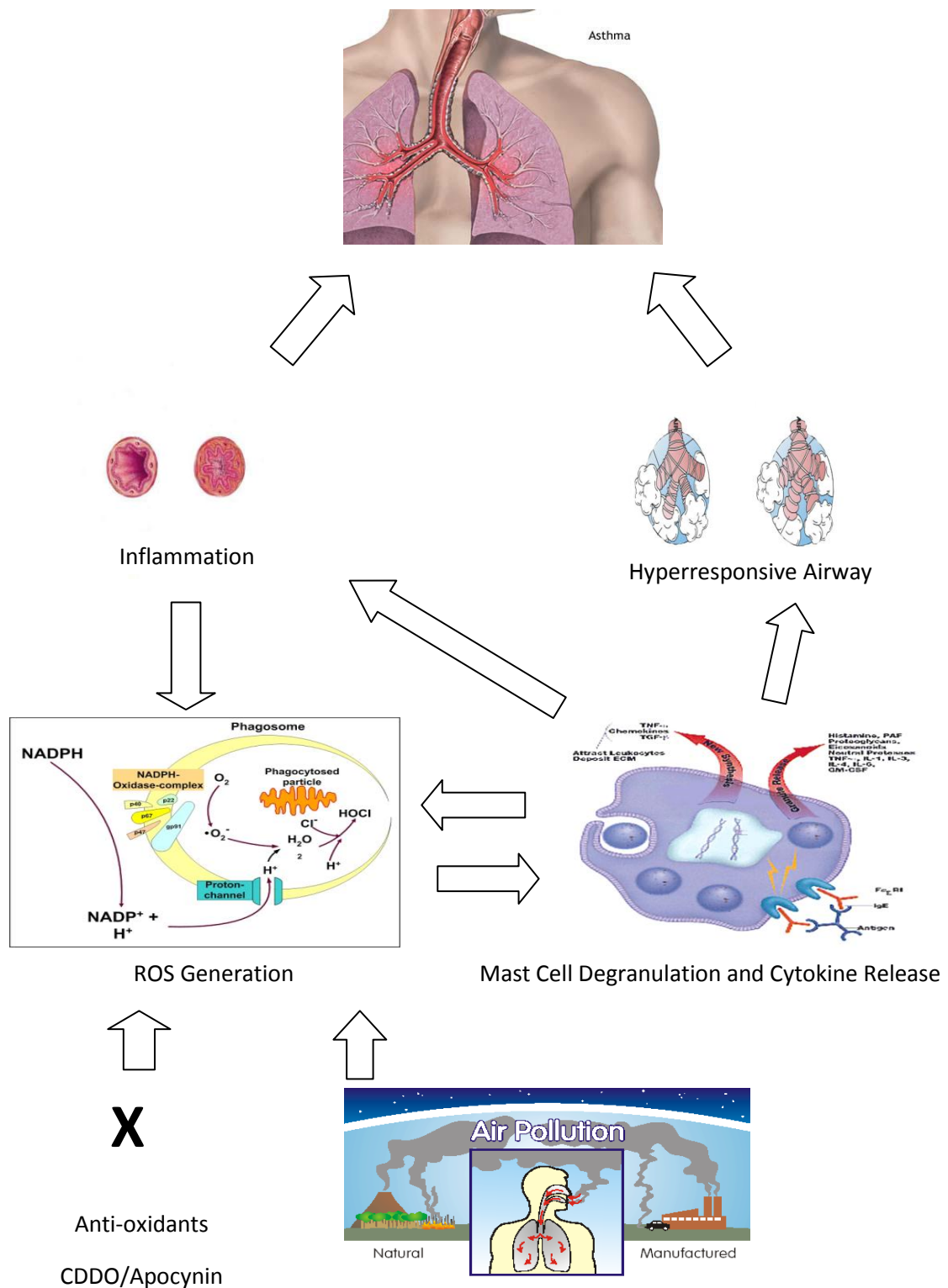


**Figure 1.** Summary of particulate induced lung inflammation model (images obtained from NIH MedlinePlus)

## **CHAPTER 2. Effect of sodium sulfite on mast cell degranulation and oxidant stress**

### **Introduction**

Sulfur dioxide (SO<sub>2</sub>) is 1 of the 6 major criteria air pollutants monitored closely by the Environmental Protection Agency because of its widespread distribution and health effects [69]. Sulfur dioxide is generated during the combustion of fossil fuels and from the isolation of metals from ores. Oxides of sulfur have also been shown to be major constituents of other proallergic pollutants, including diesel exhaust particles and fine particulate matter [52;70;71]. Sulfur dioxide has been shown to induce bronchoconstriction in patients with mild asthma [72]. These reactions occur within minutes of exposure and can be severe. Industrial exposures to high levels of SO<sub>2</sub> have been associated with long-term respiratory complications in exposed workers [73]. Asphyxiation of healthy individuals during high-level exposure to SO<sub>2</sub> has also been reported [74]. Pharmaceutical agents that have been used to treat SO<sub>2</sub>-induced bronchoconstriction include  $\beta$ -agonists, mast cell stabilizers, and cysteinyl-leukotriene receptor antagonists [75;76].

Whereas the pulmonary responses to SO<sub>2</sub> have been documented, little is known about the cellular mechanisms responsible for the observed health effects. Sulfur dioxide is a highly soluble gas that rapidly forms sulfite ions in solution [77]. Meng and Zhang compared chromosomal changes in a Chinese hamster ovary cell line exposed to sulfite ions in vitro with those observed in factory workers exposed to high levels of SO<sub>2</sub> for a long duration [78]. Other studies demonstrated sulfite-induced activation of human neutrophils in vitro by the induction of reactive oxygen species (ROS) and cellular oxidases [79;80].

Given the rapidity of the SO<sub>2</sub>-induced bronchoconstriction and the beneficial effects of mast cell stabilizers, we reasoned that SO<sub>2</sub> exposure may promote the release of allergic mediators from mast cells and basophils. In this study, we examine the capability of sulfite to directly activate mast cells and basophils independent of IgE. We found that not only does sulfite induce mast cell mediator release, but it does so through novel redox-sensitive pathways.

## **Materials and Methods**

### *Reagents*

Bovine serum albumin (BSA), N-acetyl-L-cysteine, tetramethylthiourea, 2,7-dichlorofluorescein diacetate (DCFH-DA), sodium sulfite (Na<sub>2</sub>SO<sub>3</sub>), and mouse IgE anti-dinitrophenyl (DNP) antibodies were purchased from Sigma-Aldrich Corp (St Louis, MO). The DNP-BSA was purchased from Biosearch Technologies Inc (NOVATO, CA). Anti-human IgE was purchased from BD Biosciences (San Diego, CA). Dulbecco modified Eagle medium (DMEM), fetal calf serum (FCS), streptomycin, penicillin, and Hanks balanced salt solution (HBSS) were purchased from Gibco BRL (Grand Island, NY).

### *Hexosaminidase Release Assay*

Rat basophilic leukemia (RBL-2H3) cells were cultured in DMEM supplemented with 10% FCS, 100 IU/mL of penicillin, and 100  $\mu$ g/mL of streptomycin. Cells were cultured at 37°C in a humidified atmosphere with 5% carbon dioxide (CO<sub>2</sub>). Cells were plated at 5  $\times$  10<sup>3</sup> per well in a 96-well plate and incubated overnight at 37°C in DMEM

supplemented with 5% FCS. The next day, cells were washed twice in Tyrodes buffer, pH 7.3 (137mM sodium chloride, 5.6mM glucose, 2.7mM potassium chloride, 0.5mM sodium dihydrogen phosphate, 1mM calcium chloride, and 10mM HEPES), followed by incubation in experimental conditions with Na<sub>2</sub>SO<sub>3</sub> (0.5, 0.75, 1, 2, and 5mM) diluted in Tyrodes buffer. After 30 minutes at 37°C, the reaction was stopped with an equal volume of ice-cold Tyrodes buffer. For IgE control wells, cells were preincubated for 1 hour with DNP specific IgE (200 ng/mL), followed by incubation with DNP-BSA (100 ng/mL) for 30 minutes. These concentrations of IgE and DNP were found in dose-response studies to induce maximal degranulation. The supernatants were harvested, and any cells present were removed by centrifugation at 100g for 5 minutes. 1.2% Triton-x solution was applied to obtain total release. The optical density at 405 nm was determined using an automated ELISA microplate reader (FLUOstar Optima; BMG Labtech, Durham, NC). The percentage release was calculated using the following equation: [(experimental release \_ spontaneous release)/Triton X release] x 100.

#### *Serotonin Release Assay*

These experiments were performed as described elsewhere [81]. Briefly, RBL-2H3 cells were plated at  $1 \times 10^4$  per well in a 96-well plate in DMEM supplemented with 5% FCS and 1Ci/mL of [<sup>3</sup>H] serotonin for 18 hours. Cells were then washed with HBSS, followed by incubation with experimental conditions. After incubation, supernatants were harvested, and any cells present were removed by centrifugation. Total cellular content of serotonin was quantified in the supernatant of cells lysed with Triton X. Radioactivity was measured using an automated liquid scintillation counter (1450 Micro-Beta;

PerkinElmer, Fremont, CA). The percentage release was calculated as described previously herein.

#### *Histamine Release Assay*

All studies involving human subjects were approved by the institutional review board at The University of Texas Medical Branch. After informed consent was provided, a 25-mL sample of peripheral blood was obtained by venipuncture and placed in heparin-containing tubes. The blood was mixed with an equal volume of HBSS, and mononuclear cells were isolated by density gradient centrifugation over Ficoll-Paque Plus (Amersham Biosciences, Uppsala, Sweden). The mononuclear cell fraction—containing basophils—were washed and resuspended in HBSS. A total of  $2.5 \times 10^5$  peripheral blood lymphocytes were exposed to either  $\text{Na}_2\text{SO}_3$  or anti-human IgE (1 g/mL) in HBSS for 45 minutes at 37°C. The supernatant was harvested and stored at -20°C. The released histamine was quantified by EIA (IBL, Hamburg, Germany) according to the manufacturer's instructions.

#### *Determination of Intracellular ROS Generation*

A total of  $3 \times 10^4$  RBL-2H3 cells were plated per well in a 96-well plate in DMEM with 5% FCS and incubated overnight at 37°C in 5%  $\text{CO}_2$ . Cells were then washed twice with phosphate-buffered saline (PBS) before loading with 50  $\mu\text{M}$  DCFH-DA in PBS for 20 minutes at 37°C. The cells were washed with PBS and then incubated in experimental conditions in PBS in duplicate and immediately placed in an automated fluorometer (FLUOstar Optima), with an excitation wavelength of 480 nm and emission

of 530 nm. The antioxidants tetramethylthiourea (50\_μM) and N-acetyl-L-cysteine (10mM) were prepared in PBS mixed with and without sulfite and then added to wells. In experiments using , cells were preincubated with 100\_μM diphenyleneiodonium for 30 minutes at 37°C, followed by 2 washes with PBS before DCFH-DA loading. The inhibitors themselves did not induce fluorescence. Results were calculated by subtracting spontaneous fluorescence in wells containing PBS alone and are expressed in relative fluorescence units.

### *Cellular Viability*

Cell viability was evaluated using propidium iodide staining. Cells were plated at  $3 \times 10^4$  per well in a 12-well plate in culture medium and incubated overnight at 37°C in 5% CO<sub>2</sub>. Cells were washed twice with HBSS before treatment with experimental conditions, followed by incubation for 30 minutes at 37°C. The cells were then harvested with trypsin plus 0.1% EDTA, washed twice with PBS with 0.5% BSA, and stained with propidium iodide in PBS with 0.5% BSA. Fluorescence was evaluated using a flow cytometer (FACScan; Becton Dickinson, San Jose, CA).

### *Statistical Analyses*

All analyses were performed on the means of 3 individual experiments, and experimental samples were performed in duplicate. Sulfite dose-dependent degranulation was analyzed using the Spearman correlation method. For studies using the inhibitors tetramethylthiourea and diphenyleneiodonium, a paired 2-sample for means *t* test was used, with a 95% confidence interval ( $P \leq .05$ ).

## Results

### *Na<sub>2</sub>SO<sub>3</sub> Induces Degranulation of RBL-2H3 Cells*

To determine whether Na<sub>2</sub>SO<sub>3</sub>, the principal ion of SO<sub>2</sub>, had an effect on mast cell degranulation, RBL-2H3 cells were exposed to varying concentrations of Na<sub>2</sub>SO<sub>3</sub>. As shown in Figure 2, sulfite induced degranulation of RBL-2H3 cells with a maximum degranulation of 13% observed in wells containing 2mM sulfite. Optimal IgE cross-linking induced degranulation of 14.3%. A significant correlation was observed between sulfite concentration and percentage degranulation. No measurable pH change was observed at the concentrations of sulfite used in the experiments.

We considered whether sulfite-induced mediator release was the result of cellular injury and death associated with loss of membrane integrity. Membrane integrity was unaffected by the highest concentration of sulfite (5mM) used in these experiments, as demonstrated by propidium iodide staining (Figure 3). This is in contrast to the cell death induced by 1M formaldehyde. Cell viability was also unaffected by the lower concentrations of sulfite (data not shown). Thus, an activation-dependent induction of mast cell mediator release was considered.

### *Sulfite-Induced Degranulation Is Independent of Extracellular Calcium*

Mast cell degranulation has previously been shown to depend on increases in cytosolic free calcium [82;83]. In particular, calcium mobilized from extracellular sources is important in IgE mediated degranulation, and depletion of extracellular calcium abrogates mediator release. To investigate the role of extracellular calcium in sulfite-induced degranulation, we performed degranulation (serotonin release) assays in



calcium-free media containing 1mM EDTA to further deplete extracellular calcium. Depletion of extracellular calcium did not cause a statistically significant alteration in sulfite-induced serotonin release at any of the concentrations of sulfite tested (Figure 4). These findings indicate that sulfite-induced degranulation may rely solely on the release of intracellular stores of calcium, a distinct difference from IgE-mediated degranulation.

#### *Na<sub>2</sub>SO<sub>3</sub> Can Induce ROS in RBL-2H3 Cells*

Because the sulfite ion has oxidative potential, this was considered as a possible mechanism of cellular activation. To evaluate whether Na<sub>2</sub>SO<sub>3</sub> exposure induced intracellular ROS, RBL-2H3 cells were loaded with the redox-sensitive dye DCFH-DA, which fluoresces when oxidized by ROS. The DCFH-DA-loaded cells were exposed to sulfite (0.5 and 5mM) for 60 minutes. Exposure to sulfite induced ROS in a dose-dependent manner (Figure 5). Hydrogen peroxide, 5mM, was used as a positive control. The ROS generation increased throughout the experiment (60 minutes), with 2.3- and 2.7- fold increases from 10 to 60 minutes for 0.5 and 5mM sulfite, respectively. Thus, cellular activation and subsequent degranulation may be secondary to signals generated through intracellular ROS.

#### *Antioxidants Block ROS Generation and Degranulation*

To further investigate the possibility that degranulation was directly linked to the generation of intracellular ROS, the ROS scavengers tetramethylthiourea and N-acetyl-L-cysteine were used to block ROS. As shown in Figure 6a and b, both scavengers were effective at reducing the DCFH fluorescence induced by 5mM sulfite by approximately

80% and 91%, respectively. Furthermore, we show that sulfite-induced degranulation is also inhibited by tetramethylthiourea at 1, 2, and 5mM Na<sub>2</sub>SO<sub>3</sub> (Figure 7) and by N-acetyl-L-cysteine. Cell viability evaluated by propidium iodide staining was unaffected by the antioxidants (data not shown). These results confirm that the degranulation observed after exposure to sulfite depended on the generation of an intracellular signal through ROS.

### *Role of Cellular Nicotinamide Adenine Dinucleotide Phosphate Oxidase in ROS*

#### *Induction and Degranulation*

To further explore the mechanism whereby sulfite induces the high levels of intracellular ROS, we considered the possible role of cellular nicotinamide adenine dinucleotide phosphate (NADPH) oxidases, which have been implicated in the generation of ROS after oxidant stresses [84]. To investigate whether cellular NADPH oxidase(s) was involved, we used the flavoenzyme inhibitor diphenyleneiodonium to block the intracellular generation of superoxide. The RBL-2H3 cells treated with 100\_μM diphenyleneiodonium before challenge with sulfite demonstrated reduced levels of ROS generation (Figure 8). Specifically, at 30 minutes, ROS generation by 0.5 and 5mM sulfite was decreased by 79% and 71%, respectively. Diphenyleneiodonium also significantly inhibited the degranulation induced by 1 and 2mM sulfite, respectively ( $P = .046$ ) (Figure 9).

### *Human Basophil Exposure to Na<sub>2</sub>SO<sub>3</sub> Induces Histamine Release*

To evaluate whether sulfite also induces degranulation of human basophils, peripheral blood mononuclear cells were isolated from 2 volunteers and exposed to 1, 2, and 5mM Na<sub>2</sub>SO<sub>3</sub>. Results for each volunteer are expressed as a percentage of total histamine released by cell lysis. The 5mM sulfite induced degranulation of 13% and 10% for volunteers 1 and 2, respectively. Anti-human IgE induced degranulation of 14.8% and 16% for volunteers 1 and 2, respectively (Figure 10). Ionomycin induced a degranulation of 45% and 33% for the 2 volunteers, respectively. These results confirm that sulfite-induced mediator release is an important trigger in human basophils comparable with mediator release induced by IgE cross-linking.

### **Discussion**

Sulfur dioxide is a highly soluble gas, rapidly forming sulfite and sulfate ions in solution [77]. Previous studies have documented reproducible DNA damage in vivo by SO<sub>2</sub> exposure and by sulfite exposure in vitro [78]. In addition, Beck-Speier et al showed that sulfite activates neutrophils [79]. The concentrations of Na<sub>2</sub>SO<sub>3</sub> used in this study were based on toxicity studies and previous reports documenting the effect of sulfite on neutrophils. Although industrial exposures to SO<sub>2</sub>, ranging from 5 to 200 ppm, have been documented, isolated exposures as high as 1,000 ppm have been reported [73;74]. In this study, we used sulfite concentrations of 40 to 400 ppm (0.5–5mM) in solution. Although SO<sub>2</sub> is an extremely soluble gas, the concentration of sulfite generated in solution would be difficult to calculate and, to our knowledge, has not been fluid. Based on the evidence that the physiologic effects of SO<sub>2</sub> occur very rapidly, and that the effects

can be attenuated by pretreatment with cromolyn, we hypothesized that SO<sub>2</sub> activates airway mast cells. To test this hypothesis, we exposed RBL-2H3 cells, a well-characterized mast cell model, to Na<sub>2</sub>SO<sub>3</sub>. We found that sulfite was capable of inducing degranulation of RBL-2H3 cells and that generation of intracellular ROS seemed to be the major mechanism triggering the response. These results are consistent with the growing body of literature that supports the role of oxidative stress as a key factor in pollutant-induced airway hyperresponsiveness and asthma [58;72;85]. Our results also show that sulfite can induce the formation of ROS in RBL-2H3 cells. Exposure to sulfite in the presence of the antioxidants tetramethylthiourea and N-acetyl-L-cysteine significantly abrogated this ROS response. Cellular NADPH oxidases are crucial in the generation of intracellular ROS. In neutrophils, intracellular killing depends on a functional NADPH oxidase [86]. The NADPH oxidase has been shown to be activated in neutrophils after sulfite exposure.

Neutrophils from patients with chronic granulomatous disease, who lack a functional NADPH oxidase, do not show activation in the presence of sulfite [87]. We observed that pretreatment of RBL-2H3 cells with the NADPH oxidase inhibitor diphenyleneiodonium inhibited sulfite-induced ROS formation and degranulation by 70%. These data implicate cellular NADPH oxidase as a key factor in the oxidative response to sulfite challenge.

The source of calcium in sulfite-mediated degranulation was investigated by performing sulfite exposure in the presence of calcium-free medium and a cation chelator (EDTA). We did not observe any significant inhibition of sulfite-mediated degranulation when extracellular calcium was depleted. Given the requirement for calcium flux in

degranulation, this finding suggests that intracellular free calcium mobilization is induced by sulfite treatment and is sufficient for sustaining the sulfite-induced degranulation.

To address whether the phenomenon we observed in rat mast cells could be reproduced in human basophils, we investigated the effect of sulfite exposure on peripheral blood mononuclear cells isolated from volunteers. Our results show that sulfite exposure also induced histamine release from human peripheral blood basophils.

Although it is possible that another cell secreted a histamine-releasing factor that induced basophil histamine release, our in vitro data support a direct effect of sulfite on basophils.

These results suggest that airway inflammatory cell mediator release induced by sulfite may be responsible for the observed physiologic effects of SO<sub>2</sub>. Solubilization of SO<sub>2</sub> also produces sulfuric acid, with subsequent lowering of the pH in bronchial lining fluid. This has been shown to induce bronchospasm putatively through cholinergic activation [88]. Our results suggest that the sulfite ion in the absence of excess hydrogen ion itself may be contributing to bronchospasm through direct activation of mast cells. In addition to the direct health effects of SO<sub>2</sub>, there is increasing evidence that sulfur oxides are a significant constituent of fine particulate matter and diesel exhaust particles, both of which have been implicated in allergic disease [52;71;89]. They also showed that extracts of diesel exhaust particles are capable of directly activating the release of inflammatory mediators and TH2-priming cytokines from basophils isolated from allergic and nonallergic patients [90]. Given the high concentration of sulfur oxides in diesel exhaust particles and fine particulates, it is interesting to speculate that they may be one of the constituents that mediate the health effects of these pollutants by activating mast cells in the airways. Increases in pollution have been associated with the rise in

asthma and other allergic diseases, particularly in urban areas. There is increasing evidence that pollutant-induced oxidative stress is a key step in this allergic priming. Our data document, for the first time, that the sulfite ion is capable of inducing mast cell degranulation through a ROS-mediated pathway and also implicate cellular NADPH oxidase in this phenomenon.

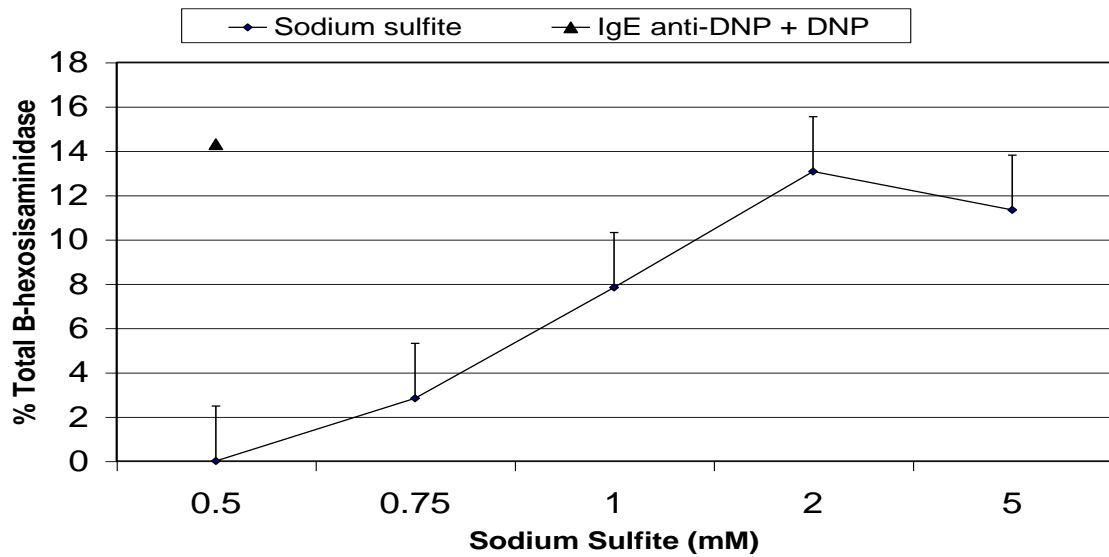


**Figure 2.**  $\beta$ -hexosaminidase assay. Demonstrating sodium sulfite induced degranulation. RBL-2H3 cells were exposed to increasing concentrations of sodium sulfite (filled circles) or IgE anti-DNP + DNP (filled triangle). n=3. Physiological range of degranulation is approximately 10 – 20% of total.

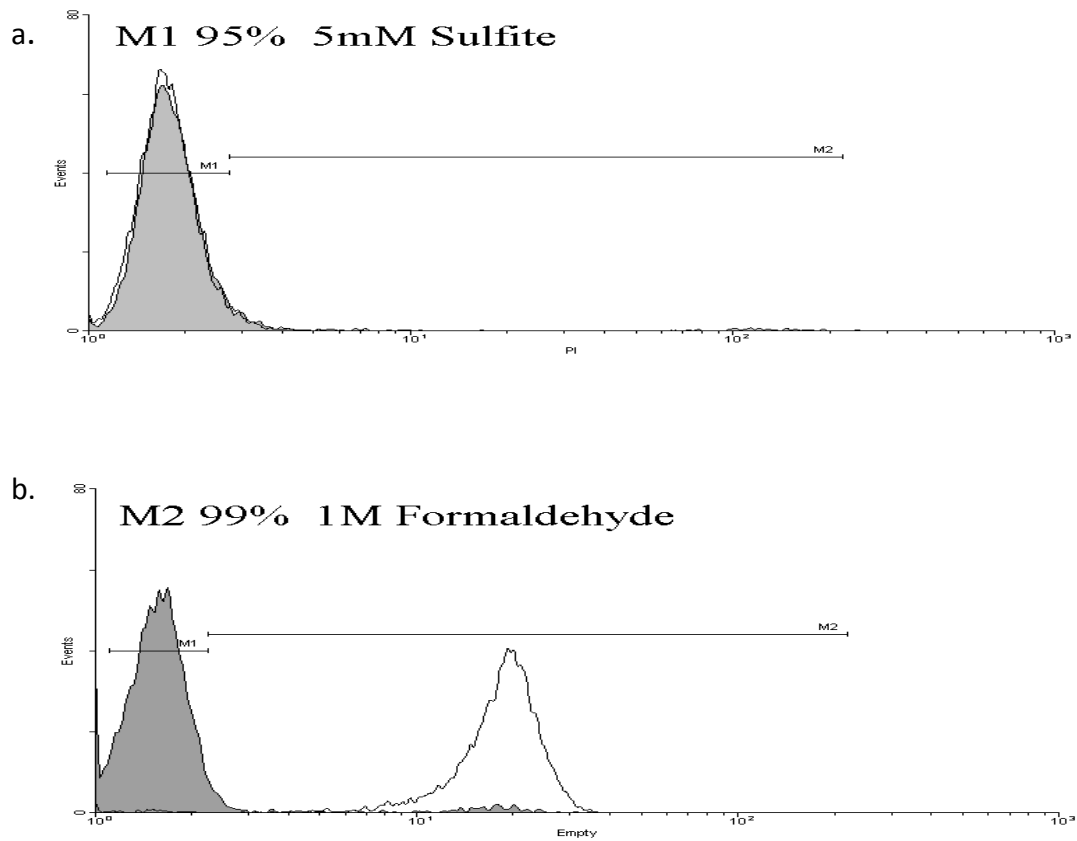


**Figure 3.** Propidium iodide staining to assess cell viability. Cells were incubated in HBSS alone (shaded histogram), or with either a. sodium sulfite (5mM) (empty histogram upper panel) or b. formaldehyde (1M) (empty histogram lower panel). Cells were then removed, stained with propidium iodide and analyzed by flow cytometry. Representative of 3 independent experiments

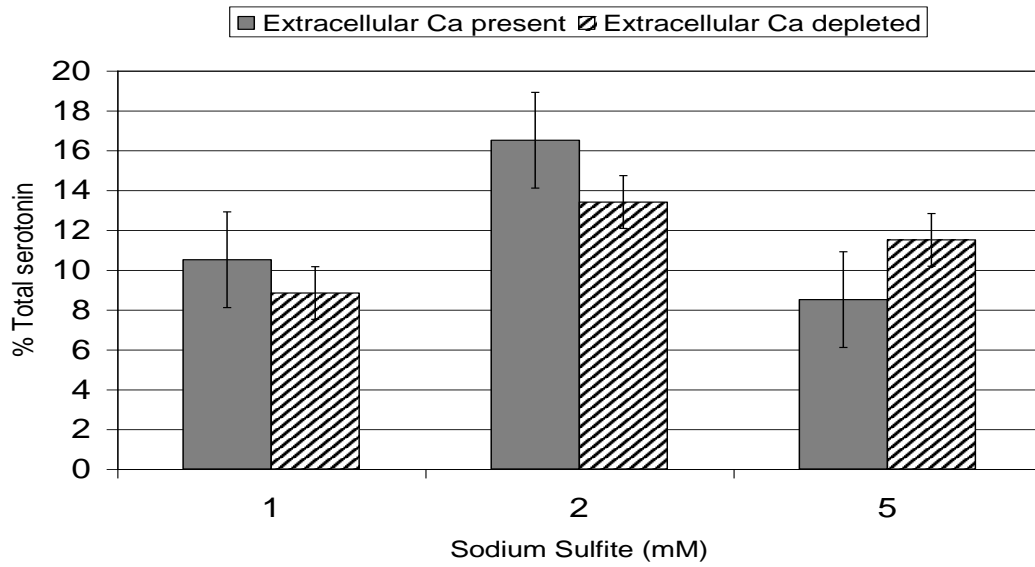


**Figure 4** Sulfite induced degranulation is unaffected by extracellular calcium depletion. RBL-2H3 cells were incubated with sodium sulfite diluted in HBSS (grey bars) or calcium free HBSS containing 1 mM EDTA (hatched bars). Supernatants were harvested and released serotonin quantified. n=3

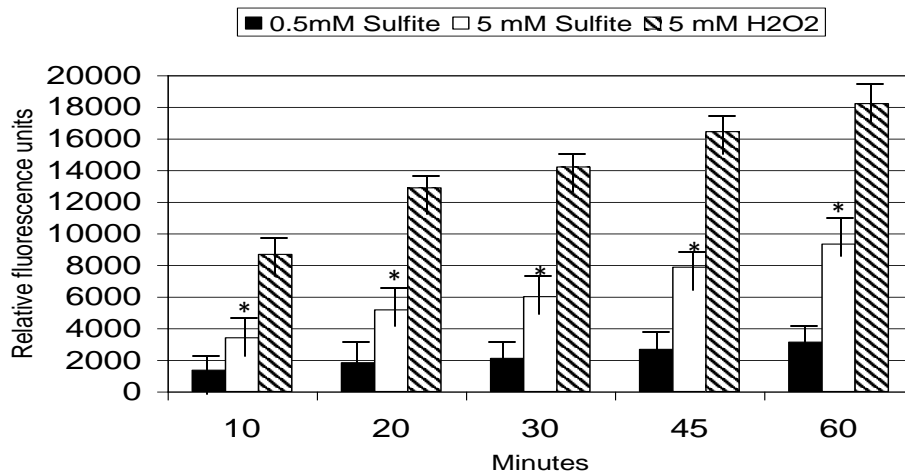


**Figure 5** Sodium sulfite induces ROS formation. Cells were exposed to 0.5 mM sulfite (black bars), 5mM sulfite (clear bars) and 5 mM H<sub>2</sub>O<sub>2</sub> (hatched bars) as a positive control. Fluorescence was determined at 10, 20, 30, 45, and 60 minutes. n=3, p<0.05.

\* Indicates statistical significant increase above negative control.



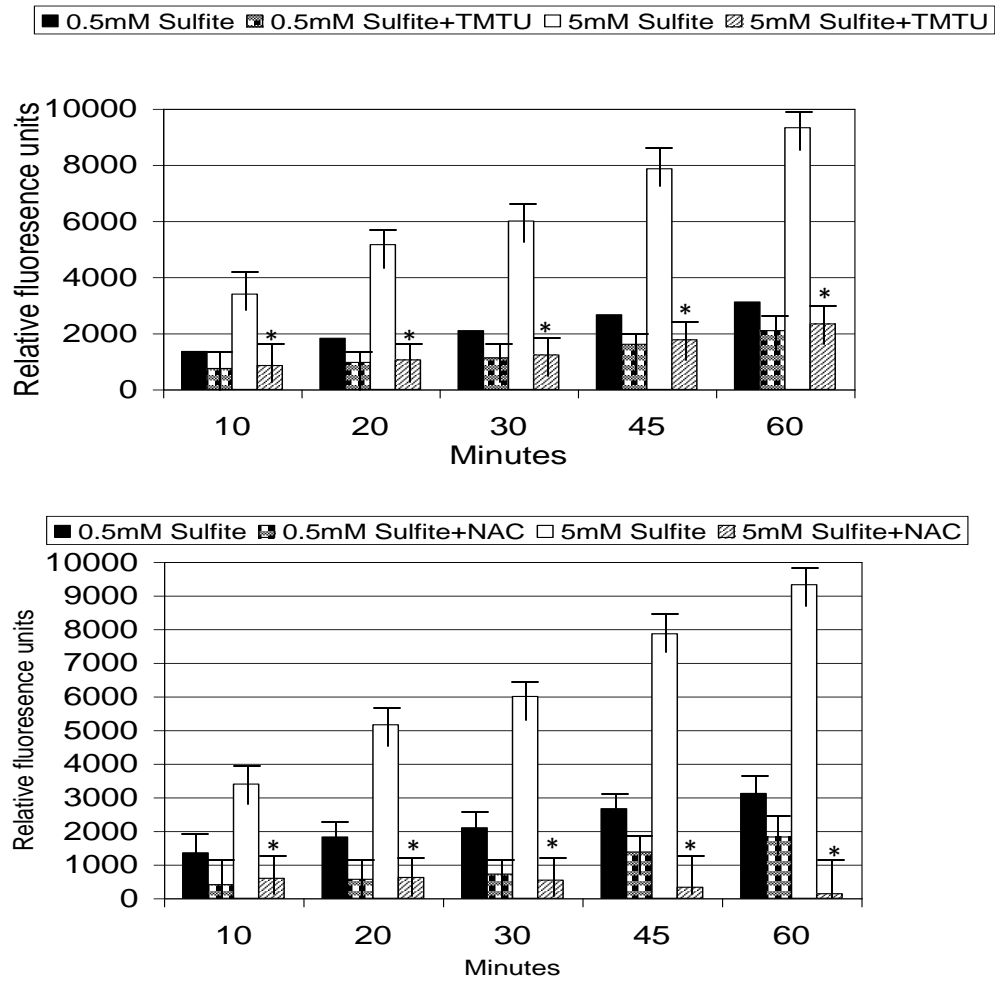


**Figure 6 a and b.** Intracellular ROS generated by sulfite exposure is inhibited by antioxidants TMTU and NAC. Cells were exposed to 0.5 mM sulfite (black bars) or 5 mM sulfite (clear bars) alone or 0.5 mM sulfite with 50  $\mu$ M TMTU (checked bars) or 5 mM Sulfite with 50  $\mu$ M TMTU (hatched bars) (4A). In figure 4B 10 mM NAC is the inhibitor instead of TMTU. Fluorescence was determined at 10, 20, 30, 45, and 60 minutes.

\* Indicates statistically significant drop from 5mM sulfite. n=3, p<0.05.

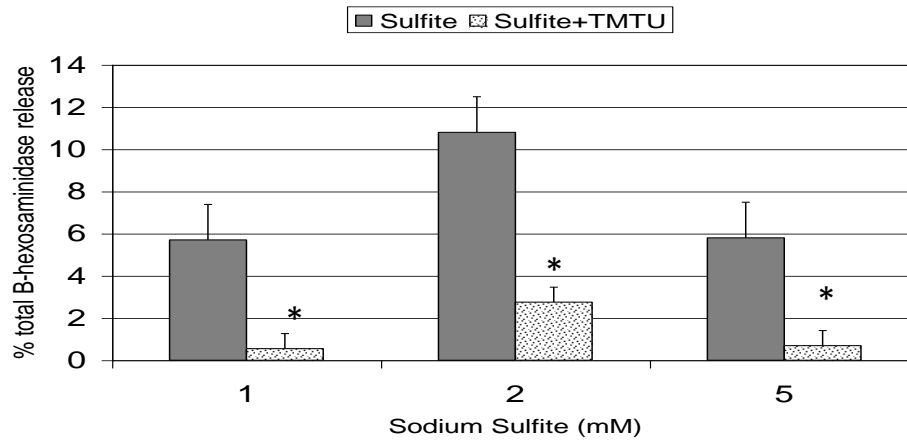


**Figure 7.** Inhibition of sulfite induced degranulation by TMTU. RBL-2H3 cells were exposed to sodium sulfite (grey bars) in Tyrodes buffer with or without 50  $\mu$ M TMTU (patterned bars) and  $\beta$ -hexosaminidase release determined. n=3, p<0.05.  
\* Indicates statistically significant drop from sulfite treatment

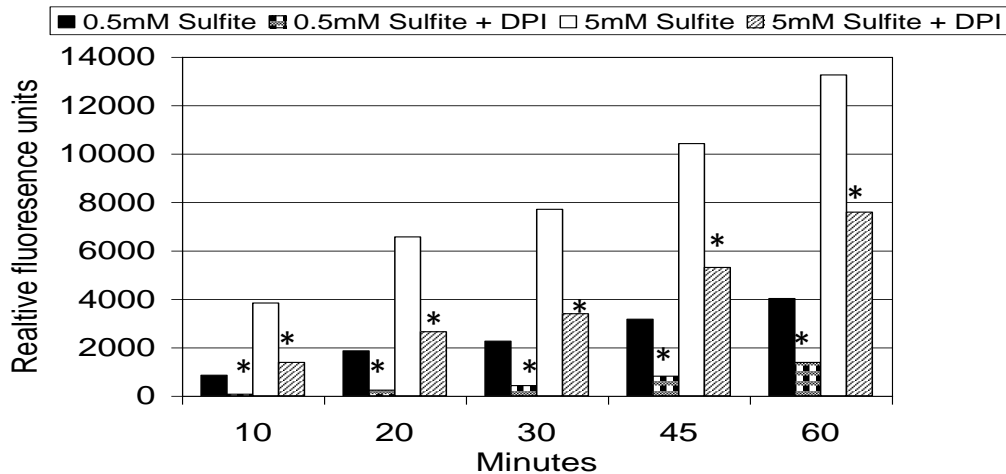


**Figure 8.** Inhibition of cellular flavoenzymes inhibits sulfite induced ROS generation. ROS induced by 0.5 mM sulfite (black bars), 5 mM sulfite (clear bars) are shown. Checked and hatched bars indicate ROS formation in cells pretreated with DPI. n=3, p<0.05.  
\* Indicates statistically significant drop from adjacent sulfite treatment

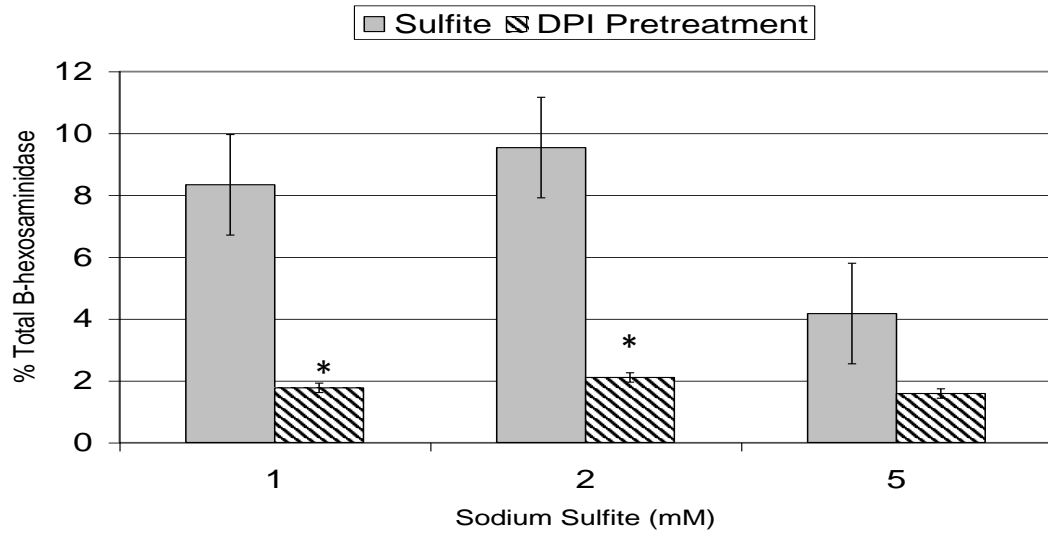


**Figure 9.** Inhibition of sulfite induced degranulation by DPI. RBL-2H3 cells were exposed to sodium sulfite in Tyrodes buffer alone (grey bars) or Tyrodes buffer containing 100  $\mu$ M DPI (hatched bars). n=3, p<0.05.  
\* Indicates statistically significant drop from sulfite treatment

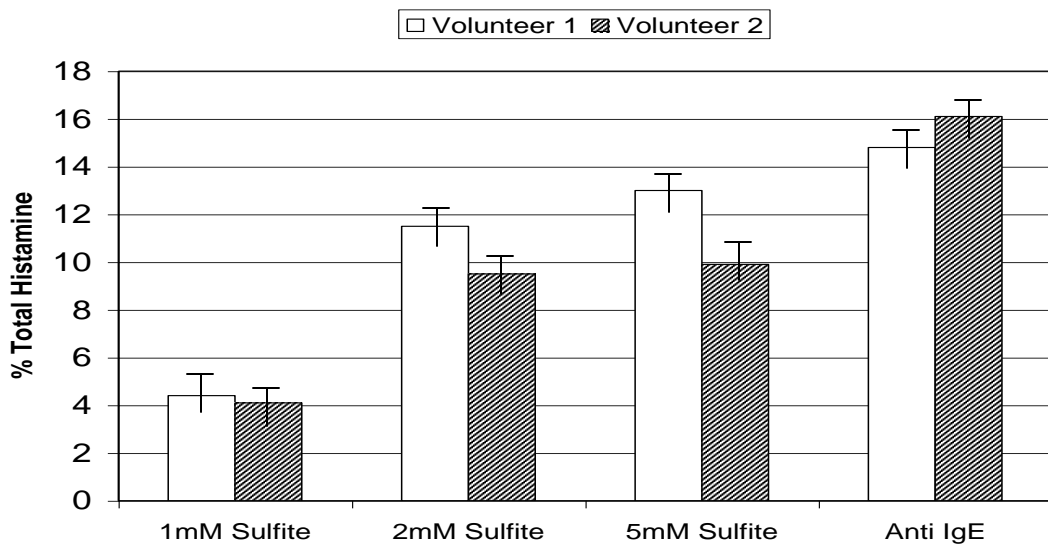


**Figure 10.** Sulfite induced histamine release from PBL. Results for two volunteers are shown and are represented as percent of total histamine released by triton X lysis. Anti-IgE mediated release for each volunteer is also shown.

## **CHAPTER 3. Acrolein Induced Oxidative Stress and Allergic Inflammation in Mast Cells**

### **Introduction**

It is thought that oxidative stress may contribute to the release of inflammatory mediators [91]. Previously, we have shown that sodium sulfite, the soluble form of sulfur dioxide, induces intracellular oxidant stress and degranulation in mast cells in a similar model system and the introduction of anti-oxidants, tetramethylthiourea (TMTU) and n-acetyl-cysteine (NAC) demonstrated reduction of the inflammatory response [92].

Exposure to other common air pollutants, such as ozone, has also been associated with the production of oxidative stress [93]. Acrolein, a major constituent of combustion products, is classified as a likely human carcinogen and a known respiratory irritant [42]. It is also known to produce protein and DNA adducts in high concentration exposures [94]. As one of the more common components of anthropogenic combustion pollution, it poses a serious health risk to exposed populations. Airborne aldehydes may be a contributing factor to the increase in asthma and allergic disease in world urban populations.

In this study, we hypothesize that acrolein acts directly upon mast cells to induce the release of inflammatory mediators and that activation is linked to the production of intracellular production of reactive oxygen species (ROS).

## Methods

### *Reagents*

Bovine serum albumin (BSA), N-acetyl-1-cysteine (NAC), tetramethylthiourea (TMTU), (DPI), 2[prime],7[prime]-dichlorofluorescein diacetate (DCFH-DA), Acrolein ( $C_3H_4O$ ), and mouse IgE anti-dinitrophenyl (DNP) antibodies were purchased from Sigma-Aldrich (St Louis, MO). DNP-BSA was purchased from Biosearch Technologies Inc (NOVato, CA). Dulbecco Modified Eagle Medium (DMEM), fetal calf serum (FCS), streptomycin- penicillin, and Hanks balanced salt solution (HBSS) were purchased from Gibco BRL (Grand Island, NY).

### *Cell culture*

RBL-2H3 cells were obtained from American Type Cell Collection (ATCC) were cultured in DMEM supplemented with 10% FCS, 100 IU/ml penicillin, and 100  $\mu$ g/ml streptomycin (Gibco BRL, Grand Island, NY) at 37 °C in a humidified atmosphere with 5%  $CO_2$ .

### *Mast cell degranulation*

As described in the review by Rashid *et al.* RBL-2H3 cells were established as an efficient and reliable alternative to the wild-type mast cell in inflammatory research [95]. These experiments were performed as described previously [92]. Briefly, RBL-2H3 cells were plated at  $1 \times 10^4$  per well in a 96-well plate in DMEM supplemented with 5% FCS and 1  $\mu$ Ci/mL of [ $H^3$ ]serotonin overnight. Cells were then washed with HBSS, followed by application of experimental conditions. After incubation, supernatants were harvested,

and any cells present were removed by centrifugation. Total cellular content of serotonin was quantified in the supernatant of cells lysed with Triton X100. Radioactivity was measured by scintillation spectroscopy (1450 MicroBeta; PerkinElmer, Fremont, CA) and the percentage release calculated: (experimental – spontaneous)/(total-spontaneous). For calcium depletion experiments, cells were labeled with [ $H^3$ ]serotonin and then washed and assayed with calcium free HBSS plus 1 mM EDTA.

#### *Determination of Intracellular ROS Generation*

RBL-2H3 cells were washed with phosphate-buffered saline (PBS) before loading with 50 $\mu$ M DCFH-DA in PBS for 20 minutes at 37°C. The cells were then washed with PBS and then incubated in experimental conditions in PBS and immediately placed in an automated fluorometer (FLUOstar Optima, BMG Labtech, Durham, NC), with an excitation wavelength of 480 nm and emission of 530 nm. The antioxidants, TMTU (50 $\mu$ M) and NAC (10 mM) were prepared in PBS and mixed with and without acrolein before adding to wells. In experiments using DPI, cells were incubated with 100  $\mu$ M DPI for 30 minutes at 37°C, followed by two washes with PBS before DCFH-DA loading. The inhibitors themselves did not induce fluorescence. Results were calculated by subtracting spontaneous fluorescence in wells containing PBS alone and are expressed in relative fluorescence units.

#### *Cellular viability measurements*

Cell viability was evaluated using several methods. Propidium iodide (Calbiochem, San Diego, CA) staining was used to assess cellular membrane integrity. Cells were incubated for 30 minutes with acrolein. The cells were then harvested with

trypsin plus 0.1% EDTA, washed twice with PBS with 0.5% BSA, and stained with propidium iodide 1 µg/ml) in PBS with 0.5% BSA. Fluorescence was evaluated by flow cytometry (FACScan; Becton Dickinson, San Jose, CA).

A second method of analyzing cell viability used the reduction of tetrazolium dye to assess mitochondrial activity as an indication of cell health. The MTT assay was performed according to manufacturer protocols (Cayman, Ann Arbor, MI). Briefly, cells were incubated with acrolein for 30 minutes. Cells were washed with PBS/10% FCS. MTT [3-(4,5-dimethylthiazol-2-yl)-2,5-diphenyltetrazolium bromide] was added to the cells for 4 hours at 37° C. The supernatant removed and replaced with isopropanol and the optical density (540 nm) read in an automated plate reader (FLUOstar Optima).

A third method for assessing cellular viability is known as the JAM (“just another method”) assay [96] and assesses the amount of intact non-fragmented DNA within cells. RBL-2H3 cells were incubated with 1 µCi/ml 3H-thymidine overnight. Cells were washed and incubated with acrolein. After incubation, cells were harvested on a semi-automated harvester and DNA deposited onto glass fiber filters, which was dried and placed into scintillation fluid and counts enumerated by scintillation spectroscopy. Total raw counts were compared between experimental conditions.

#### *Intracellular Calcium Measurement*

Intracellular calcium was determined using the FLIPR Calcium 3 Assay Kit (Molecular Devices, Sunnyvale, CA), which utilizes a calcium sensitive fluorescent dye, according to manufacturer’s instructions. Briefly, RBL-2H3 cells were grown to confluency on 96-well plates. Medium was removed and 100 µl of the FLIPR Calcium 3 assay reagent in HBSS + 20 mM Hepes was placed into well and the plate incubated at

37°C for 1 hour. After placing varying concentrations of acrolein, the plate was immediately placed into an automated microplate reader (FluoStar Optima) and fluorescence determined (excitation 480 nm, emission 530 nm).

#### *Cytokine, chemokine, and leukotriene assays*

RBL-2H3 cells were cultured with acrolein with and without DNP for 30 minutes. RNase protection assays (RPA) were performed according to the manufacturer's instructions (RiboQuant<sup>TM</sup>, BD Biosciences Pharmingen, San Diego, CA).

RBL-2H3 cells were cultured with acrolein with and without DNP for 30 minutes. Cells were then washed and allowed to incubate another 24 hours. Culture supernatants were harvested and immediately frozen at -20°C until analysis. Cytokines were measured using a rat 9-plex: IL-1 $\alpha$ , IL-1 $\beta$ , IL-2, IL-4, IL-6, IL-10, GM-CSF, IFN $\gamma$  and TNF $\alpha$  (Bio-Rad, Hercules, CA) and read on a Bio-Plex system (Bio-Rad) according to the manufacturer's instructions. The assay performances reports a detection limit of <10 pg/ml with a dynamic range of 0.2 - 32,000 pg/ml. 14,15-leukotriene C4 (LTC4) levels were assessed using an EIA according to manufacturer's instructions (Cayman) and optical density read (520 nm) on an automated plate reader (FLUOstar Optima).

#### *Statistical Analyses*

All analyses were performed on the means of 3 individual experiments, and experimental samples were performed in duplicate. Degranulation was analyzed using the Spearman correlation method and individual comparisons were made using a paired 2-sample for means *t* test was used, with a 95% confidence interval ( $P < 0.05$ ).



## Results

### *Acrolein induces mast cell degranulation*

In experiments to detect the direct effect of acrolein on mast cell degranulation, RBL-2H3 cells exposed to acrolein induced a progressive increase in the release of [ $H^3$ ]serotonin from 1-10,000 ppm (Figure 11). Subsequently, we investigated the potential ability of acrolein to synergize with IgE cross-linking. To accomplish this, RBL-2H3 cells were sensitized with anti-DNP-IgE (200 ng/ml) for one hour, washed and then exposed to DNP-BSA with or without acrolein. Using concentrations of DNP-BSA (1 ng/ml), that induced suboptimal degranulation, we found that not only was there no synergy, but that there was, in fact, suppression of serotonin release at acrolein concentrations of 100-10,000 ppm (Figure 11). This suggested alternative mechanisms existed for acrolein-induced degranulation versus IgE-crosslinking

### *Acetaldehyde and Formaldehyde induce mast cell degranulation*

Acetaldehyde and Formaldehyde are also important environmental pollutants. It has been concluded that:

VOCs such as formaldehyde and acetaldehyde have to be considered as priority pollutants with respect to their health effects. It has been pointed that in renovated or completely new buildings, the VOCs concentration levels are often several orders of magnitude higher. The main sources of acetaldehydes in homes include building materials, laminate, linoleum, wooden varnished, and cork/pine flooring. It is also found in plastic water-based and matt emulsion paints, in wood ceilings, and wooden, particle-board, plywood, pine wood, and chipboard furniture [97].

The use of acetaldehyde is important in industrial processes, and can be measured in waste water and air. "Sources of acetaldehyde include fuel combustion emissions from stationary internal combustion engines and power plants that burn fossil fuels, wood, or

trash, oil and gas extraction, refineries, cement kilns, lumber and wood mills and paper mills. Acetaldehyde is also present in automobile and diesel exhaust [98].” Acetaldehyde is also one of the main chemicals identified in tobacco smoke. Acetaldehyde in combination with nicotine, can lead to increased addiction to cigarette smoking. Acetaldehyde is a probable or possible carcinogen in humans [99].

Formaldehyde is an important precursor to many other chemical compounds, especially for polymers. Because of its ubiquitous use and potential for adverse health effects, exposure to formaldehyde is of particular interest in toxicity studies. On 10 June 2011, the US National Toxicology Program described formaldehyde as "known to be a human carcinogen"[100]. Formaldehyde forms during the oxidation (or combustion) of methane and carbonaceous compounds, especially seen in forest fires, automobile exhaust, and tobacco smoke[101]. In combination with sunlight, oxygen, methane and other hydrocarbons, formaldehyde becomes an important component of smog.

In order to examine whether other aldehydes initiate degranulation similarly to acrolein, RBL-2H3 cells were treated with formaldehyde and acetaldehyde in a dose dependent fashion. Both acetaldehyde and formaldehyde caused a significant rise in degranulation between 1ppm and 10 ppm (Figure 12). Cellular toxicity for these two aldehydes was ruled out as the primary cause of degranulation at this dose as it was with acrolein (data not shown).

### *Intracellular Calcium Concentration*

To further explore acrolein-induced degranulation mechanisms, it has been shown previously that IgE-dependent mast cell degranulation is dependent on the influx of extracellular calcium [102;103]. However, we have shown previously that degranulation by a strong oxidant stimulus occurred in the absence of extracellular calcium [92]. Thus, intracellular calcium release in RBL-2H3 cells exposed to acrolein was determined. Calcium levels increased at 0.01 ppm acrolein, and demonstrated a statistically significant increase at 10 ppm (Figure 13). To determine if degranulation was dependent upon the influx of extracellular calcium, serotonin release was determined after extracellular calcium depletion (Figure 14), which demonstrated no effect. Thus, we concluded that calcium stores from intracellular sources may be sufficient to induce degranulation in response to acrolein, a distinct difference from the mechanism reported previously for IgE-mediated degranulation [103].

### *Acrolein induces generation of reactive oxygen species*

In previous studies, the generation of intracellular reactive oxygen species (ROS) was associated with mast cell activation and degranulation [92]. Thus, we sought to investigate the mechanism of degranulation by determining the generation of intracellular ROS after acrolein exposure. Using an ROS sensitive fluorescent dye, DCFH-DA, acrolein exposed RBL-2H3 cells showed significant increases in intracellular ROS with increasing acrolein concentrations. Intracellular ROS levels increased modestly but significantly with 0.01 ppm and more substantially at 10 ppm, which was equivalent to ROS levels after exposure to 100 mM H<sub>2</sub>O<sub>2</sub> (Figure 15). To investigate further, we

treated cells with ROS scavengers, TMTU or NAC, which significantly reduced both ROS production and serotonin release (Figure 16). To investigate if flavoenzymes, such as those located within NADPH oxidase or mitochondrial complex II were involved in ROS generation by acrolein, cells were treated with DPI prior to exposure to acrolein. No change in serotonin release was observed.

#### *Acrolein induces expression of inflammatory cytokines*

An additional indicator of mast cell activation is secretion of inflammatory mediators, which may occur with or without degranulation [104]. Cytokine mRNA expression was assessed in an RNase protection assay. While acrolein induced an increase in IL-6 and TNF $\alpha$  mRNA at 0.0001 ppm this was not sustained at higher concentration (0.1 ppm) (Figure 17). DNP cross-linking also induced significant levels of TNF and IL-6, but this was reduced by addition of .0001 ppm acrolein.

We measured the presence of cytokines in culture supernatants of RBL-2H3 cells activated with increasing concentrations of acrolein and in the presence of DNP/ $\alpha$ DNP-IgE. Elevated levels of cytokines (Figure 18) were detected after exposure of RBL-2H3 cells only to higher concentrations (10,000 ppm) of acrolein. However, in contrast to degranulation experiments, there was an enhancement of cytokine release in combination with IgE cross-linking to low (1 ng/ml) and high (50 ng/ml) concentrations of DNP. All other concentrations of acrolein yielded undetectable or near undetectable levels. Levels of LTC<sub>4</sub> were increased with both 1000 and 10,000 ppm acrolein (Figure 19).

### *Acrolein induces cellular toxicity in mast cells*

Acrolein is known to have significant cellular toxicities. To investigate the level of toxicity in our system, several methods were utilized. The MTT assay (Figure 20) assesses the ability of cells with functional mitochondria to reduce a tetrazolium dye and is routinely used as an assessment of viability and/or cell growth. Increasing doses of acrolein incubated with RBL-2H3 cells for 30 minutes caused a dose-dependent reduction in the ability of the cells to reduce the dye, beginning at 10 ppm and significantly at 100 ppm. This can be interpreted as loss of cellular viability and/or a loss in mitochondrial function.

PI stains the DNA of cells whose membrane integrity is compromised. In order to assess membrane integrity, RBL-2H3 cells were treated with acrolein for 30 minutes, stained with propidium iodide (PI) and analyzed by flow cytometry (Fig 21). At 10 ppm acrolein few cells stained positive with PI, but at doses of 100 and greater, increasing numbers of cells demonstrated positive staining. These data imply a significant loss of membrane integrity at 100 ppm acrolein.

The JAM assay measures the loss of pre-labeled DNA from cells due to the fragmentation of DNA from apoptotic cells and is considered a sensitive measure of apoptotic cell death [96]. RBL-2H3 cells treated with acrolein for 30 minutes demonstrated a modest loss (20%) of DNA at acrolein concentrations of 1-100 ppm, while higher doses showed a progressive increase in loss up to 80% at 10,000 ppm (Figure 22). The Jam was repeated in human A549 epithelial cells to confirm the effects were not cell specific (Figure 23). Similar results were seen in both cell types. These experiments suggested that DNA fragmentation and loss may occur at low levels (1 ppm)

but that substantial cell death and loss of DNA does not occur until much higher levels (>100 ppm). Together these data indicate that acrolein is toxic to mast cells beginning at concentrations as low as 1 ppm, but that significant cell death/mitochondrial dysfunction, increased membrane permeability and loss of DNA occurs at concentrations of 100-1000 ppm.

## **Discussion**

Acrolein is a major component of urban air pollution. It is released in emissions and effluents from its manufacturing. Acrolein is also found in many other combustion processes especially cigarette smoking and petrochemical fuels. It is found in the environment as a result of being applied to water and waste water as a slimicide and aquatic herbicide. Additionally, it can be created through photo-oxidation reactions of hydrocarbon pollutants found in air, and from land disposal of sludge materials [42;105;106]. Acrolein is fairly reactive and therefore unstable. In general, people may be exposed to acrolein through inhalation of contaminated air. Acrolein exposures have been associated with increased mucous production [107], tumor formation [108], DNA adducts [109], and airway hypersensitivity [110]. Epidemiologic studies have shown the physiologically relevant range of acrolein exposure is between 0.5 ppm and 50 ppm. The average American daily exposure is estimated to be in the range of 0.5 to 1.5 ppm [111-113].

The results of our experiments show a bimodal response of mast cells to acrolein exposure. High levels of exposure (> 10 ppm) lead to evidence of increasing cellular toxicity with dosage, while lower levels, in the daily exposure range ( $\leq$  1 ppm), result in

ROS generation and degranulation with an absence of toxicity. Thus, our data indicates a correlation between exposure of acrolein and the induction of an inflammatory state in mast cells *in vitro* in a narrow range. Additionally, the lowest concentrations of acrolein (< 0.5 ppm) show little to no effect on mast cell degranulation; those lower concentration exposures may induce an early state of activation of the inflammatory process as evidenced by upregulation of intracellular ROS and calcium beginning at 0.01 ppm. Generation of intracellular ROS and calcium release from intracellular stores may herald the initial activation of mast cell pro-inflammatory pathways. Acrolein exposure between 1 ppm and 10 ppm induces degranulation and results in the creation of substantial levels of intracellular reactive oxygen species, which is suppressed, in part, by antioxidant scavengers.

Acrolein at higher concentrations (100 ppm and greater) induces toxicity and cell necrosis. Our data demonstrating cytokine and leukotriene release at the highest levels of acrolein exposure (1000-10,000 ppm), is likely not physiologically relevant other than in situations of very high toxic exposures. It is more likely that release of preformed cytokines resulted from the loss of cellular membrane integrity and not active secretory processes. This level of exposure might be represented by direct cigarette smoke or direct exposure to wood fires or acrolein processing [42;105]. The toxicity we observe is similar to that seen in previous studies [114;115], where acrolein was shown to induce oxidative cellular toxicity through the depletion of GSH as well as the induction of the MAP Kinase signaling pathway leading to cellular growth cycle arrest and cell necrosis. The highly electrophilic nature of acrolein likely induces DNA cross-links, resulting in mutation and the inability of repair mechanisms to recover damaged DNA [116]. As was

seen in our data, a study by Keher, Kozekov, and Rahman also show that concentrations of acrolein below those toxic doses show no evidence of cell necrosis, while still inhibiting cell growth [114;116;117].

Acrolein toxicity has been linked to two major intracellular signaling pathways resulting from its strong electrophilic nature. It tends to form adducts with the thiol groups of glutathione (GSH) in the cytosol and the nucleus, thus depleting cellular GSH and causing oxidant imbalance. GSH depletion leads to activation of apoptosis, most likely through an alteration of the activity of NF- $\kappa$ B [117]. Alternatively, acrolein may directly bind transcription factors leading to activation of cell death mechanisms. Kehrer and Biswal further suggest that the oxidative imbalance and the effects thereof are a result of changes in GSH status, rather than the formation of oxidation products themselves, which is further bolstered by evidence that anti-oxidants alter cellular states not through blockade of ROS but through attenuation of GSH imbalance. Indirect depletion of GSH may also result from ROS generated by damage to the mitochondrial electron transport chain [118]. It is known that mast cells degranulate, in part, due to a sudden shift in cytosolic calcium levels [119]. Acrolein may directly induce calcium pathways or indirectly induce calcium influx via the PKC/JNK signaling pathway [120]. Additionally, intracellular calcium shifts may also influence the activation state of NF- $\kappa$ B [121].

Taken together, these reports corroborate the combined effects we have shown in our experiments. Acrolein exposure leads to both cellular toxicity at higher concentrations and activation of calcium-dependent degranulation pathways resulting from a shift in oxidative balance. The results corroborated the concept that acrolein,



through the induction of oxidative stress, promotes mast cell degranulation. The release of mediators from mast cells in response to acrolein implicates acrolein as a component of urban air pollution that may potentially promote asthma and allergic disease. While several pathways for ROS generation by mast cells have been investigated, including the enzymes NADPH oxidase and xanthine oxidase [122]. The strongest evidence for IgE/antigen mediated ROS generation centers on the eicosanoid pathway and the enzymes COX1 and 5 LO [123]. IgE-independent pathways for ROS generation remain elusive. Several studies implicate a major role of oxidative stress in mast cell mediated inflammation. The oxidative stress is a result of an anti-oxidant/oxidant imbalance. Reduction in the efficacy of superoxide dismutase (SOD) seems to play a significant role in this imbalance [124]. More specifically, the transcription factor Nrf2, which is responsible for SOD and glutathione generation might be bound or damaged by exogenous stimuli, leading to reduction of the anti-oxidant generation pathway. The importance of Nrf2 in mast cell inflammatory processes was shown by [125]. Further study of mast cell intracellular pathways will help to elucidate the mechanisms bridging the production of cellular oxidative stress and a state of hypersensitive inflammation.

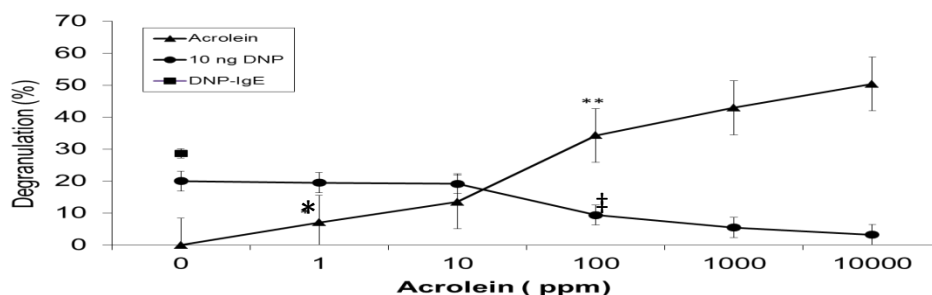


**Figure 11.** Degranulation of RBL-2H3 cells. Degranulation upon exposure to acrolein or acrolein with DNP/anti-DNP IgE cross-linking. RBL-2H3 cells were radio-labeled with  $H^3$  - serotonin for 24 hours prior to exposure. RBL-2H3 degranulation increases with exposure while acrolein blocks the DNP-IGE response inversely with exposure.  $n=3$ .

\*Denotes statistical significance between negative control and 1 ppm ( $p < 0.05$ )

\*\* Denotes statistical significance between 1 ppm and 100 ppm acrolein ( $p < 0.05$ )

‡ Denotes statistical significance between DNP positive control and 100 ppm Acrolein + 10 ng DNP ( $p < 0.05$ )

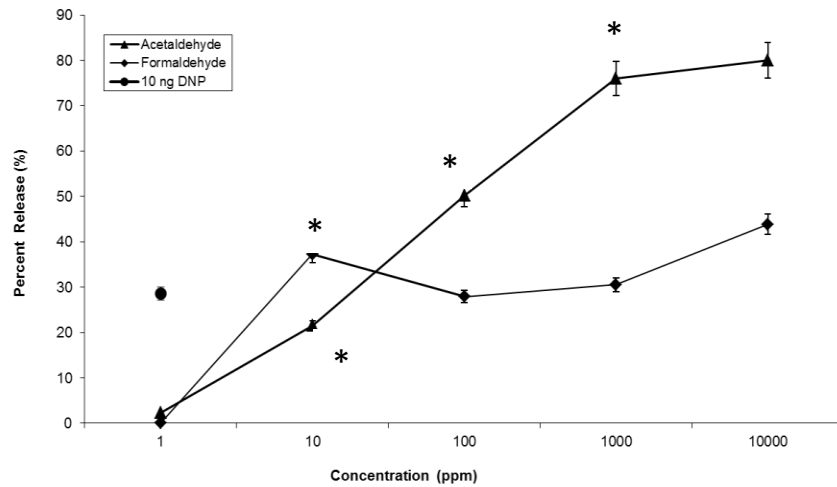


**Figure 12.** Degranulation of RBL-2H3 cells in response to treatment with acetaldehyde or formaldehyde. RBL-2H3 cells were radio-labeled with  $H^3$  - serotonin for 24 hours prior to exposure. RBL-2H3 degranulation increases with exposure to both acetaldehyde and formaldehyde.  $n=3$ ,  $p<0.05$ .

\* Indicates Statistical significance between indicated treatment and previous treatment

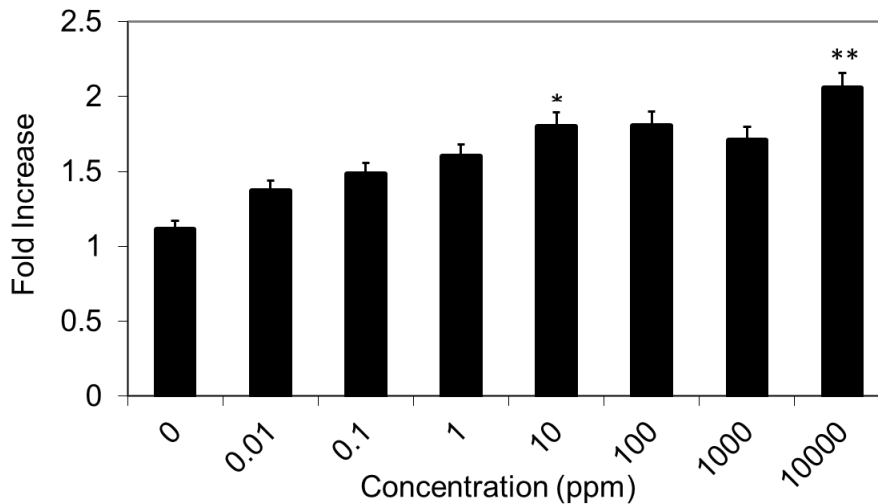


**Figure 13.** Detection of release of intracellular  $Ca^{2+}$ . RBL-2H3 cells were treated with the FLIPR fluorescence kit and injected with increasing concentrations of acrolein. Fluorescence was detected at wavelengths 485 excitation/520 emission. Values are fold increase of the post-injection fluorescence over the pre-treatment measures. Results show a steady rise in  $Ca^{2+}$  release with increasing concentrations of acrolein.

\*Indicates Statistically significant increase from negative control ( $p < 0.05$ ,  $n = 3$ )

\*\* Indicates statistical significance between 10 and 10,000 ppm ( $p < 0.05$ ,  $n = 3$ )

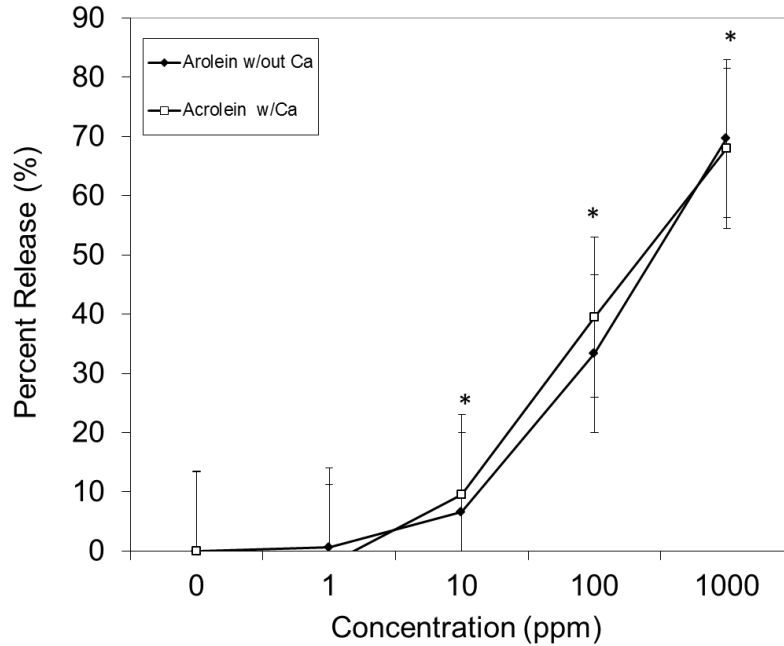


**Figure 14.** Effect of  $\text{Ca}^{2+}$  depletion on acrolein induced degranulation. RBL-2H3 cells were depleted of calcium, tritiated serotonin and treated with increasing concentrations of acrolein in a calcium depleted media. Results reveal no significant influence

\*Indicates statistical significance between indicated treatment and previous treatment.  $n=3$ ,  $p<0.05$

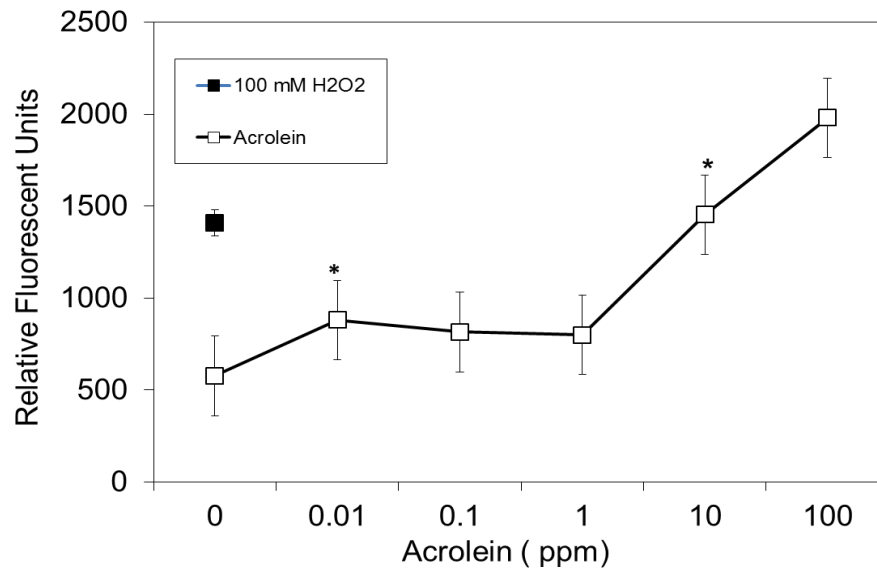


**Figure 15.** Reactive oxygen species as measured by DCFH-DA fluorescence. RBL-2H3 cells were pulsed with DCFH-DA and treated with either PBS or acrolein. Relative fluorescence was read at excitation 480 nm and emission 530 nm wavelengths. ROS is shown to increase at low concentrations of acrolein and then again at higher exposures.

\*Indicates statistical significance between the indicated concentration and the previous concentration ( $p < 0.05$ ,  $n = 3$ )

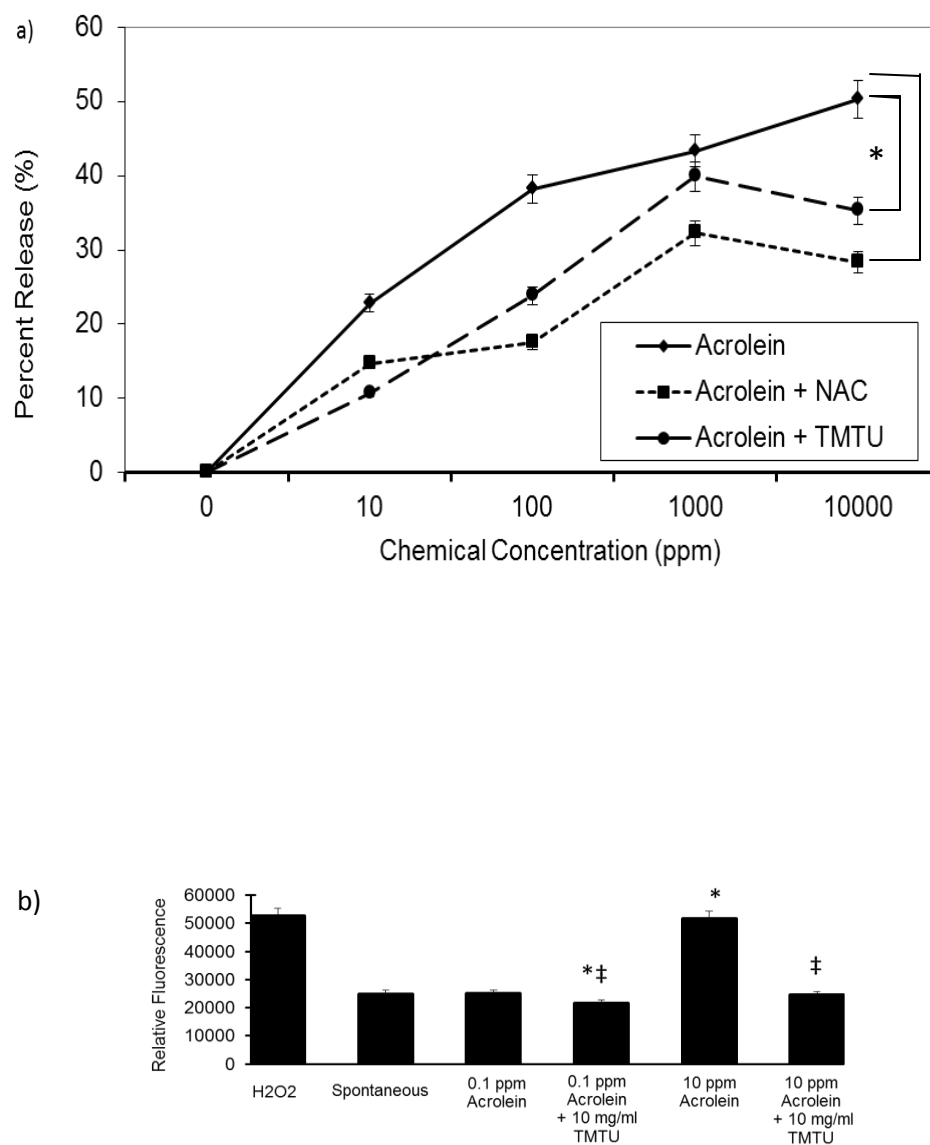


**Figure 16. a.** Acrolein induced degranulation in RBL-2H3 cells treated with  $H^3$  labeled serotonin. Cells were treated with anti-oxidants TMTU and NAC. **b.** Acrolein induced ROS generation in RBL-2H3 cells measured by DCFH-DA fluorescence compared to cells treated with antioxidant TMTU. Treatment with anti-oxidants significantly reduce both degranulation and ROS generation associated with acrolein exposure.

\* indicates statistical differences from spontaneous fluorescence ( $p < 0.05$ ,  $n = 3$ )

‡ indicates statistical difference from cells without anti-oxidant ( $p < 0.05$ ,  $n = 3$ )

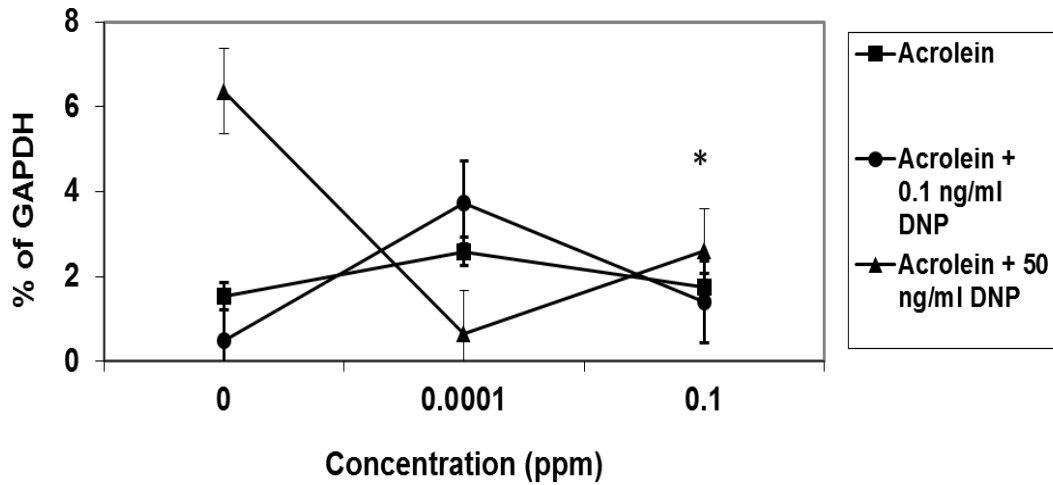
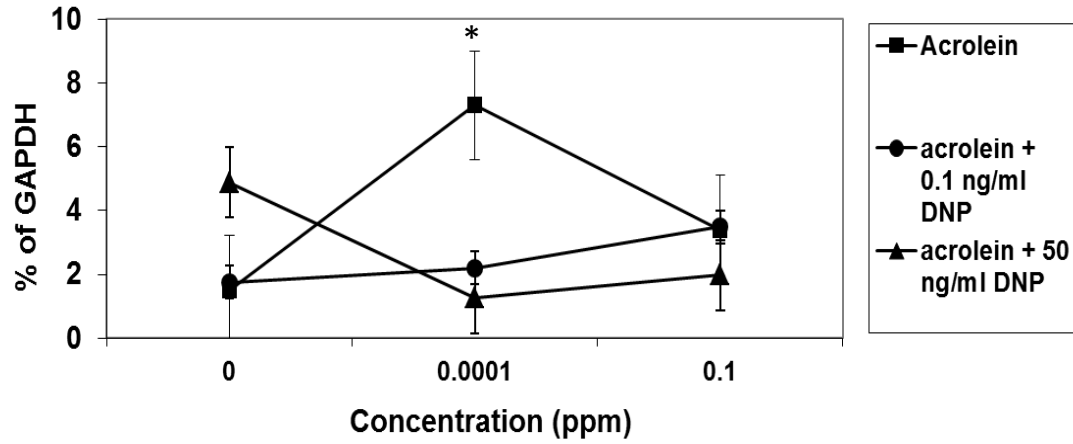


**Figure 17.** a) TNF- $\alpha$  (a) and IL-4 (b) mRNA expression as measured by RNase protection assay. RBL-2H3 cells were treated for 30 minutes with acrolein with or without anti-DNP-IgE/DNP. Densitometry was utilized to quantify the resultant blots. Acrolein alone induced expression of cytokines at 0.0001 ppm. Acrolein reduced cytokine mRNA produced by IgE crosslinking. \*indicates statistical difference from previous concentration within the same treatment ( $p < 0.05$ ,  $n = 3$ ). ‡indicates statistical difference between treatments at marked concentration ( $p < 0.05$ ,  $n = 3$ ).

	IL-1a	IL-1b	IL-2	IL-4	IL-6	IL-10	IFN $\gamma$	TNFa	GM-CSF
acrolein									
10,000 ppm	61	160	49	10	903	460	128	241	41
+ DNP 0.1	98	366	118	18	1594	853	231	415	85
+ DNP 50	136	509	170	22	2167	1184	292	558	107

**Figure 18.** Cytokine production in RBL-2H3 cells exposed to acrolein. Cell supernatant was utilized in the Bioplex multiplexbead array.  
\*results are expressed as pg/ml culture supernatant

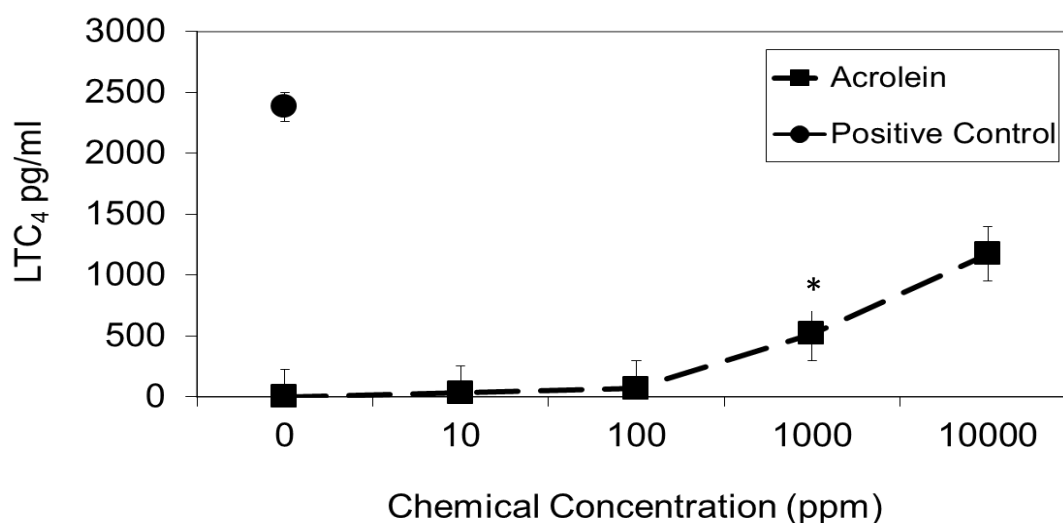


**Figure 19.** Leukotriene C<sub>4</sub> release from RBL-2H3 cells. Cells were treated with increasing doses of acrolein. The treated cells were then examined for LTC<sub>4</sub> expression was measured by absorbance ( $\lambda = 520$  nm). Leukotriene release was only observed at high concentrations of acrolein exposure. n=3, p<0.05

\* Indicates statistical significance from the prior concentration of acrolein treatment

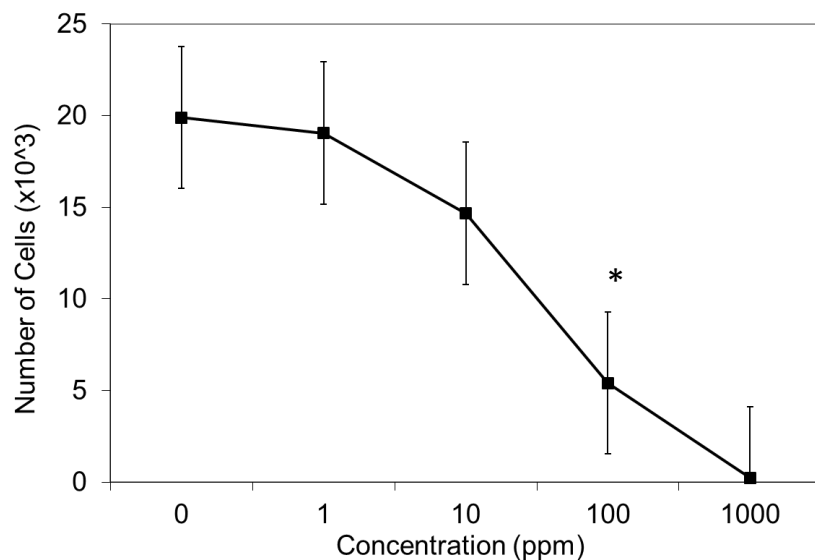


**Figure 20.** MTT assay. Assessed cell mitochondrial viability in RBL-2H3 cells treated with increasing concentrations of acrolein. Mitochondrial viability drops at 100 ppm. \*Indicates statistical difference from previous lower concentration ( $p < 0.05$ ,  $n = 3$ )

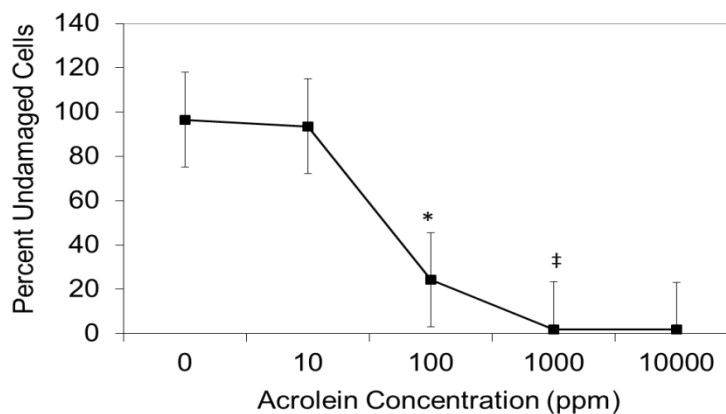
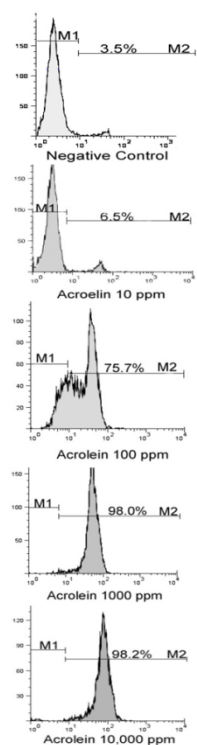


**Figure 21.** Propidium Iodide staining of RBL-2H3 cells exposed to acrolein. Flow cytometry of RBL-2H3 cells exposed to increasing doses of acrolein and stained with propidium iodide to examine cell toxicity. A dramatic drop in cell viability occurs at 100 ppm acrolein exposure. \*indicates statistical difference from negative control ( $p < 0.05$ ,  $n = 3$ ) †indicates statistical difference from previous concentration ( $p < 0.05$ ,  $n = 3$ )

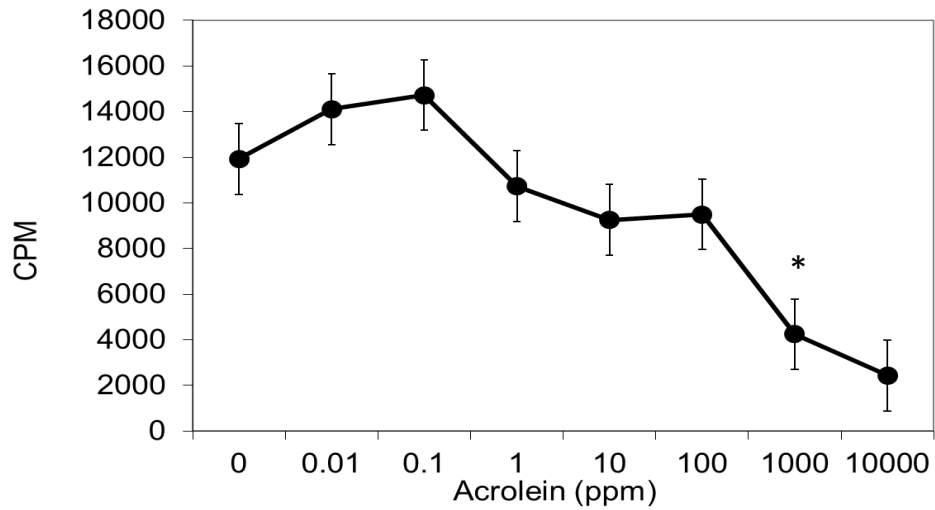


**Figure 22.** JAM Assay. RBL-2H3 Cells were pulsed with  $H^3$ -thymidine and treated with increasing doses of acrolein or PBS control. Cell growth rates were measured via incorporation of  $H^3$ . A statistically significant drop in cell replication is shown at 1000 ppm acrolein exposure.  
\* Indicates statistical difference between indicated concentration and negative control ( $p < 0.05$ ,  $n = 3$ )

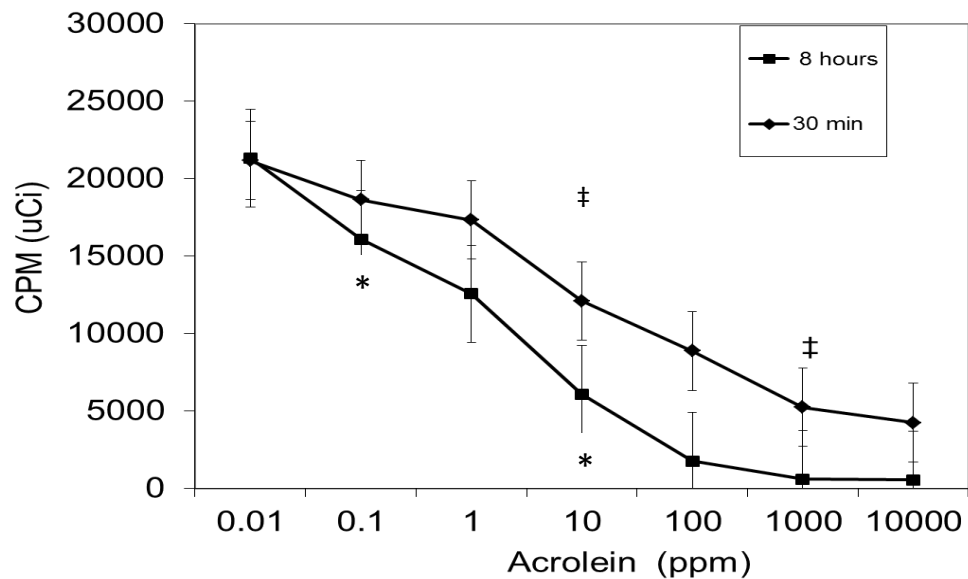


**Figure 23.** JAM Assay with A549 cells. Human lung epithelial A549 cells were pulsed with  $H^3$ -thymidine and treated with increasing doses of acrolein or PBS control. Cell growth rates were measured via incorporation of  $H^3$ . A549 cells began to show toxicity to acrolein exposure at 10 ppm for 30 min exposure and 0.1 ppm for an 8 hour exposure.  
‡ Indicates statistical difference between indicated concentration and previous concentration 30 min ( $p < 0.05$ ,  $n = 3$ )  
\* Indicates statistical difference between indicated concentration and previous concentration 8 hour ( $p < 0.05$ ,  $n = 3$ )



## CHAPTER 4. Effects of Sulfur Dioxide Exposure in an Animal Model of Asthma

### Introduction

It has been established that sulfates are a primary component of particulate air pollution [48] [52]. Sulfur dioxide is created through the burning of sulfur or of burning materials that contain sulfur:  $S_8 + 8 O_2 \rightarrow 8 SO_2$  [57]. Fossil fuels such as coal and petroleum often have abundant sulfur compounds. Therefore, their combustion generates sulfur dioxide.  $SO_2$  oxidation forms sulfuric acid, which can lead to acid rain. The production of calcium silicate cement can form sulfur dioxide as well when is a by-product of combustion in the manufacture of calcium silicate cement when  $CaSO_4$  is heated with coke and sand [57]. In the +4 oxidation state, sulfur oxides are reducing agents and thus do not pose a significant health risk, however most combustion products are in the reduced form such as  $SO_3^{-2}$ . Sulfur oxides in the +4 state can be further oxidized by halogens [126]. Sulfur dioxide is also the oxidizing agent in the Claus process, a key procedure utilized by oil refineries. During the Claus process, sulfur dioxide is reduced by hydrogen sulfide to give elemental sulfur [126]. As previously discussed,  $SO_2$  is highly soluble and dissolves readily in water to form ions of sulfite and sulfuric acid ( $SO_2 + H_2O \rightleftharpoons HSO_3^- + H^+$ ) ( $2 SO_2 + 2 H_2O + O_2 \rightarrow 2 H_2SO_4$ ).  $SO_2$  behaves chemically similar to ozone due the valence structure of electrons. Sulfur and oxygen both contain six valence electrons, leading to similar shape and reactivity. Sulfite can form in the environment as a result of reactions between aqueous bases and sulfur dioxide ( $H_2SO_4 + Na_2S_2O_5 \rightarrow 2 SO_2 + Na_2SO_4 + H_2O$ ). This reaction can take place in reverse, breaking down sodium metabisulfite through the addition of an aqueous acid

[126]. Additionally, when an aqueous base is exposed to sulfur dioxide, the reaction produces physiologically available sulfite salts. Diesel exhaust is also a major source of sulfate containing particles and, therefore, roadways associated with increased urbanization can contribute to increased levels of sulfates [53] [51] [51]. With increased urbanization, comes the increased risk of respiratory inflammation as shown in numerous epidemiologic studies [12;127].

The mechanistic link between fine and ultrafine particles and the development of airway hypersensitivity remains incomplete. We have shown that both acrolein and sulfite can induce ROS production in mast cells, leading to the release of inflammatory mediators. We also showed the ROS is released independent of extracellular  $\text{Ca}^{2+}$  and it can be reduced by treatment with antioxidants. The results for sulfite were consistent with a membrane based-NADPH oxidase generation of ROS upon cellular exposure. Translation of cellular findings to the complexities of living organisms is imperative in the understanding of disease states. In order to further investigate the pathophysiology of oxidative stress induction of airway hypersensitivity in response to oxidant pollutant insult, we extended our studies into a whole animal model.

This portion of our examination an animal model of allergic asthma was employed using a mucosal sensitization paradigm [128]. In this approach, it has been shown that it is a mast cell dependent process. Mice were exposed to a sub-optimal dose of OVA (0.1%) to examine the ability of  $\text{SO}_2$  to enhance allergic sensitization. Mice were exposed to a physiologically relevant level of  $\text{SO}_2$  (1 ppm) in exposure chambers in order to simulate the sulfite component of ambient particulate air pollution. In addition, the role of ROS production was investigated by administering apocynin, a known

inhibitor of NADPH oxidase, to a portion of the animals via drinking water. We hypothesized that exposure to SO<sub>2</sub> would enhance allergic sensitization and airway hyperresponsiveness in mice, and that this effect could be ameliorated with treatment by an inhibitor of NADPH oxidase.

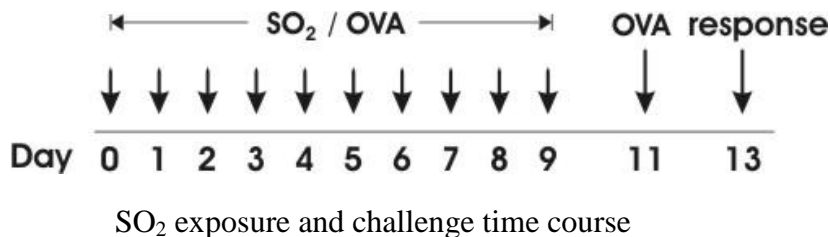
## **METHODS**

### *Animal protocol*

Animal experiments were performed according to the National Institute of Health Guide for Care and Use of Experimental Animals and approved by UTMB Animal Care and Use Committee. 6 week old C57BL/6 mice were obtained from Jackson Laboratory (Bar Harbor, Maine) and housed in pathogen-free environments. Ovalbumin (OVA Grade V; Sigma) and SO<sub>2</sub> exposures was performed on a minimum of three mice per experimental condition. Exposure chamber cages were labeled to identify the mice in each experimental group. Two or three large food pellets were replaced after each day of exposure and all water bottles were cleaned and refilled with purified water or water plus Apocynin (10 ml per L). Mice were sensitized by daily inhalational exposures to OVA (0.1%) in sterile saline for 20 min. over 10 days at the end of each day of SO<sub>2</sub> exposure. Two days after mucosal sensitization, mice were challenged with 1% OVA by nebulization daily for 20 minutes per day over the course of 3 days. 48 hours later challenged mice were tested for lung function, lung histology, oxidative stress, cytokine production, and OA-specific T-cell proliferation and serum IgE and IgG1 levels.

### *SO<sub>2</sub> Exposure*

SO<sub>2</sub> exposures were performed for groups of mice in 0.85 m<sup>3</sup> whole body stainless steel exposure chambers. The flow rates through each chamber were maintained at 0.425 m<sup>3</sup>/min or 30 chamber changes per hour. Mice were exposed sulfur dioxide for a period of 6 hours/day for 10 days at 1 ppm SO<sub>2</sub>. Air controls are included with each experiment. Air is HEPA-filtered prior to entry into the chambers and sulfur dioxide gas is introduced into the exposure chamber via an air stream mixing chamber. During the exposure, chamber air is sampled every 30 minutes and analyzed on a Shimadzu GC17A gas chromatograph equipped with a flame photoionization detector (Shimadzu Corp, Columbia, MD) or by rosaniline hydrochloride spectrophotometry [129]. The gas chromatograph is calibrated each day with a sulfur dioxide gas standard (Aeriform, Pasadena, Texas) prior to the day's sampling.



### *Plethysmography*

Airway hyperreactivity (AHR) was measured in unanesthetized mice as previously described [130]. Briefly, mice were placed within small volume (~600 ml) Plexiglas chambers, which allowed for free movement. Mouse breathing patterns (Buxco, Inc., Sharon, CT, U.S.A.), were continuously monitored as a function of chamber pressure. Methacholine (MCh) dissolved in phosphate-buffered saline (pH=7.4) was administered in increasing doses (0 – 50 mg/ml) as an aerosol (to the mice within the

chambers, by using a DeVilbiss ultrasonic nebulizer, connected to an aerosol driver and pump apparatus. Then administration of MCh concentration over 2 min., followed by a 3 min. observation and continued data collection period. The enhanced pause (Penh) variable was calculated [131]. The measured response was taken as the highest Penh value achieved during the administration and observation periods.

#### *Tissue harvesting and processing*

At the completion of lung function experiments, animals were sacrificed using an overdose of ketamine (60-70 mg/kg) plus xylazine (5-10 mg/kg) followed by opening the chest cavity. Blood for testing IgE levels was removed by needle aspiration from the heart. Blood was allowed to clot, and the serum collected by centrifugation at 1200 g for 10 minutes, and frozen at -20°C. The thoracic lymph nodes were isolated from the paratracheal and parabronchial regions. For standard histology, lungs were inflated with 10% formalin, removed and fixed in 10% formalin, embedded in paraffin. Three to four µm sections were stained with hematoxylin and eosin or toluidine blue by standard techniques (Vel-Lab, Houston, Tx).

#### *Bronchoalveolar lavage (BAL)*

Tracheas were opened by incision of the cricothyroid membrane and cannulated with a plastic cannula. The lungs were lavaged five times with 0.8 ml ice-cold sterile PBS. Supernatant from the first 0.8 ml was aliquoted and frozen at -20°C until analysis for cytokines and chemokines. The remaining cellular fractions were combined, counted on a hemocytometer, and cytocentrifuge preparations made. Slides are stained Wright-

Giemsa (Dif-Quick) and counted into major groupings: mononuclear cells, eosinophils, neutrophils, and macrophages by standard morphology. A minimum of 200 cells were counted per preparation and the absolute count of each cell type calculated.

#### *T-cell stimulation*

T-cell proliferation and cytokine production was assessed in draining lymph node T-cells. The thoracic lymph nodes were isolated from the paratracheal and parabronchial regions, transferred to cold PBS and gently homogenized on a 70 mm Falcon<sup>TM</sup> cell strainer (BD Pharmingen) in order to obtain a single cell suspension. Cell suspensions were washed, resuspended in culture medium (RPMI 1640 containing 10% FCS, 1% glutamine, 50 mg/ml penicillin-streptomycin and 50 mM b-mercapto-ethanol) and total cell number counted. Cells were cultured in triplicate in 96-well round-bottom plates for 5 days with OVA (10 mg/ml) at 37°C in 5% CO<sub>2</sub>. Each *in vitro* stimulation was performed in triplicate. Supernatants were harvested, and kept at -20°C. <sup>3</sup>H-thymidine (1 µCi/well) was added for the last 18 hours of culture, plates harvested onto glass fiber filters and counted in an automated scintillation counter.

#### *Heme-oxygenase-1 and glutathione*

Freshly harvested lungs were washed with PBS, blotted dry, weighed, and homogenized in 20 ml/gram of 10% metaphosphoric acid. Supernatants were collected after 5 minutes at room temperature and stored at -80°C. Glutathione plays a critical role in cellular defense against oxidative stress in tissues and cells. Within cells, glutathione exists in reduced (GSH) and oxidized (GSSG) states. In healthy cells and tissue, more

than 90% of the total glutathione pool is in the reduced form (GSH) while less than 10% exists in the disulfide form (GSSG). The high GSH concentration is because the enzyme that transitions it from its oxidized state (GSSG), glutathione reductase, is constitutively active and inducible upon oxidative stress. Total and oxidized glutathione were assessed using the enzyme recycling method according to manufacturer's instructions (Cayman Chemical Company, Ann Arbor MI).

For heme-oxygenase-1 (HO-1) measurements, lungs were homogenized in PBS with 1% NP40. Supernatants were collected and stored at -80°C. Samples were assessed for mouse HO-1 by EIA according to manufacturer's instructions (Takara Bio, Otsu, Japan).

#### *Bioplex array assay*

Cytokine analysis was performed according to manufacturers' instructions (BioRad). Multiplex assays using antibody-bound polystyrene microspheres (Luminex xMAP technology) with (capture) antibody that were mixed with samples. After washing, a secondary FITC-conjugated (detection) antibody was then bound to the captured antigen and the samples passed through a detector (flow cytometer), where fluorescence intensity for each bead type was deconvoluted and quantitated. The published assay performances include a detection limit of <10 pg/ml with a dynamic range of 0.2 - 32,000 pg. [132].

#### *Airway smooth muscle reactivity.*

Airway smooth muscle reactivity was measured as previously described. Briefly, mouse trachea (4-6 cartilaginous rings and associated airway smooth muscle) was

dissected from freshly sacrificed mice, a wire holder attached through the lumen of the ring, placed in a 37°C bath (Radnoti, Inc.) with oxygenated (95% O<sub>2</sub>/5% CO<sub>2</sub>) Krebs-Henseleit buffer (in mM: NaCl 118, CaCl<sub>2</sub> 2.8, MgSO<sub>4</sub> 1.2, KH<sub>2</sub>PO<sub>4</sub> 1.2, NaHCO<sub>3</sub> 25, dextrose 11.1), and connected to signal transducers that convert tension to digital data. Trachea were exposed to both KCl and increasing doses of MCh (10<sup>-12</sup> to 10<sup>-6</sup> M) for 5 min [133]. Atropine was then applied to inhibit MCh tension.

*Measurement of OVA-specific antibody in serum.*

OVA-specific serum IgE was quantified using a two-step sandwich ELISA. Purified anti-mouse IgE monoclonal antibody (mAb) (PharMingen, 02111D, clone R35-72) was used as a capture antibody and coated onto 96-well plates. After addition of serum samples, OVA was added (10 mg/ml) and detected with horseradish peroxidase (HRP)-conjugated anti-OVA IgG (Biotrend, Germany; 1:20,000). OPD development was quantified and IgE levels calculated by reference to mouse IgE standard curves (PharMingen, 03121D). OD was determined on an automated ELISA plate reader (Molecular Device Corp., Sunnyvale, CA).

Serum levels of OVA-specific IgG1 were measured by ELISA. 96-well plates (Immunlon2; Dynatech, Chantilly, VA) were coated with OVA (5 mg/ml). After addition of serum samples, an alkaline phosphatase-labeled rat anti-mouse IgG1 (02003E; BD PharMingen) and developed according to manufacturer's instructions.



### *Statistical Analysis*

Individual group means were compared with parametric (T-test) or non-parametric (Mann-Whitney U) tests if data was not normally distributed with values of  $P < 0.05$  considered significant. A Friedman repeated measures ANOVA on Ranks was performed on plethysmography and tracheal ring contractility assays to establish normality followed by acquisition of a significant “F” statistic ( $P < 0.05$ ) by repeated measures ANOVA. Post-hoc discrete data analyses between groups and within MCh concentrations was performed using Student-Newman Kuels test or Holm-Sidak post-hoc pairwise comparison.

## **Results**

### *Airway Hyperresponsiveness*

Whole animal plethysmography was performed on sensitized and challenged mice. In sensitized animals, MCh initiated rapid and vigorous responses, resulting in shallow rapid breathing patterns, thus indicating AHR and constricted airways similar to asthma. 24 hours after OVA challenge, mice that had undergone OVA sensitization showed a slight increase in AHR at the highest dose of MCh (50 mg/ml) (Figure 24a). This modest response was expected due to the suboptimal sensitization paradigm. Mice treated with SO<sub>2</sub> also showed a modest but significant increase in the level of response to MCh challenge. However, in OVA-sensitized mice exposed to SO<sub>2</sub> demonstrated a significant increase in AHR over OVA alone, indicating that SO<sub>2</sub> substantially enhances the AHR associated with allergic airway sensitization. Further, mice sensitized to OVA in the presence of SO<sub>2</sub> and concomitantly treated with apocynin, a known inhibitor of

NADPH oxidase, displayed a marked decrease in response to MCh (Figure 24b). These findings support the original hypotheses that SO<sub>2</sub> enhances allergen sensitization and AHR, and that the mechanism may be via activation of NADPH oxidase. 48 hours after OVA challenge, the SO<sub>2</sub> effect seen at 24 hours is attenuated and non-significant (Figure 25a and b).

Interestingly, mice that received apocynin alone in the absence of OVA sensitization nor SO<sub>2</sub> exposure showed a significant rise in response to MCh, and OVA plus apocynin showed a synergistic effect on increasing AHR (Figure 26a). This effect of apocynin persisted at 48 hours for OVA sensitized mice, but not for non-sensitized mice (Figures 26b). Thus, apocynin did not appear to improve the AHR in Ova sensitized mice, but rather caused it to worsen. These data suggest that blocking NADPH oxidase actually may induce hyperresponsiveness and may suggest a need for NADPH oxidase-mediated signaling in order to maintain airway tone in healthy and allergen-sensitized animals. However, animals undergoing a mild oxidative stress, such as 1 ppm SO<sub>2</sub>, appear to benefit from NADPH oxidase blockade.

To further investigate the mechanisms of AHR, an isolated tracheal ring contractility assay was performed. Tracheal ring contractility is an alternative method to assessing airway hyperresponsiveness that directly measures tracheal airway smooth muscle contractile force [134]. In these experiments, trachea were harvested 48 hours after challenge. OVA sensitized and challenged mice had a significant rise in airway MCh response compared to negative controls (Figure 27a). SO<sub>2</sub> exposure alone had only a slight insignificant increase on contractility. Surprisingly, mice receiving both SO<sub>2</sub> and OVA, displayed a significant reduction in smooth muscle contraction and apocynin

treatment resulted in an increase in contractility (Figure 27b). Similarly, while SO<sub>2</sub> exposure alone resulted in a slight insignificant rise in contractile force, apocynin treatment caused a significant increase in contractile force (Figure 27c). Finally, control animals exhibited a reduction in contraction with apocynin. OVA sensitized and challenged mice demonstrated an increase in contraction, similar to plethysmography (Figure 27c).

Together these data do not corroborate the plethysmography data other than in OVA sensitized mice. However, apocynin appears to counteract all SO<sub>2</sub> effects, again supporting the contention that SO<sub>2</sub> is likely acting through NADPH oxidase. However, in these experiments, SO<sub>2</sub> appeared to have a “protective” effect on smooth muscle contractile responses. Several potential explanations can be considered. For one, SO<sub>2</sub> may affect a number of inflammatory cell subsets, in particular, mast cells, as we have shown in Chapter 1. While the trachea typically contains ample numbers of mast cells, the experimental procedure of removing the trachea and immersing in a physiologic solution/bath may remove inflammatory mediators, and other mediators released from other cells may also be critical for contractile responses. Alternatively, the effects of SO<sub>2</sub> may differ in various lung compartments due to changes in inflammatory cell infiltrate and neurological receptors. Nonetheless, the results are intriguing and require further investigation to fully explain.

#### *Lung mast cells*

To determine if there was increased mast cell recruitment in mice exposed to SO<sub>2</sub> versus mice exposed only to air, mast cells were counted and averaged over mm length of airway. Airway length was directly measured *ex vivo* under dissection microscopy. The

air treated mice had an average of 3.7 cells per mm airway while mice exposed to 1 ppm SO<sub>2</sub> had an average of 4.3 mast cells per mm airway. The majority of mast cells were seen in the adventitia in both air treated mice and SO<sub>2</sub> exposed mice (Figure 28a).

Although there appears to be an increase in mast cell numbers in the airway and adventitia, there were no statistically significant differences in mast cell counts per location or per length of airway. Thus indicating no substantial increase in mast cell immigration or proliferation within the lungs of SO<sub>2</sub> exposed mice in response to the environmental insult or the subsequent OVA challenge (Figure 28b).

#### *Airway inflammation*

Bronchoalveolar lavage cell differentials were assessed to determine the inflammatory response to airway sensitization and the impact of SO<sub>2</sub> exposures. In mice exposed to SO<sub>2</sub> there was no increase in inflammatory cells compared with controls. As expected, there was a significant increase in the percentage of eosinophils in mice sensitized to OVA (Figure 29). OVA sensitized mice, that were also exposed to SO<sub>2</sub>, showed an insignificant increase from OVA sensitized mice. However, mice sensitized to OVA with SO<sub>2</sub>, that were also treated with apocynin, had a significant decrease in eosinophil percentage. Thus, apocynin appears to attenuate airway inflammation in mice exposed to SO<sub>2</sub> and allergen. Additionally, apocynin did not appear to alter the inflammatory response in control mice, OVA sensitized mice, nor SO<sub>2</sub> exposed mice.

### *Allergen-specific immune responses*

Specific antigens can induce T cell activation, resulting in cytokine production, cytokine receptor expression, and ultimately proliferation of activated T cells. One of the more common methods to assess T-cell activation is to assess T-cell proliferation upon in vitro stimulation of T cells with antigen [135]. In this study, OVA-specific T-cell responses from the draining lymph nodes of OVA-sensitized and SO<sub>2</sub> exposed mice were assessed. In these experiments, SO<sub>2</sub> exposed mice had an increase in T-cell proliferation (Figure 30). Both SO<sub>2</sub> alone and SO<sub>2</sub> with OVA challenge enhanced T cell proliferation. Taken together, this data indicated that SO<sub>2</sub> appears to enhance T-cell responsiveness in both a non-specific and antigen-specific fashion.

Oxidant pollutants are not typically associated with allergic sensitization. However, evidence has emerged that oxidant pollutants may enhance pre-existing allergic disease. The mechanism by which it occurs is unclear. We sought to determine if allergen-specific IgE responses were enhanced with SO<sub>2</sub>. IgE antibodies are primarily associated with allergic processes, and unlike humans, IgG<sub>1</sub> may also be enhanced in allergic immune responses in mice.

As anticipated OVA-specific IgE was significantly increased over controls in OVA challenged mice. Mice exposed to SO<sub>2</sub> and OVA, however, had significantly decreased levels of IgE. Apocynin, however, countered that effect and IgE rose even higher than OVA sensitized animals alone (Figure 31). In contrast, IgG<sub>1</sub> displayed a different pattern of response. While there was a rise in IgG<sub>1</sub> with OVA challenged animals (Figure 32), OVA sensitized mice had a slight increase with SO<sub>2</sub> that was significantly reduced by apocynin. Conversely, control mice exposed to SO<sub>2</sub> alone, or

apocynin alone had substantial increases of IgG<sub>1</sub>. Thus, SO<sub>2</sub> appears to reduce OVA-specific IgE production while enhancing IgG<sub>1</sub> production, both of which are countered by apocynin.

### *Cytokine Expression*

Cytokines are small molecule signaling proteins, known as immunomodulating agents, which are expressed by cells to issue instructions to surrounding cells and tissue. Essentially, all nucleated cells, including epithelial cells and tissue specific macrophages exposed to the environment produce cytokines such as IL-1, IL-6, and TNF- $\alpha$  [136]. Once bound to their specific receptor, cytokines initiate an intracellular signaling cascade that results in cellular function change and DNA transcription of more cytokines and surface receptors. Alternatively, cytokines can down-regulate further cell signaling molecules and receptors. Cytokines can be divided into two immunological categories: type 1, which serve to initiate cellular immune responses (IL-6, IFN- $\gamma$ , TGF- $\beta$ , IL-12, RANTES, MIP-1 $\alpha$ , TNF- $\alpha$ ), and type 2 (IL-4, IL-10, IL-13, IL-5.), which favor antibody responses. Inflammatory cytokines can be induced by oxidant stress (TNF- $\alpha$ , IL-6, IL-1 $\beta$ ) [137;138]. Since cytokine signaling can lead to subsequent release of still other cytokines and result in increased oxidant stress, they play an important role in chronic inflammation. Cytokines were measured via multiplex luminescent beads in both whole lung homogenate and bronchoalveolar lavage.

In bronchoalveolar lavage, type 2 inflammatory cytokines displayed similar patterns of expression. IL-13 was not increased for OVA alone, however SO<sub>2</sub> exposed mice, in combination with OVA displayed a significant rise (Figure 33a). IL-13 dropped

significantly with administration of apocynin. As expected, IL-4 was significantly higher in OVA sensitized animals (Figure 33b). When combined with SO<sub>2</sub>, IL-4 levels were high, and those animals receiving apocynin showed a dramatic drop. IL-5 displayed the same results as IL-4, with OVA sensitized mice higher than controls, SO<sub>2</sub> exposed mice significantly increased over OVA alone, and apocynin treatment significantly reducing that effect (Figure 33c). Proinflammatory type 1 cytokines IL-1a, IL-6, IL-12, and IFN- $\gamma$  exhibited increased expression only in the mice both OVA challenged and exposed to SO<sub>2</sub> (Figures 33 d-g). Additionally, the SO<sub>2</sub> exposed mice that were treated with apocynin showed a significant decrease in the aforementioned cytokines. RANTES was increased in OVA exposed mice and treatment with apocynin significantly reduced the level expressed (Figure 33h). There was not a significant rise with SO<sub>2</sub> exposure for RANTES. Cytokines not reported (IL-10, TGF- $\beta$ , MIP-1 $\alpha$ , IL-1 $\beta$ ) were too low to measure with accuracy.

### *Glutathione*

Glutathione is the major intracellular low-molecular-weight thiol composed of glutamic acid, cysteine, and glycine. An increased GSSG-to-GSH ratio is considered to be an indicator of oxidative stress.

The present study exhibited oxidative stress in mice challenged with OVA, in the presence or absence of SO<sub>2</sub> (Figure 34). Mice subsequently treated with apocynin had a significant reduction of total glutathione. While there was not a significant difference between SO<sub>2</sub> treated mice and those exposed to only air, mice receiving apocynin in the absence of any exogenous stimulus displayed a significant rise in oxidative stress.

### *Heme Oxygenase-1*

Heme oxygenase-1 (HO-1) provides cytoprotection against oxidative stress. While its main function is heme degradation, HO-1 can also play a role in inflammation and apoptosis. HO-1 acts to help reduce tissue damage in response to other proinflammatory stimuli. The upregulation of HO-1 takes place in response to phenomenon such as hypoxia and exposure to bacterial lipopolysaccharide, and reactive oxygen/nitrogen species [139]. The presence in tissue of HO-1 can then be utilized as a measure of oxidative stress brought on by exogenous sources.

In the present study, apocynin conferred a reduction of HO-1 effect in the mice exposed to SO<sub>2</sub> (Figure 35). Alternatively, the mice receiving clean air had higher levels of HO-1 in those receiving apocynin. The SO<sub>2</sub> treated animals had higher levels of HO-1 in general, than the control mice. Further, OVA challenged mice experienced a significant rise in HO-1 over the saline controls.

### *Nitric Oxides*

NO<sub>x</sub> has been recognized for its ability to regulate diverse activities. Nitrite (NO<sub>2</sub><sup>-</sup>) and nitrate (NO<sub>3</sub><sup>-</sup>), have been used in the indirect measurement of NO<sub>x</sub> since they are more stable. [140;141]. NO is produced through the reaction of L-Arginine, NADPH, and O<sub>2</sub> to NO and Citrulline [142-144]. Inducible (iNOS) production can be observed in several cell types of importance to the immune system including chondrocytes, epithelial cells, hepatocytes, and glial cells [145]. In general, iNOS is



induced by endotoxin and inflammatory cytokines. NO-mediated activation is implicated with a range of biological functions including inflammation [146].

These experiments showed a significant increase in total NO<sub>x</sub> with OVA challenge. Interestingly, apocynin treated mice had a significant rise in NO<sub>x</sub> as well, although not as high as OVA (Figure 36a). SO<sub>2</sub> exposed mice also showed signs of stress with an increase in NO<sub>x</sub>, but when combined with OVA, SO<sub>2</sub> paradoxically displayed a reduced effect, decreasing NO<sub>x</sub> expression (Figure 36b).

## **Discussion**

In these experiments it has been demonstrated that SO<sub>2</sub> exposure enhances the allergic inflammatory process. The effect, however, is time dependent and seems to be ameliorated by 48 hours after OVA challenge. While inflammatory cell location was not influenced, lymphocytes were increased, inflammatory cytokines expression was enhanced, and T cell stimulation was raised. Mice that were exposed to SO<sub>2</sub> and OVA challenged also displayed increased airway hypersensitivity as seen in whole body plethysmography and tracheal ring contractility. These data indicate that SO<sub>2</sub> exposure does in fact worsen the state of allergic airway pathology beyond that seen in OVA sensitized animals. IgE did not seem to play a role in the SO<sub>2</sub> mediated effects however. While IgE expression rose, as expected, in the OVA sensitized mice, those exposed to SO<sub>2</sub> actually displayed a decrease in IgE. Alternatively, IgG<sub>1</sub> increased as a result of SO<sub>2</sub> exposure. IgG binds directly to foreign antigen and stimulates longer-term inflammatory processes while IgE is bound to mast cells and must be cross-linked for immediate

activation. It therefore is possible that the SO<sub>2</sub> molecules are part of a longer-term inflammatory pathway.

Cytokine expression seems to play an important role in the inflammatory response to exogenous air pollutants. Clearly, SO<sub>2</sub> exposure enhanced the allergic sensitization with respect to cytokine expression. The data in this study suggests that hyperresponsiveness, while independent of mast cells, may be controlled by enhanced expression of IL-13 and IL-4. A mixed inflammatory model has been revealed with an additional increase in pro-inflammatory cytokines IL-6 and IFN- $\gamma$ . Similar to the reduced hyperresponsiveness seen with the addition of apocynin treatment, the expression of cytokines dropped from the SO<sub>2</sub> exposed mice that also received OVA challenge. This effect may indicate that SO<sub>2</sub> enhancement of airway hyperresponsiveness and inflammation may be due to oxidative stress generated through the NADPH oxidase pathway.

Additionally, it was shown that oxidative stress is enhanced by the presence of the SO<sub>2</sub>. HO-1, GSSH, and NO<sub>x</sub> were all enhanced by OVA challenge alone as well as by SO<sub>2</sub> exposure. These experiments thus indicate that an imbalance in the oxidative state plays an important role in both allergic inflammation and the inflammatory process enhanced through exposure to environmental pollutant. This balance can be restored through treatment with an antioxidant.

The NADPH oxidase inhibitor apocynin was able to ameliorate the effects of SO<sub>2</sub>. In mice treated with apocynin, airway hypersensitivity was reduced and inflammatory cytokines expression dropped. IgG<sub>1</sub> expression was lower in apocynin treated animals,

while IgE expression went back up. Oxidative stress was also reduced in apocynin treated mice. In contrast to the SO<sub>2</sub> exposed mice, animals receiving only OVA challenge or saline exhibited the opposite reaction to apocynin. Apocynin actually increased all measures of oxidative stress and hypersensitivity in OVA alone treated mice. Taken together these data indicate that the oxidative balance is delicate and can be overwhelmed in situations where cells are unable to produce enough antioxidant naturally to compensate for shifts in pro-oxidant pathways. Negative feedback may play a role, whereas providing cells an anti-oxidant shuts off the natural anti-oxidant pathways, rendering the cells vulnerable to further oxidative stress. Alternatively, it is possible that allergic sensitization through a classic IgE dependent pathway causes shifts in oxidative balance through a differing pathway than the exogenous environmental insult. In this manner, decreasing the activity of NADPH oxidase restored the balance in SO<sub>2</sub> exposed mice, while it enhanced the inflammatory processes of the OVA challenged animals.

The mechanisms of oxidative balance and the signaling pathways utilized by cells in response to allergic inflammatory pathways, both in classic IgE dependent sensitization and IgE independent exogenous insult require further study.

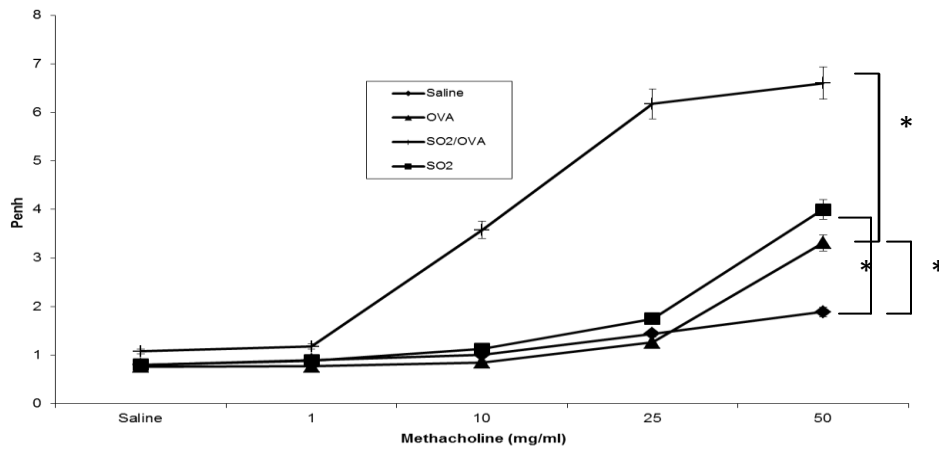


**Figure 24a.** Whole animal plethysmography 24 hours post-OVA challenge expressed as raw Penh. OVA sensitized mice had a significant rise in Penh over negative controls.  $\text{SO}_2$  exposed mice also displayed a significant rise in Penh over controls. Those exposed to  $\text{SO}_2$  and OVA showed a significantly higher Penh compared to OVA alone.

\* Indicates statistical significance ( $P < 0.05$ ) between treatments,  $n = 7$

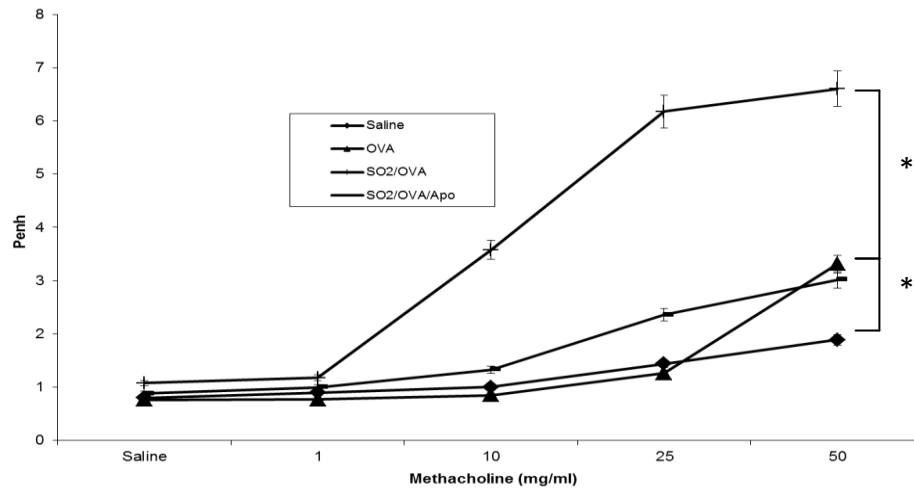


**Figure 24b.** Whole animal plethysmography 24 hours post-OVA challenge expressed as raw Penh.  $\text{SO}_2$  alone and OVA alone displayed a similar rise in Penh over negative controls. Mice sensitized to  $\text{SO}_2$  and OVA had a significant rise in Penh over OVA alone.

\* Indicates statistical significance between treatments,  $p < 0.05$ ,  $n = 7$

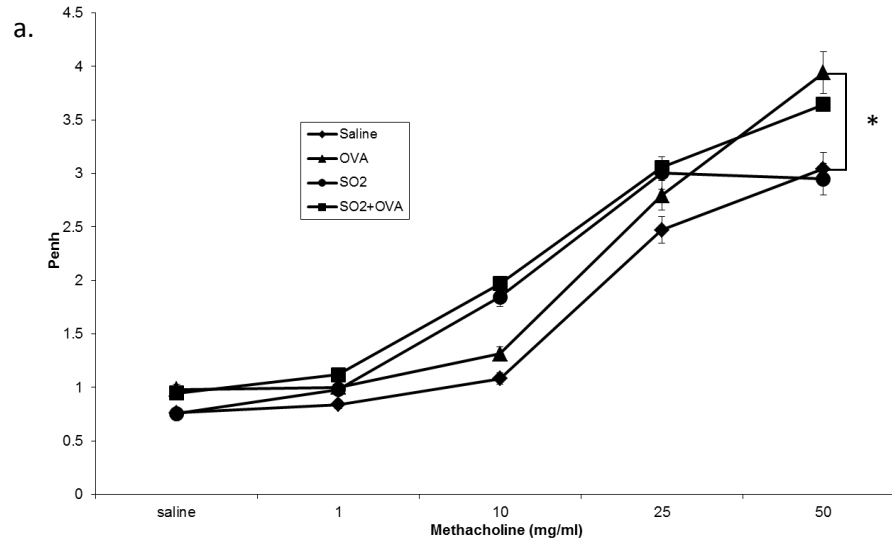


**Figure 25a.** Whole animal plethysmography 48 hours post-ova challenge expressed as raw Penh for mice exposed to SO<sub>2</sub> plus OVA challenge. OVA sensitized mice had a significant rise in Penh over saline. There is no significant difference for SO<sub>2</sub> exposed mice when compared to OVA

\* Indicates statistical significance between treatments,  $p \leq 0.05$ ,  $n=7$ .

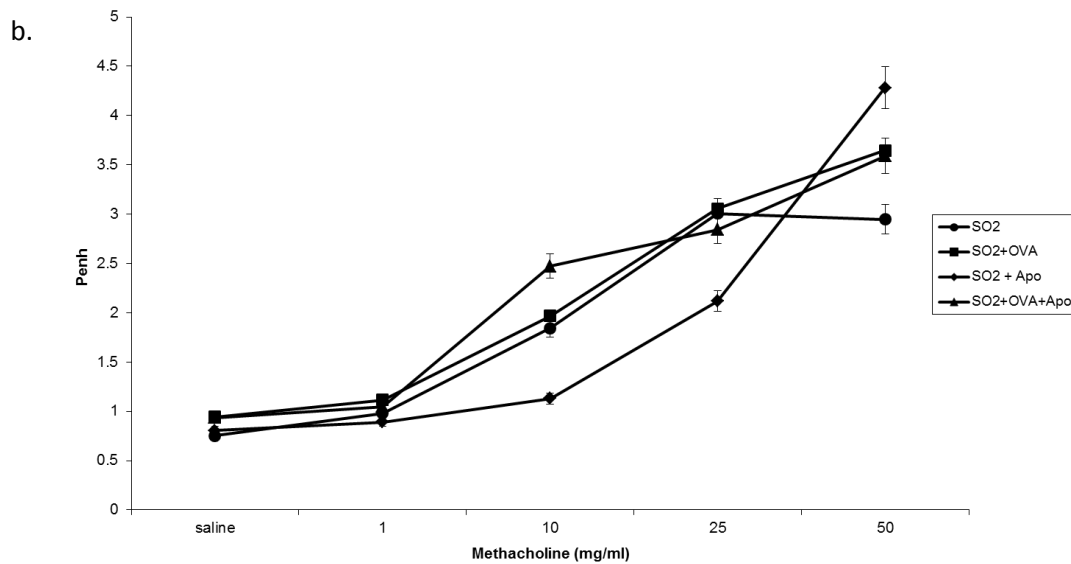


**Figure 25b.** Whole animal plethysmography 48 hours post-OVA challenge expressed as raw Penh for mice exposed to SO<sub>2</sub> plus OVA challenge. There was no significant differences between SO<sub>2</sub> + OVA and those treated with OVA + apocynin, n=7.

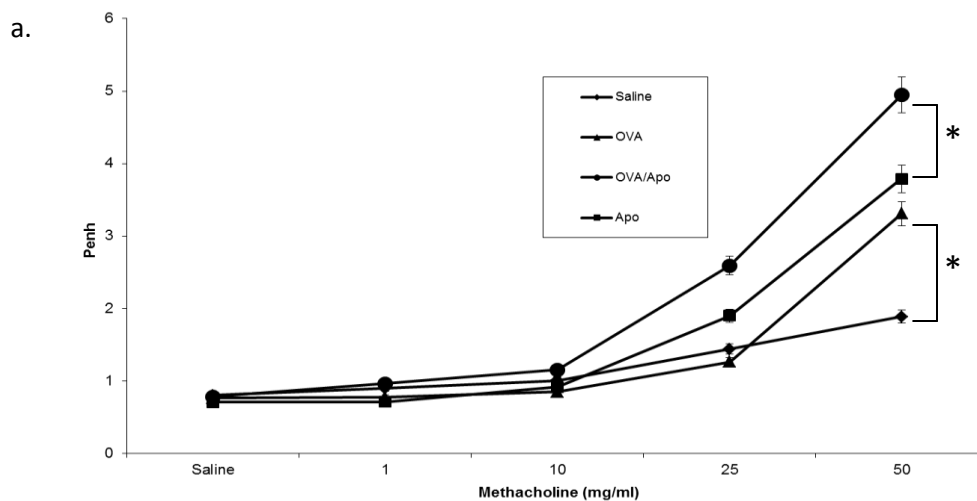


**Figure 26a.** Whole animal plethysmography 24 hours post-ova challenge expressed as raw Penh for mice exposed to air only. OVA sensitized mice had a significant rise in respiratory pauses. Mice receiving treatment with apocynin also displayed significantly higher Penh values, with those that were OVA sensitized showing the most significant change.

\*Indicates statistical significance between treatments, p<0.05, n=7

b.

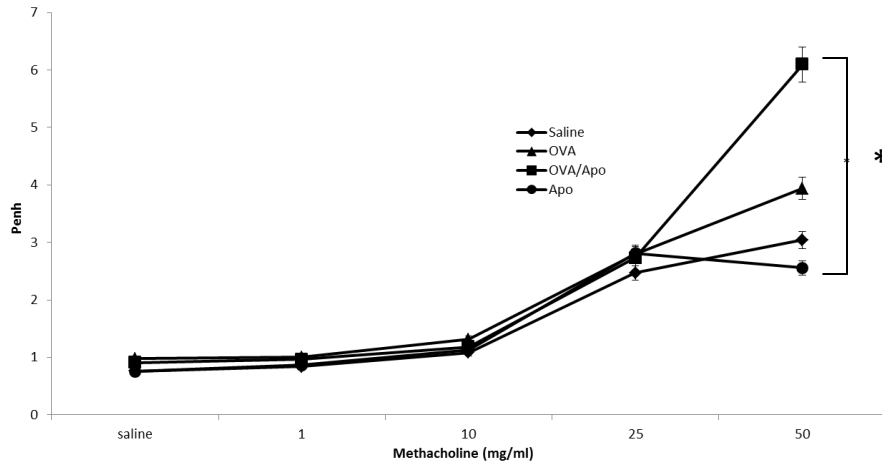


**Figure 26b.** Whole animal plethysmography 48 hours post-ova challenge expressed as raw Penh for mice exposed to SO<sub>2</sub> plus OVA challenge. Those receiving OVA + apocynin had a significantly higher Penh to the saline alone animals, but not those receiving OVA challenge. \* Indicates statistical significance between treatments  $p \leq 0.05$ ,  $n=7$

a.

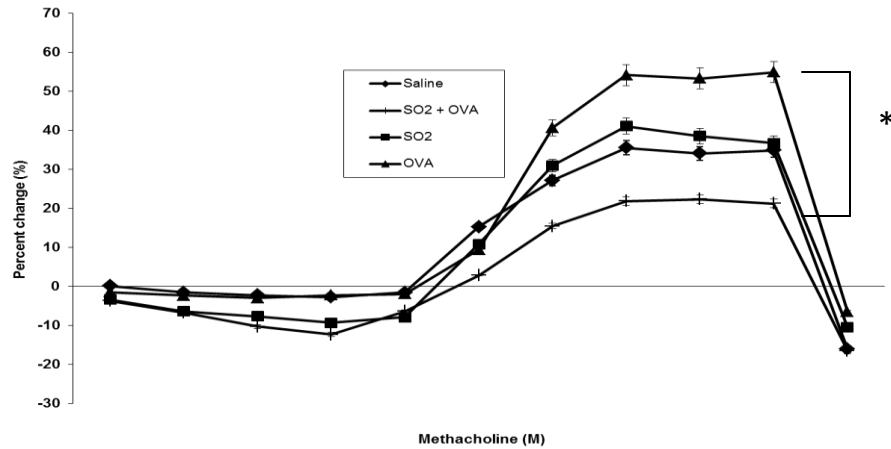


**Figure 27a.** Trachea Ring Assay measuring smooth muscle contractility in sacrificed mice post OVA challenge exposed to SO<sub>2</sub> plus OVA. Points represent percent change from negative control at increasing doses of methacholine beginning with saline and ending with atropine (methacholine doses range  $1 \times 10^{-8}$  mM to 0.1 mM). SO<sub>2</sub> exposed and OVA sensitized mice did not show a significant change from negative control. SO<sub>2</sub> + OVA sensitized mice displayed significantly lower contractility than those exposed to OVA alone. \* Indicates statistical significant differences between treatments,  $p \leq 0.05$ ,  $n=7$

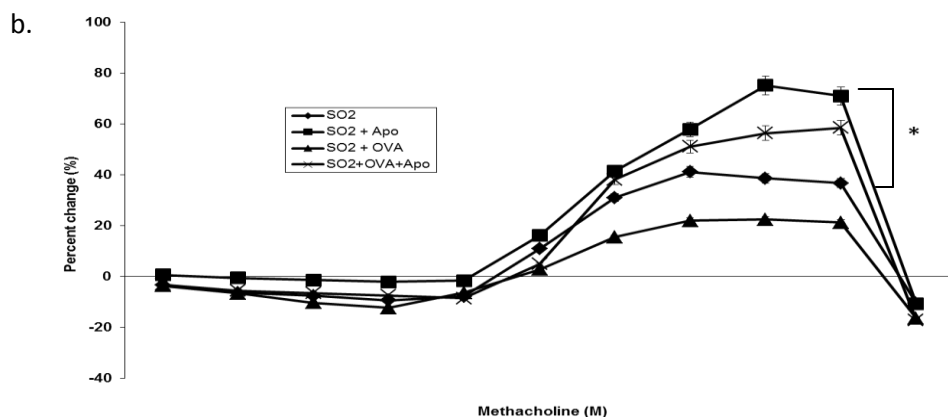


**Figure 27b** Trachea Ring Assay measuring smooth muscle contractility in mice post OVA challenge in mice exposed to SO<sub>2</sub> plus OVA. Points represent percent change from negative control at increasing doses of methacholine beginning with saline and ending with atropine (methacholine doses range  $1 \times 10^{-8}$  mM to 0.1 mM). SO<sub>2</sub> exposed and OVA sensitized mice did not show a significant change from SO<sub>2</sub> alone. Those mice treated with apocynin, however, had significant increases in contractility than those exposed to SO<sub>2</sub> alone.

\* Indicates statistical significant differences between treatments  $p \leq 0.05$ ,  $n=7$ .

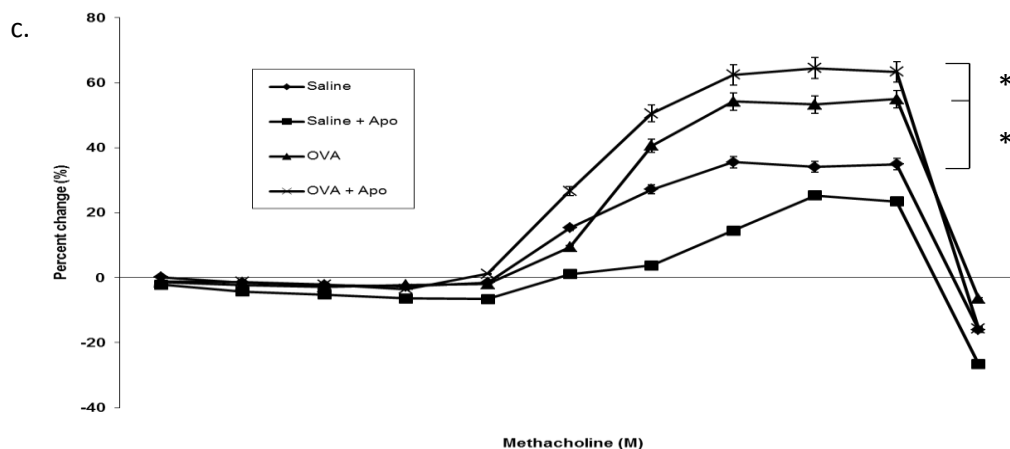


**Figure 27c** Trachea Ring Assay measuring smooth muscle contractility in sacrificed mice post ova challenge exposed to air only. Points represent percent change from negative control at increasing doses of methacholine beginning with saline and ending with atropine (methacholine doses range  $1 \times 10^{-8}$  mM to 0.1 mM). Contractility was significantly higher for OVA sensitized mice but there was a significant rise in those sensitized mice treated with apocynin.

\* Indicates statistical significant change between treatments  $p \leq 0.05$ ,  $n=7$



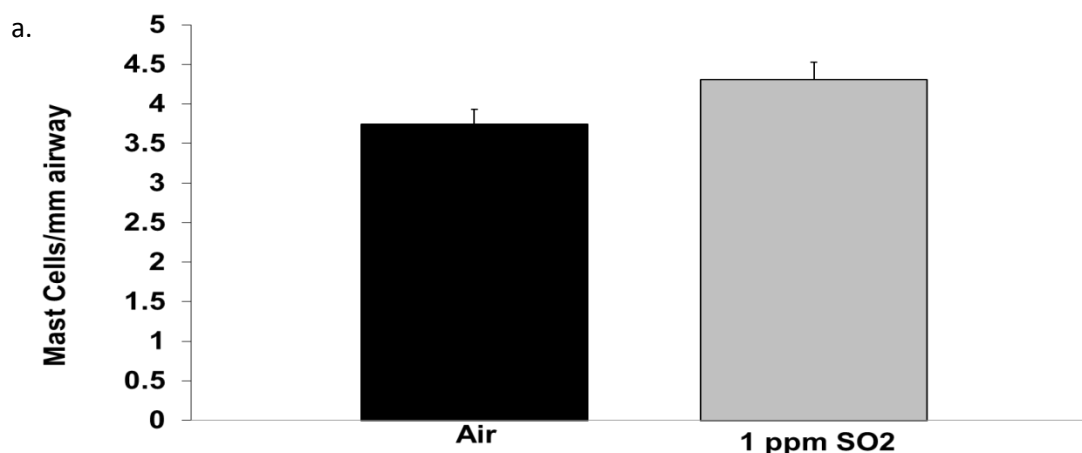


**Figure 28a.** Average number of mast cells per millimeter of murine airway. Mice were sacrificed 48 hours after OVA challenge. Trachea were surgically removed and measured for length. Mast cells were isolated from BAL, stained and enumerated. There was no difference observed between SO<sub>2</sub> exposed mice and those exposed only to air, n=7.

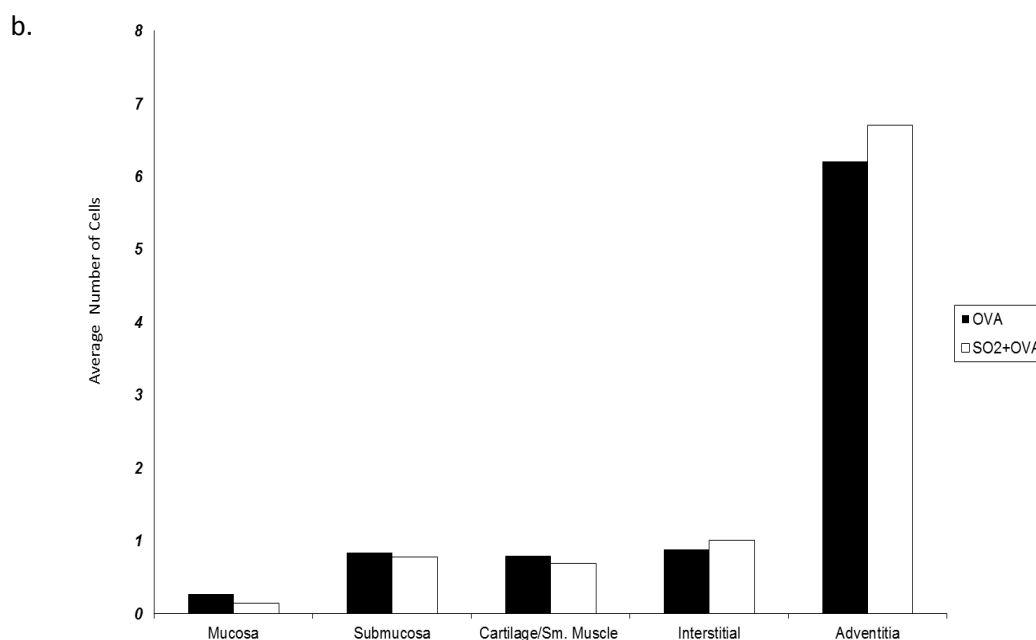


**Figure 28b.** Average number of mast cells per histologic location in murine airway. 48 post OVA challenge, mice were sacrificed and whole lungs were fixed with formalin and paraffin embedded for histologic slicing and staining. Prepared histology slides were enumerated for cell differentials under light microscopy. There were significantly more cells in the adventitia of the airway but no difference between SO<sub>2</sub> exposed mice and those exposed only to air, n=7.

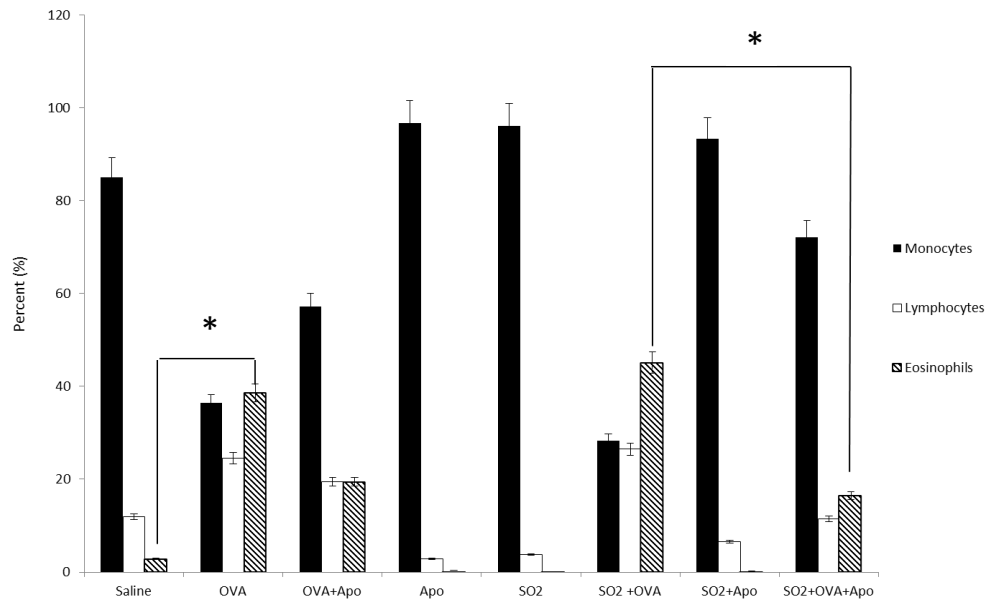


**Figure 29.** Differential cell counts in treated mice. BAL was obtained from mice 48 hours after OVA challenge. Results show an expected increase in eosinophils in mice receiving OVA sensitization. SO<sub>2</sub> plus OVA was similar to OVA alone and apocynin treated mice had a significant reduction in eosinophils. All treatments were compared statistically. Only significant differences are indicated.

\*indicates statistically significant differences between indicated treatments,  $p < 0.05$ ,  $n = 7$ .

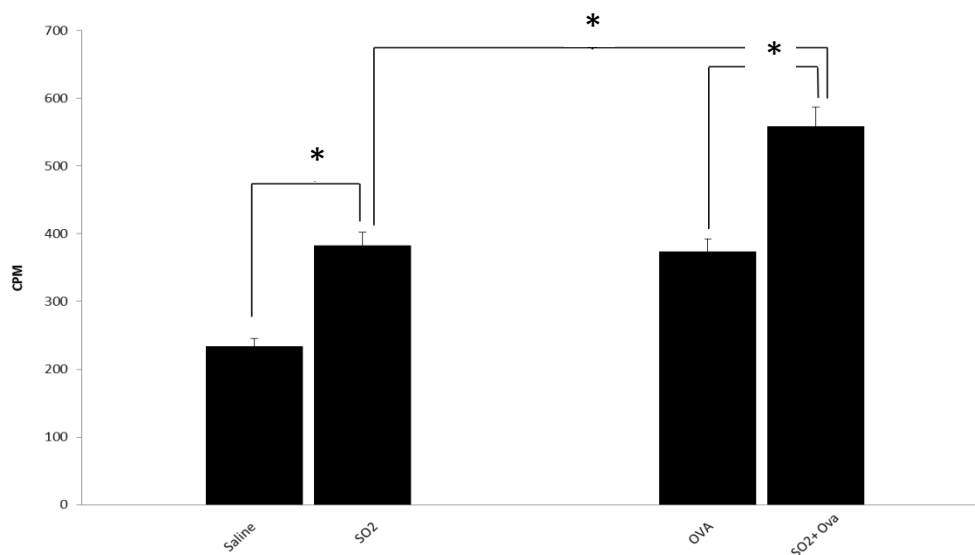


**Figure 30.** T cell proliferation in treated mice. T cells were isolated from draining lymph nodes 48 hours post mouse ova challenge and sacrifice. Isolated cells were incubated with H<sup>3</sup> thymidine. Incorporated thymidine was read for  $\beta$  counts and expressed as CPM. Mice exposed to SO<sub>2</sub> had significantly higher T cell expansion than those exposed to air only in both OVA sensitized animals and unsensitized animals.

\* Indicates statistical significance  $p \leq 0.05$ ,  $n = 7$ .

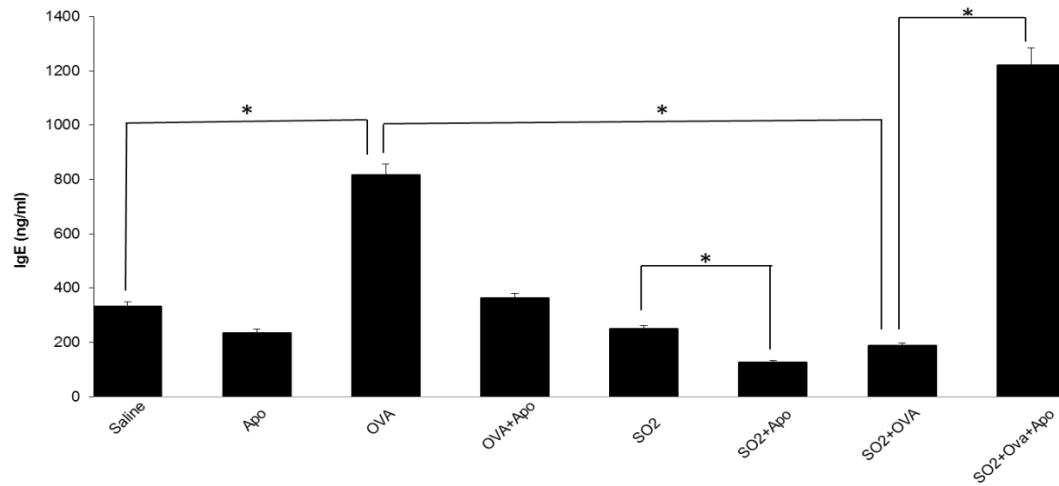


**Figure 31.** IgE Measured by ELISA. IgE in serum obtained from cardiac puncture 48 hours post OVA challenge. OVA sensitized mice showed a significant rise in IgE expression. Mice exposed to SO<sub>2</sub> and OVA sensitized had a significantly lower IgE expression that was reversed when treated with apocynin while apocynin reduced IgE expression in mice receiving SO<sub>2</sub> alone. \* Indicates statistical significance  $p \leq 0.05$ ,  $n=7$ .

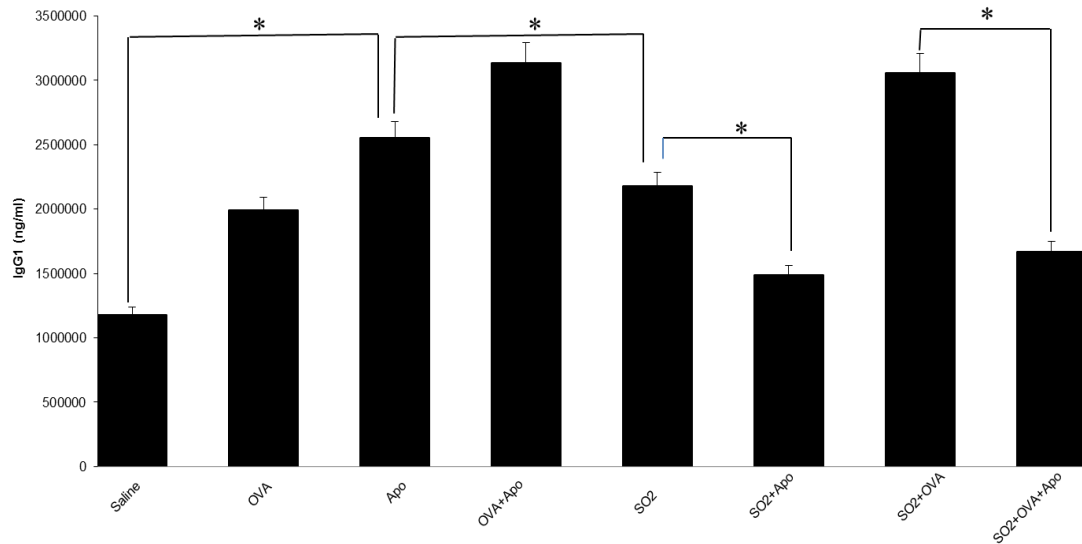


**Figure 32.** IgG1a Measured by ELISA. IgG1a in serum obtained through cardiac puncture of sacrificed mice 48 hours post OVA challenge  
 \*Indicates statistical significance  $p \leq 0.05$ ,  $n=7$   
 data without connecting bars are not statistically significant

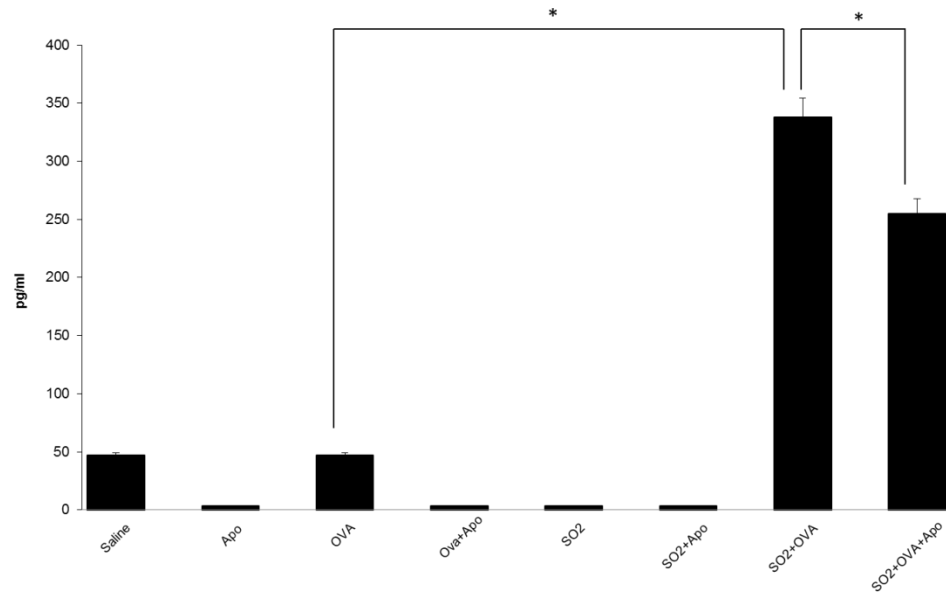


**Figure 33a.** IL-13 measured in BAL. 48 hours post ova challenge by multiplex bead array. SO<sub>2</sub> exposed mice that were sensitized to OVA showed a significant rise over OVA alone sensitized mice. Apocynin treatment significantly reduced expression of IL-13 in SO<sub>2</sub> exposed and OVA sensitized mice.

\* Indicates statistical significance between indicated treatments  $p \leq 0.05$ ,  $n=7$

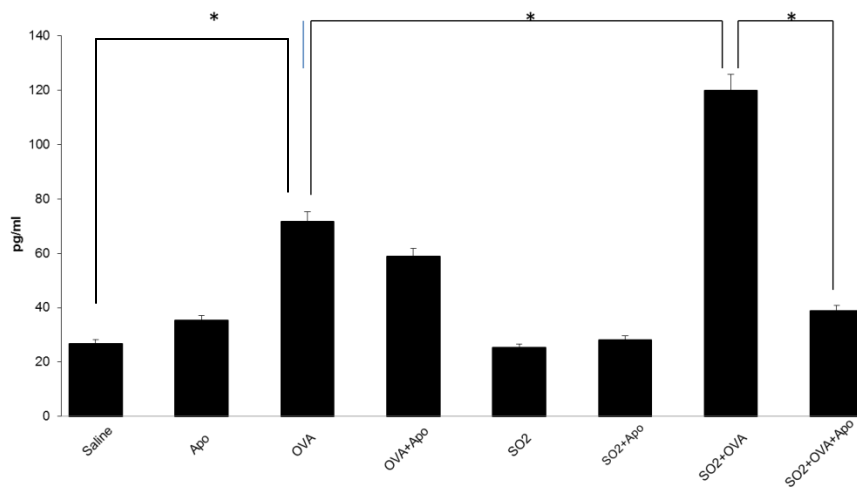


**Figure 33b.** IL-4 measured in BAL. 48 hours post ova challenge by multiplex bead array. OVA sensitized mice had a significant rise in IL-4 over negative controls. SO<sub>2</sub> exposed mice that were sensitized to OVA showed a significant rise over OVA sensitized mice. Apocynin treatment significantly reduced expression of IL-4 in SO<sub>2</sub> exposed and OVA sensitized mice.

\* Indicates statistical significance between indicated treatments  $p \leq 0.05$ ,  $n=7$

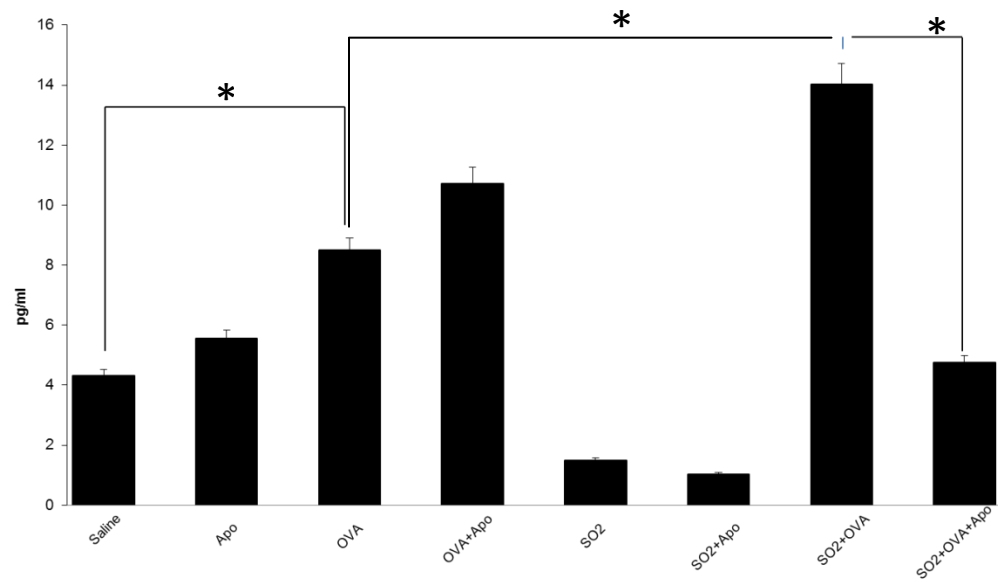


**Figure 33c.** IL-5 measured in BAL. 48 hours post ova challenge by multiplex bead array. OVA sensitized mice had a significant rise in IL-5 over negative controls. SO<sub>2</sub> exposed mice that were sensitized to OVA showed a significant rise over OVA alone sensitized mice. Apocynin treatment significantly reduced expression of IL-5 in SO<sub>2</sub> exposed and OVA sensitized mice,  $p < 0.05$ ,  $n = 7$ .

\* Indicates statistical significance between indicated treatments  $p \leq 0.05$

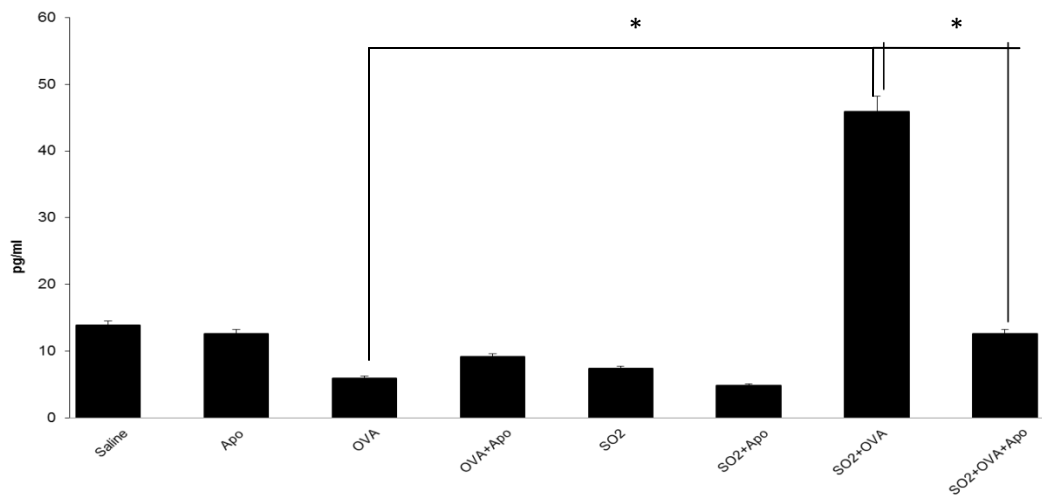


**Figure 33d.** IFN- $\gamma$  measured in BAL. 48 hours post ova challenge by multiplex bead array. SO<sub>2</sub> exposed mice that were sensitized to OVA showed a significant rise over OVA alone sensitized mice. Apocynin treatment significantly reduced expression of IFN- $\gamma$  in SO<sub>2</sub> exposed and OVA sensitized mice.

\* Indicates statistical significance between indicated treatments  $p \leq 0.05$ ,  $n = 7$ .

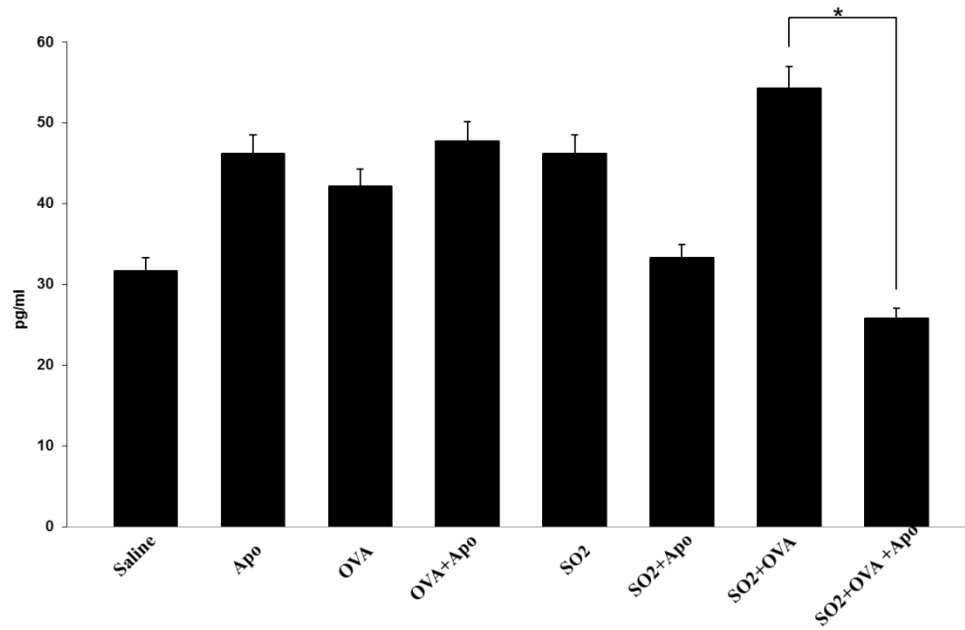


**Figure 33e.** IL-1a measured in BAL. 48 hours post ova challenge by multiplex bead array. A significant reduction in IL-1a expression was demonstrated in mice exposed to SO<sub>2</sub> and treated with apocynin.

\* Indicates statistical significance  $p \leq 0.05$ ,  $n=7$ .

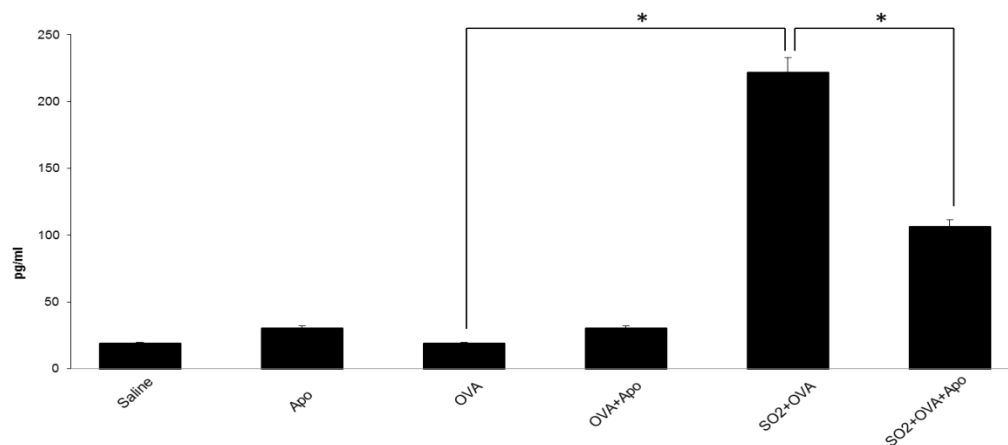


**Figure 33f.** IL-6 measured in BAL. 48 hours post ova challenge by multiplex bead array. SO<sub>2</sub> exposed mice that were sensitized to OVA showed a significant rise over OVA alone exposed mice. Apocynin treatment significantly reduced expression of IL-6 in OVA sensitized mice.

\* Indicates statistical significance between indicated treatments  $p \leq 0.05$ ,  $n=7$ .

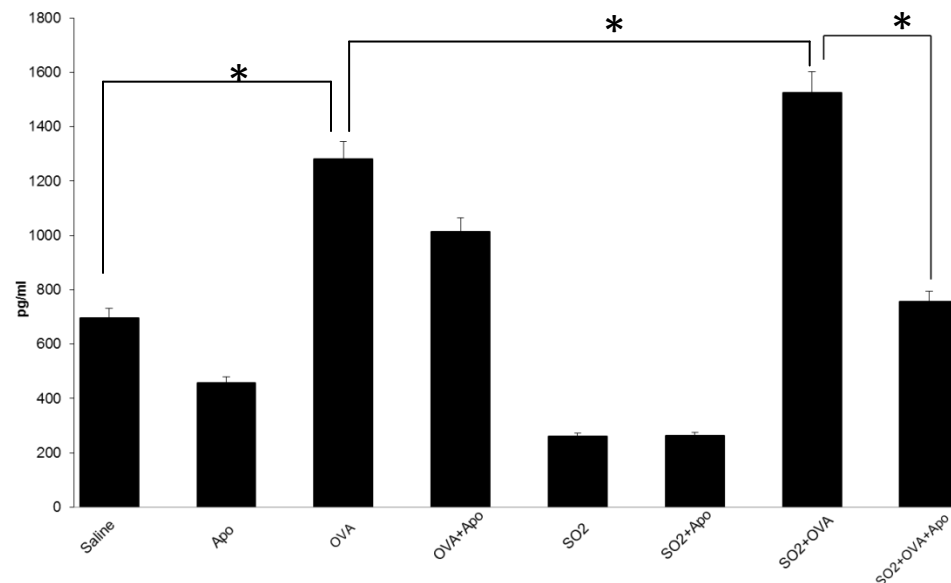


**Figure 33g.** IL-12 measured in BAL. 48 hours post ova challenge by multiplex bead array. OVA sensitizes mice had a significant rise in IL-5 over negative controls. SO<sub>2</sub> exposed mice that were sensitized to OVA showed a significant rise over OVA alone sensitized mice. Apocynin treatment significantly reduced expression of IL-12 in SO<sub>2</sub> exposed and OVA sensitized mice.

\* Indicates statistical significance between treatments  $p \leq 0.05$ ,  $n=7$ .

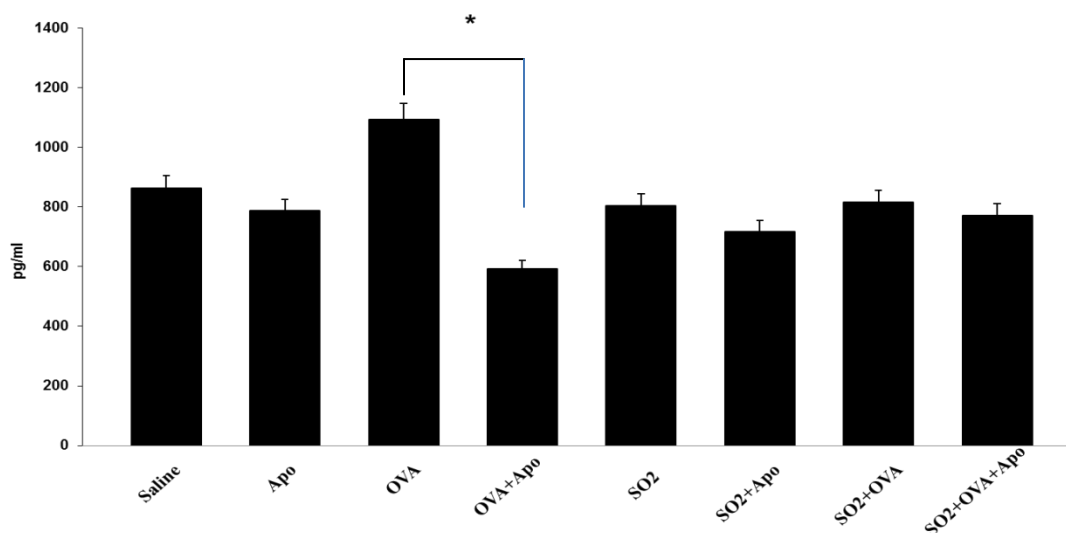


**Figure 33h.** RANTES measured in BAL. 48 hours post ova challenge by multiplex bead array. Apocynin treatment significantly reduced expression of RANTES in OVA sensitized mice.

\* Indicates statistical significance  $p \leq 0.05$ ,  $n=7$ .

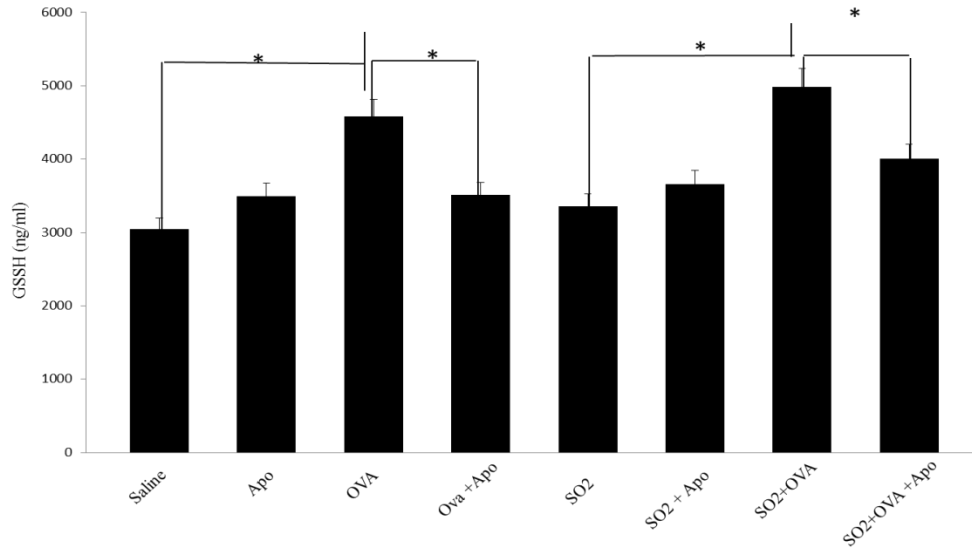


**Figure 34.** Glutathione 48 hours post ova challenge. There was no difference seen between SO<sub>2</sub> exposed mice and those receiving only air. GSSH levels were, however, affected by the treatment with apocynin. OVA sensitized animals displayed a significant Total Glutathione measured by ELISA in whole lung homogenate in total GSSH expression and those receiving apocynin reduced GSSH back to background levels.

\* Indicates statistical significance  $p \leq 0.05$ ,  $n=7$ .

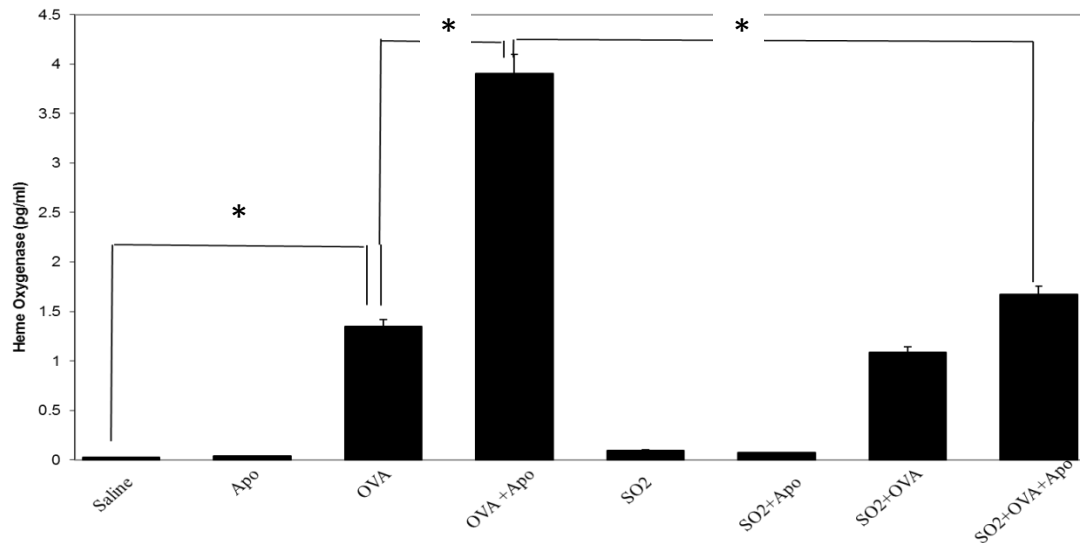


**Figure 35.** Heme Oxygenase-1 measured in whole lung homogenate by ELISA. HO-1 examined 48 hours post ova challenge. In both SO<sub>2</sub> and air exposed mice, OVA sensitization caused a significant increase in HO-1 expression. There was no apparent affect of SO<sub>2</sub>. Apocynin caused a significant rise in HO-1 in OVA sensitized mice. That effect was ameliorated, however, in the mice exposed to SO<sub>2</sub>.

\* indicates statistical significance  $p \leq 0.05$ ,  $n=7$ .



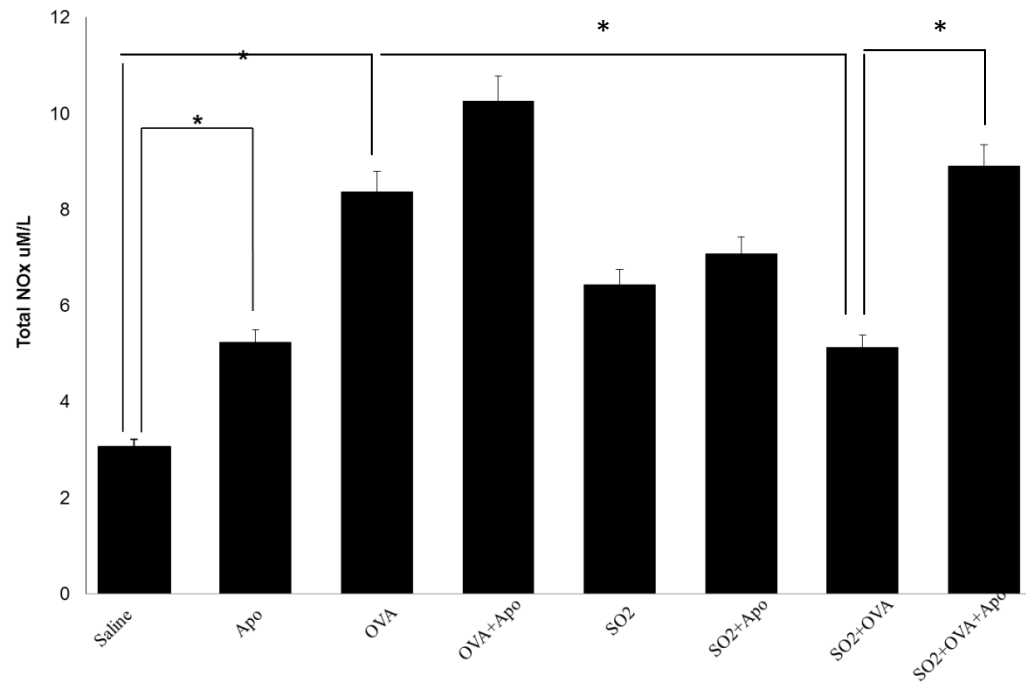


**Figure 36.** Total nitric oxides measured in BAL by ELISA. Total NOx 48 hours post ova challenge. OVA sensitized mice displayed a significant rise in total NOx. Mice that were treated with apocynin had a significant increase in NOx over the negative control animals as well as those treated with SO<sub>2</sub>.

\* Indicates statistical significance  $p \leq 0.05$ ,  $n=7$ .

## **CHAPTER 5. Amelioration of Airway hyperresponsiveness by Activation of Anti-Oxidant Responses**

### **Introduction**

Oxidant air pollutants activation of cellular NADPH oxidase may play a role in increased rates of asthma through the generation of intracellular reactive oxygen species (ROS) [84] [64]. Elevated levels of reactive oxygen species (ROS) induce cellular injury and promote airway inflammation and hyperresponsiveness (AHR) in animal models of asthma [62;122;123;147-151]. Cellular injury during ROS production can include damage to or downregulation of Nrf2 [67]. Nrf2 is a DNA binding element that leads to the transcription of anti-oxidant proteins. As ROS increases and anti-oxidant production becomes overwhelmed, or is downregulated, then cells become overwhelmed and oxidative damage to cellular membranes and DNA adduct formation can lead to chronic states of inflammation [68;114]. 2-cyano-3,12-dioxoooleana-1,9(11)-dien-28-oic acid-TFEA (CDDO) is a drug that upregulates anti-oxidant responses through the prostaglandin J/Nrf2/ARE pathway [152-156] [157]. We can utilize CDDO to examine the mechanistic pathway of asthma initiated by oxidative stress as shown in our previous investigations presented herewith. In this study it was hypothesized that allergic immune responses can be reduced by treatment with anti-oxidants that restore the oxidative balance by upregulating the Nrf2 pathway.

## Methods

### *Animal protocol*

Animal experiments were performed according to the National Institute of Health Guide for Care and Use of Experimental Animals and approved by University of Texas Medical Branch Animal Care and Use Committee. 6 week old C57BL/6 and Balb/cJ mice were obtained from Jackson Laboratory (Bar Harbor, Maine). Mice were sensitized intraperitoneally with 50 µg of Ovalbumin (OVA Grade V; Sigma-Aldrich, St Louis, MO) in 2 mg aluminum hydroxide and challenged 14 days later with nebulized 1% OVA for 3 to 6 days.

Mice were either administered CDDO-methyl ester (ME) (compound 402; Reata Pharmaceuticals Inc., Dallas, TX) in sesame seed oil by gavage or injected IP with CDDO-trifluoroethanolamine (TFEA) (compound 404; Reata) in PBS, 10% DMSO and 10% Cremaphor EL (Calbiochem/EMD Millipore, Darmstadt, Germany). At the completion of experiments, animals were sacrificed using an overdose of ketamine (70 mg/kg) and xylazine (10 mg/kg) followed by opening the chest cavity.

### *Airway smooth muscle contractility*

Mouse tracheal rings (4-6 cartilaginous rings and associated airway smooth muscle) were dissected from freshly sacrificed mice, a wire holder attached through the lumen of the ring, placed in a 37°C bath (Radnoti, Inc.) with oxygenated (95% O<sub>2</sub>/5% CO<sub>2</sub>) Krebs-Henseleit buffer (in mM: NaCl 118, CaCl<sub>2</sub> 2.8, MgSO<sub>4</sub> 1.2, KH<sub>2</sub>PO<sub>4</sub> 1.2, NaHCO<sub>3</sub> 25, dextrose 11.1), and connected via a 4-0 silk suture to tension transducers that was interfaced with an A/D board (100-Hz sampling rate), on a PC-

compatible computer running a digital data collection program (BioBench, National Instruments, Inc.). Rings were stretched to attain 500-600 mg passive tension, washed with fresh buffer over 30-60 min, and then exposed to increasing concentrations of KCl (20-60 mM), for intervals of 10-15 min./concentration. After reaching maximal tension at the highest KCl concentration, the rings were washed several times with fresh buffer over a 30 min. period. A dose-response relationship was then obtained with increasing concentrations of MCh ( $10^{-12}$  to  $10^{-6}$  M) applied for 5 min/concentration. Afterward, atropine was applied to inhibit cholinergic tone, and to establish that the prior tension increases observed were MCh dependent. At the end of the experiment, the rings were removed, blotted, and weighed.

### *Plethysmography*

Airway reactivity (AR) was measured in unanesthetized mice as previously described [130]. Mice were placed within small volume (~600 ml) Plexiglas chambers, which allowed for free movement (Buxco Research Systems, Wilmington, NC). Alterations in chamber pressure, as a function of breathing patterns was continuously monitored. MCh dissolved in normal saline (pH=7.4) was administered in increasing doses (0 – 50 mg/ml) using a DeVilbiss ultrasonic nebulizer, and aerosol pump. Each MCh concentration was administered over 2 min., followed by a 3 min. data collection period. The enhanced pause (Penh) was calculated as described [131]. Briefly, Penh was calculated by the formula  $(PEP/PIP) \times (T_e - T_r)/T_r$  where PEP=peak expiratory pressure (ml/sec), PIP=peak inspiratory pressure (ml/sec),  $T_e$ =expiratory time, and  $T_r$ =relaxation time(sec) or the time of the pressure decay to 36% of total box pressure during expiration.

The highest Penh value during the data collection period was recorded. Penh data was statistically analyzed using univariate repeated measures analysis of variance. Dose response curves to MCh were analyzed as repeated measures. Data was log transformed before analysis to equalize variances in all groups.

#### *Bronchoalveolar lavage*

Bronchoalveolar lavage (BAL) was collected by washing 1 cc of cold normal saline once. Lungs were then lavaged with a second ml of NS 3-4 times, the cellular fractions combined for cell counts and the initial 1 ml of lavage stored at -20°C for cytokine measurements. Lungs were inflated with and then immersed in 10% formalin in saline for histological analysis. Cells were counted on a hemocytometer, and cytocentrifuge preparations made. Slides were stained Wright-Giemsa (Dif-Quick) and enumerated into subsets: mononuclear cells, eosinophils, neutrophils, and macrophages/monocytes by standard morphology. At least 200 cells were counted per preparation and the absolute number of each cell type calculated.

#### *Redox assays*

BAL samples were assessed for total hydroperoxides, total anti-oxidant capacity, and pro-oxidant–antioxidant balance. Free radical exposure leads to oxidative transformation of lipids, proteins, amino acids, nucleic acids, etc. Hydroperoxides (ROOH) were measured through reduction of diethylparaphenylene-diamine according to manufacturer's instructions (Diacron International, Grosseto, Italy). Briefly, BAL samples were diluted in an acidic buffer (pH 4.8) in the presence of ferric or ferrous ions,

generating alkoxyl and peroxy radicals via the Fenton reaction. A chromogenic substrate, N,N,-diethylparaphenylene-diamine, was added, which oxidizes to form a cationic product, and absorbance analyzed at 546 nm on a FLUOstar OPTIMA plate reader (BMG Labtechnologies, Offenburg, Germany). Results were expressed as Carratelli units where 1 unit corresponds to 8 mg/ml H<sub>2</sub>O<sub>2</sub>.

Antioxidant capacity to hypochlorous acid (HClO) was determined according to the manufacturer's instructions (Diacron International (OXY-Adsorbent test). Briefly BAL samples were mixed with a solution containing HClO. N,N,-diethylparaphenylen-diamine was added and absorbance analyzed at 546 nm. The results were expressed as  $\mu$ moles HClO/mL.

The pro-oxidant-antioxidant balance (PAB) assay simultaneously measures both pro-oxidants and anti-oxidants using 3,3',5,5'-tetramethylbenzidine and its cation as a redox indicator participating in two simultaneous reactions. A standard curve was made using varying concentrations of hydrogen peroxide and uric acid, and the results expressed as HK units, which are the percentage of hydrogen peroxide on the standard curve.

#### *Measurement of OVA-specific antibody*

Blood for testing IgE levels was removed by needle aspiration from the heart, allowed to clot at 37°C. Serum was collected by centrifugation, and stored at -20°C until use. Serum levels of OVA-specific IgE were measured by ELISA as described in the previous chapter.

#### *OVA-specific T-cell proliferation*

T-cell proliferation was assessed in spleen cells. Cells were isolated from spleen by gently pressing between the frosted ends of 2 microscope slides. Cell suspensions were washed, resuspended in culture medium (RPMI 1640 containing 10% FBS, 1% glutamine, 50 mg/ml gentamicin and 50 mM  $\beta$ -mercapto-ethanol). After gradient density centrifugation with lympholyte M (Cedarlane, Burlington, NC) to isolate mononuclear cells, cells were cultured in triplicate in 96-well round-bottom plates for 5 days with varying concentrations of OVA at 37°C in 5% CO<sub>2</sub> in triplicate. <sup>3</sup>H-thymidine (1  $\mu$ Ci/well) was added for the last 18 hours of culture, plates harvested onto glass fiber filters and counted in an automated scintillation counter. Results are expressed as a stimulation index (cpm OVA/cpm medium).

#### *Glutathione and heme-oxygenase-1*

Freshly harvested lungs were washed with PBS, blotted dry, weighed, and homogenized in 20 ml/gram of 10% metaphosphoric acid. Supernatants were collected after 5 minutes at room temperature and stored at -80°C. Total and oxidized glutathione were assessed using the enzyme recycling method according to manufacturer's instructions (Cayman Chemical Company, Ann Arbor MI).

For heme-oxygenase-1 (HO-1) measurements, lungs were homogenized in PBS with 1% NP40. Supernatants were collected and stored at -80°C. Samples were assessed for mouse HO-1 by EIA according to manufacturer's instructions (Takara Bio, Otsu, Japan).

### *Statistical Analysis*

Individual group means were compared with parametric (T-test) or non-parametric (Mann-Whitney U) tests if data was not normally distributed with values of  $P < 0.05$  considered significant. A Friedman repeated measures ANOVA on Ranks was performed on plethysmography and tracheal ring tension measurements to establish normality followed by acquisition of a significant “F” statistic ( $P < 0.05$ ) by repeated measures ANOVA. Post-hoc discrete data analyses between groups and within MCh concentrations was performed using Student-Newman Kuels test or Holm-Sidak post-hoc pairwise comparison.

## **Results**

### *Airway hyperresponsiveness.*

Initial pilot experiments were performed using CDDO-ME. C56BL/6 mice were sensitized with OVA and 2 weeks later given 3 challenge doses of 1% OVA by nebulization. CDDO-ME was administered at 2 and 4 mg/kg one hour prior to each OVA challenge for a total of three total doses. Forty eight hours after the final challenge, mice were evaluated for airway hyperresponsiveness to MCh using whole body plethysmography (Figure 37a), which showed an increase in Penh in OVA challenged mice and improvement with CDDO-ME. Seventy two hours later, tracheal rings were harvested and tested for contractility, which demonstrated a dose-dependent reduction in tracheal ring contractile force in response to MCh (Figure 38).

In this series of experiments, significant toxicity was noted for the CDDO-ME compound in C57BL/6 mice. Subsequent experiments were conducted with CDDO-



TFEA and Balb/c mice, which ameliorated the toxicity issues. In addition, six daily 1% OVA challenges were given with CDDO-TFEA given 1-2 hours prior to OVA challenge to enhance the airway inflammatory response and hyperresponsiveness. Using this model, a substantial reduction of Penh in response to MCh was seen in mice treated with 6 mg/kg of CDDO-TFEA (Figure 37b). All subsequent experiments were performed in this manner.

#### *Lung inflammation and OVA-specific immune responses.*

Bronchoalveolar lavage samples were obtained from mice 48 hours after OVA challenge (Figure 39). The total inflammatory cell numbers and, in particular, eosinophils were reduced by 6 mg/kg CDDO to 58% of OVA control. However, pulmonary histology did not show a significant reduction in perivascular inflammation (data not shown). To investigate the impact on adaptive immune responses, OVA-specific IgE formation and T-cell proliferative responses were evaluated. Both OVA-specific IgE levels and T-cell proliferative responses to OVA were reduced substantially (Figure 40a and b).

#### *Oxidant stress*

To understand further the potential mechanism that CDDO modifies the airway responses to allergen challenge, we investigated the levels of oxidants and redox balance. The pro-oxidant-anti-oxidant balance assay was used to assess the overall balance of oxidants and anti-oxidants produced in the BAL fluid. OVA challenge alone skewed the oxidant/anti-oxidant balance towards an anti-oxidants response, indicating that significant endogenous antioxidant responses occur with an acute allergen challenge. The addition of

CDDO further enhanced this response at the 6 mg/kg dose (Figure 41a). To further elucidate this phenomenon, direct measurements of oxidants and anti-oxidants were performed. The production of oxidants (dROM assay) was elevated following OVA challenge, and CDDO further enhanced this increase (Figure 41b). Anti-oxidants (oxy-adsorbant assay) were also elevated by CDDO but only significantly with the 6 mg/kg dose (Figure 41c).

To further explore the basis of the anti-oxidant response in CDDO-treated mice, the levels of glutathione and HO-1 were assessed in lung tissues (Figures 42 and 42). OVA challenge increased both reduced glutathione and HO-1. Reduced glutathione increased on days one and two after the final treatment and challenge, but HO-1 levels were only increased on day 2.

## **Discussion**

In this study, we evaluated the effect of CDDO in a model of asthma. We hypothesized that an improvement in airway hyperresponsiveness and inflammatory response would occur with administration of CDDO compounds. This was based on the known effects of CDDO on activation of Nrf2 and upregulation of anti-oxidant responses. Oxidant stress is a well-described component of asthma and allergic inflammation. However, past attempts to alter the inflammation and hyperresponsiveness of asthma with anti-oxidants have met with mixed results.

Mice with disruption of the Nrf2 gene demonstrated exaggerated airway inflammation in a similar allergen-induced model of asthma [125]. The mechanism of action of CDDO compounds may underlie their effectiveness in the setting of the airway

oxidative stress in asthma. CDDO upregulate ARE via Nrf2 activation. Exactly how this activation occurs is unclear.

In our study, overall, CDDO skewed the pro-oxidant/antioxidant balance more towards an anti-oxidant response despite also increasing oxidant species. Thus, the anti-oxidant increase appears to have reduced the overall increase in pro-oxidants. In addition to improving airway hyperresponsiveness, we also demonstrated reduced airway eosinophilia and antigen-specific immune responses. OVA-specific IgE and T-cell proliferation were reduced. We did not investigate the mechanisms whereby CDDO may modify antigen-specific immune responses, but we speculate that a reduction in oxidant-mediated activation of TH2 pathways may be involved.

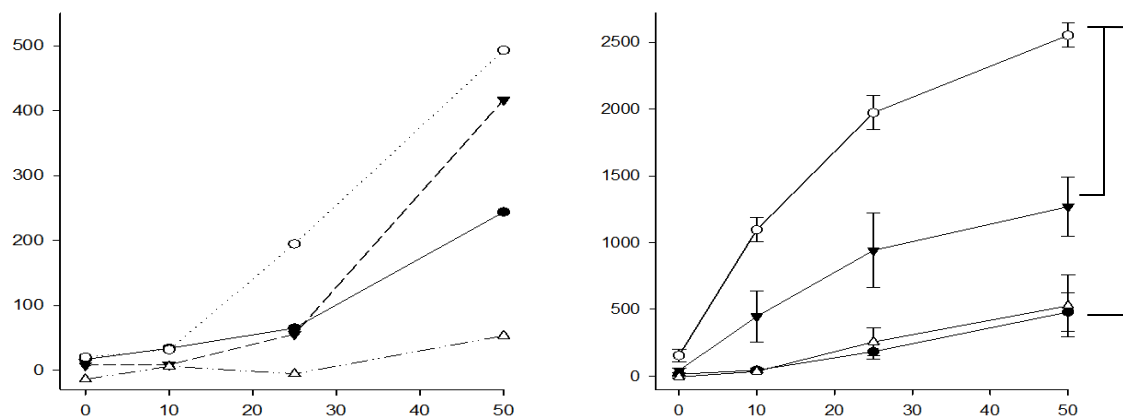


**Figure 37 . Whole body plethysmography in CDDO treated Mice.**

**a.** C57Bl/6 Mice (n=2/group except 4mg/kg, in which n=1) were assessed for enhanced pause after methacholine challenge. Statistical analysis was not performed due to the small numbers and pilot nature of the experiment. open circles = OVA, closed circles=saline, open triangles=CDDO 4mg/kg, and closed triangles=CDDO 2mg/kg.

**b.** Balb/c Mice (n=4-6 per group) were assessed for hyperresponsiveness (enhanced pause  $\pm$  SEM) 24 hours after last OVA challenge. Data are expressed as the percent of baseline Penh. Raw Penh values ranged from 0.4 (baseline) to 17.3 (50 mg/ml MCh). open circles = OVA, closed circles=saline, open triangles=CDDO 6mg/kg, and closed triangles=CDDO 3mg/kg. There was significant differences between OVA and CDDO 3mg/kg and 6 mg/kg ( $<0.001$ ) with OVA, CDDO 3mg/kg with saline ( $<0.001$ ), but no difference between saline and CDDO 6mg/kg. MCh 10 mg/ml there was a significant difference between OVA and CDDO 3mg/kg ( $p=0.002$ ), CDDO 6mg/kg ( $p<0.001$ ), and saline and at 25 and 50 there was a significant difference between CDDO 3mg/kg and 6mg/kg ( $<0.001$ ), and CDDO 3mg/kg and saline ( $<0.001$ ).

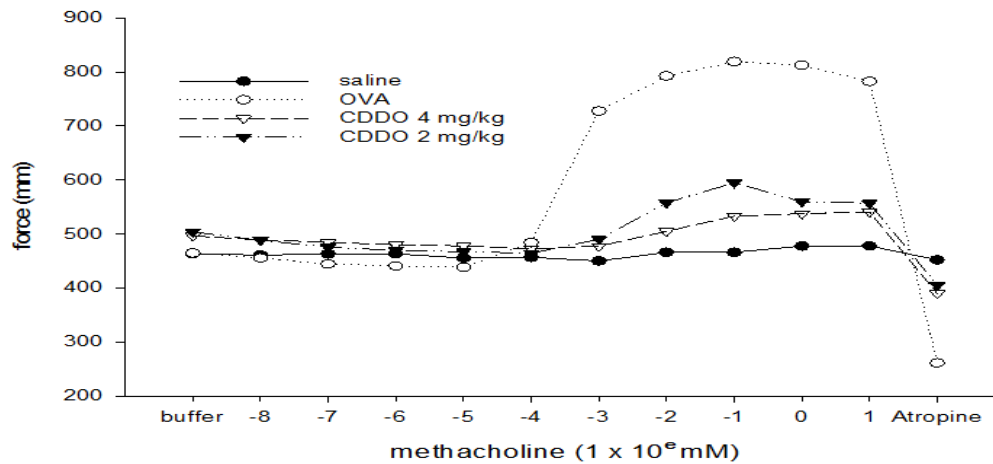


**Figure 38 .** Tracheal ring contractility in CDDO treated mice.

Tracheal rings were exposed to increasing concentrations of methacholine. Atropine was given at the end of the experiment to prove that the responses were receptor mediated. The data was normally distributed (Shapiro-Wilk test  $p=0.986$ ) with equal variance ( $p=0.888$ ). A Repeated Measures ANOVA demonstrated significant difference among treatments ( $P<0.05$ ) and a pairwise comparison (Holm-Sidak) demonstrated significant differences between all groups ( $P<0.05$ ) for all comparisons.  $n=5$

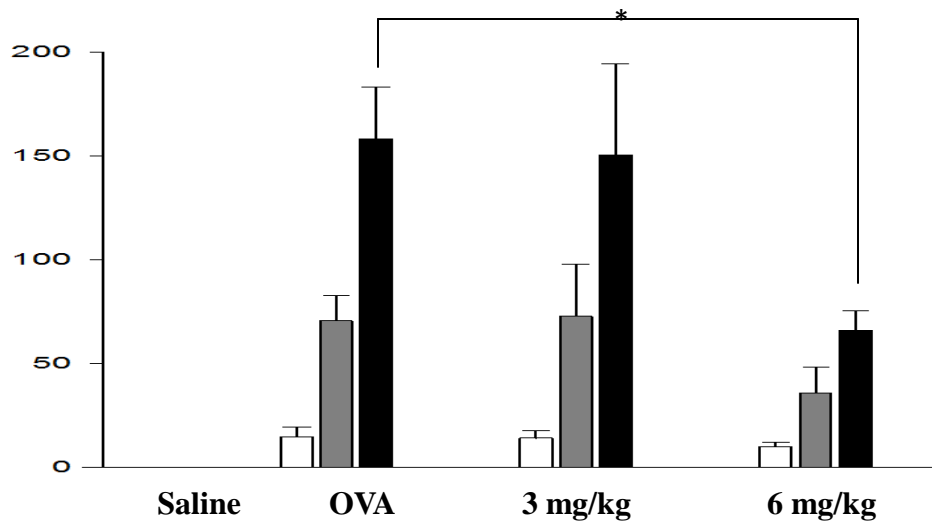


**Figure 39.** Bronchoalveolar lavage inflammatory cells in CDDO treated Mice.

BAL cells were collected 48 hours after final OVA challenge. unfilled bars=macrophages, grey bars = lymphocytes, black bars = eosinophils. Neutrophils and all cells from saline challenged mice were too few to display. There was a significant difference in total eosinophils between the OVA versus CDDO 6mg/kg groups ( $p=0.008$ ) representing a 58% drop in total BAL eosinophils.

\* Indicates significant differences from OVA control,  $n=5$

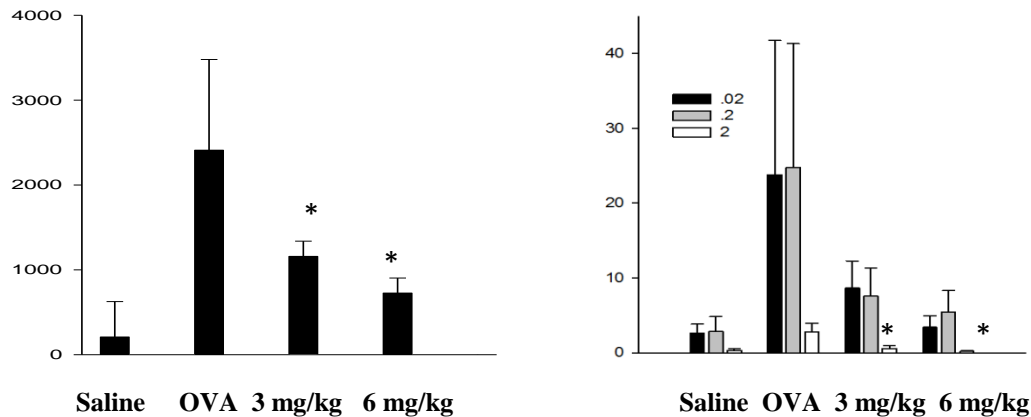


**Figure 40.** IgE and T-cell immune responses in CDDO treated mice.

**a.** OVA-specific IgE was assessed 48 hours after final challenge with OVA. There was a significant difference in the IgE levels: OVA vs CDDO 3mg/kg and CDDO 6mg/kg.

**b.** OVA-specific T-cell proliferation was assessed one week after final OVA challenge. Mononuclear spleen cells were stimulated with OVA at 0.02, 0.2 , and 2 mg/ml for 5 days. There was a significant difference in the stimulation index from OVA control animals at the 2 mg/ml concentration for CDDO 3mg/kg and CDDO 6mg/kg

\* Indicates significant differences from OVA control ,  $p \leq 0.05$ ,  $n=5$

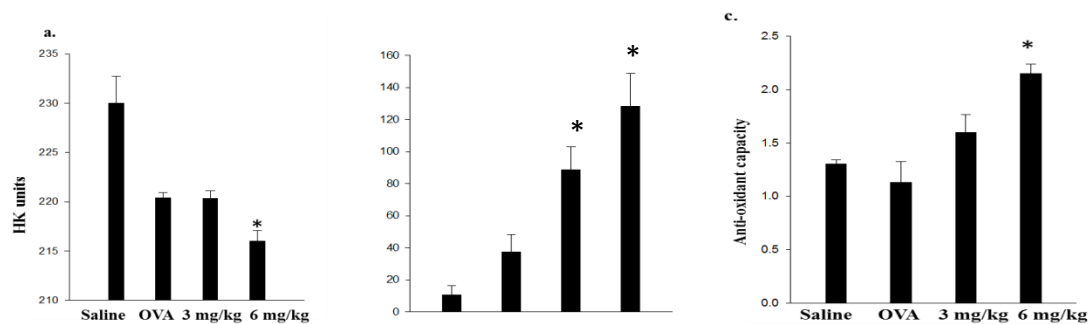


**Figure 41.** Oxidant stress response in CDDO treated mice.

Oxidant stress responses were assessed in bronchoalveolar lavage samples collected 48 hours after the final OVA challenge. **a.** Pro-oxidant/antioxidant balance was lower in OVA-treated animals compared to saline control and CDDO 6 mg/kg was lower than OVA treated animals indicated a shift towards an antioxidant response.

**b.** Total hydroperoxides (dRom assay) demonstrated an increase in production of hydroperoxides with treatment of animals with CDDO at both the 3 mg/kg and 6 mg/kg doses.

**c.** Antioxidant capacity. Animals treated with CDDO showed a trend in increased levels of total antioxidants with CDDO 3mg/kg and a significant increase with CDDO 6mg/kg compared to OVA control.

\* Indicates significant differences from OVA control  $p \leq 0.05$ ,  $n=5$

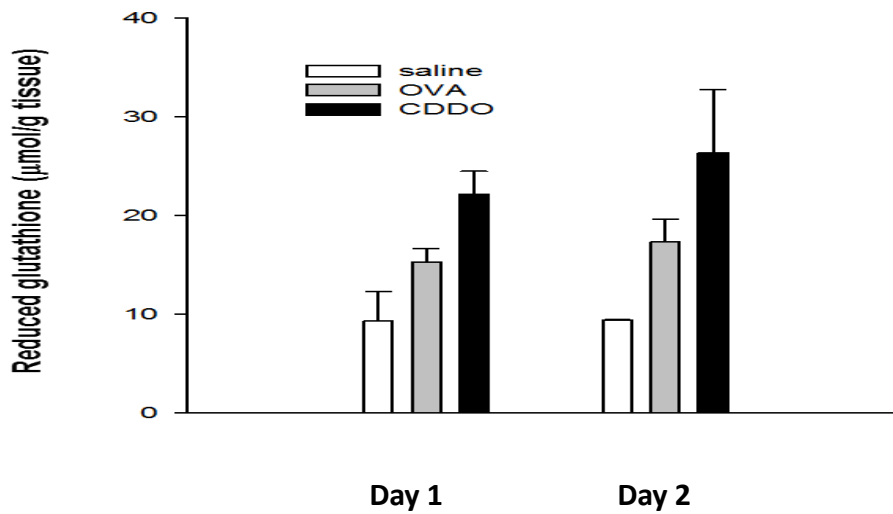


**Figure 42.** Glutathione with CDDO

Glutathione protein levels were assessed by ELISA in lung homogenates at 24 and 48 hours post OVA challenge. There were trends towards increasing reduced glutathione for both the 24 and 48 hour time points after treatment with CDDO 6 mg/kg. n=2

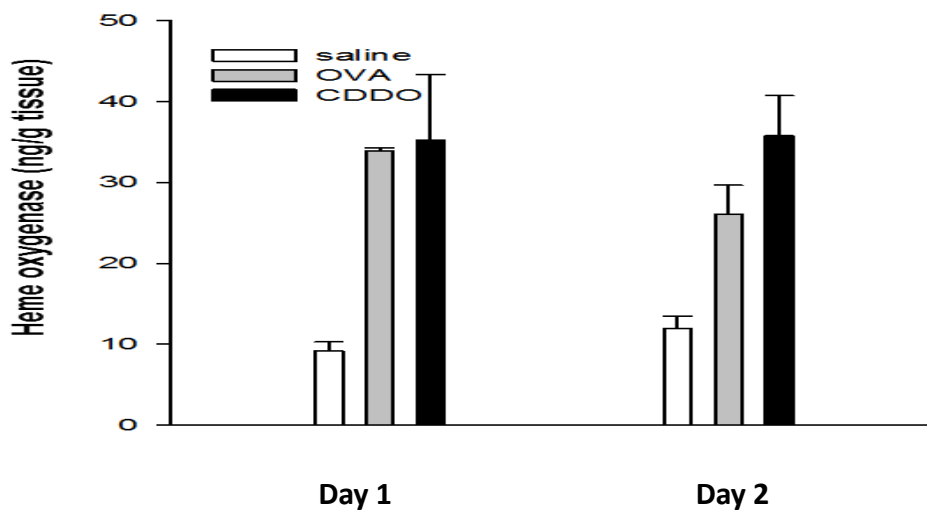


**Figure 43.** Heme-oxygenase with CDDO.

Heme-oxygenase protein levels were assessed by ELISA in lung homogenates at 24 and 48 hours post OVA challenge. There were trends towards increasing heme-oxygenase 48 hours after treatment with CDDO 6 mg/kg. n=2

## Chapter 6. CONCLUSIONS

### *SO<sub>2</sub> in vitro*

In this series of studies our aim was to establish a model of airway inflammatory initiation upon exposure to allergic stimuli that include environmental pollutants. In establishing that model, it became clear that there was a role for oxidative stress in the initiation of airway inflammation. In the first study presented herewith, it was demonstrated that rat derived mast cells and human isolated mast cells both degranulate inflammatory mediators *in vitro* when exposed to sulfite. Aqueous sulfite is used as a well-established *in vitro* model for SO<sub>2</sub>. Sulfur dioxide is one of the most ubiquitous air pollutants and a large component of diesel exhaust. Furthermore, a significant level of ROS was established upon sulfite exposure. When the cells were incubated with anti-oxidants both the ROS and the degranulation were ameliorated indicating a role for oxidative stress in pollutant exposure in allergic inflammatory processes.

### *Acrolein in vitro*

In order to establish that this model held true in other classes of common air pollutants the following study examined the role of ROS in the allergic inflammatory process when rat derived mast cells were exposed to acrolein. Acrolein is a potent aldehyde that is already known for its carcinogenic properties, but is produced from a variety of anthropogenic combustion sources, including cigarette smoke and automobile exhaust.

As with the sulfite study, it was established that acrolein induced mast cell degranulation *in vitro*, independently of direct cellular toxicity. Additionally, IgE cross-linking was blocked in the presence of acrolein, providing evidence that pollutant exposure can possibly override normal allergic processes in inflammatory cells. Cellular



exposure to acrolein also produced a significant level of ROS. The ROS was reduced when the RBL-2H3 cells were treated with anti-oxidants known to inhibit NADPH Oxidase. Reduction in ROS was accompanied by concomitant reduction in mast cell degranulation. Intracellular  $\text{Ca}^{2+}$  was shown to increase with increasing doses of acrolein exposure, indicating a possible role in ROS initiation of intracellular degranulation pathways. Depletion of extracellular calcium showed that those processes did not depend on an influx of  $\text{Ca}^{2+}$  ions. Inflammatory cytokines such as IL-4 and TNF- $\alpha$  were shown to increase from acrolein exposure, indicating a possible role in induction of a continued state of inflammation upon pollutant insult. As with the degranulation, acrolein blocked the expected cytokine expression from IgE cross-linking, thus providing further evidence that pollutant particles may interfere with established inflammatory pathways and induce inflammation through an ROS dependent initiation of degranulation.

#### *SO<sub>2</sub> in vivo*

The *in vitro* model was then extended into mice in order to establish a translation to the complex systems of living organisms. Sulfur dioxide was chosen due to the pervasive nature of SO<sub>2</sub> and sulfite-containing particles in the environment. The *in vivo* relationship between environmental pollutant and allergic inflammation proved to be more complex than the *in vitro* model. Mice were sensitized to OVA to mimic an atopic allergic state. Mice that were exposed in controlled chambers to ambient levels of SO<sub>2</sub> did demonstrate an enhanced wheezing state as seen in the whole body plethysmography. This effect was, however, time dependent and was ameliorated after 48 hours post OVA challenge. Some of the animals were given apocynin, a known inhibitor of NADPH Oxidase. Apocynin treated mice that were exposed to SO<sub>2</sub> displayed a reduced reaction

to MCh challenge, indicating a role for ROS *in vivo* similar to the *in vitro* model.

Alternatively, mice that were not exposed to SO<sub>2</sub>, had the reverse reaction to apocynin treatment. Their MCh breathing pauses went up, rather than down as with SO<sub>2</sub>. This reaction indicated a delicate balance in the oxidative state of allergic sensitized mice.

Similar to the *in vitro* model, SO<sub>2</sub> enhancement of OVA sensitization was seen in the expression of inflammatory cytokines typically associated with allergic inflammation such as IL-4, IL-6, and IL-12. Apocynin treatment reduced this effect as well again providing more evidence for a relationship between environmental pollutant induced inflammation and oxidative stress. Also similar to the *in vivo* model was the relationship between SO<sub>2</sub> exposure and IgE expression. While interference with IgE cross-linking was observed *in vitro*, in the animal study, SO<sub>2</sub> exposure resulted in reduced IgE expression when compared to the OVA alone treated mice. Likewise, treatment of those animals with apocynin caused a reverse response in IgE expression.

Further evidence of SO<sub>2</sub> enhancement of the allergic inflammatory process can be seen in the recruitment of inflammatory cells. Lymphocytes were notably increased in SO<sub>2</sub> exposed mice, as was T cell proliferation, when compared to OVA challenged mice receiving air alone. When treated with apocynin the effect of SO<sub>2</sub> was reduced, again indicating that SO<sub>2</sub> induces an imbalance in oxidative states in the airway.

Additional indications of the role of oxidative stress in mice were observed in measures of heme-oxygenase-1, glutathione, and nitric oxides. All of these indicators of oxidative stress displayed increased levels in the presence of SO<sub>2</sub>. Additionally, treatment with apocynin reduced the levels of these oxidative stress indicators after SO<sub>2</sub> exposure. Paradoxically, it has become evident that the shifts in oxidative balance taking place in

the airway are easily overwhelmed. In the absence of the exogenous environmental insult, treatment with apocynin created an increased state of oxidative stress. Rather than reducing the allergic inflammatory reactions normally seen with OVA sensitization and challenge, apocynin treatment enhanced hyperresponsiveness and inflammation.

#### *CDDO inhibition of allergic inflammation*

In light of this information, to further examine a mechanistic pathway of the oxidative imbalance caused by allergic airway inflammation, an additional mouse model was utilized. Mice were OVA sensitized and challenged as in the previous model. In order to focus on the oxidative balance, in this study, no exogenous pollutant was provided. Rather than employing an inhibitor of NADPH oxidase, the triterpenoid initiator of the Nrf2 anti-oxidant pathway, CDDO, was administered to the mice. As expected, OVA sensitization and subsequent challenge induced airway hypersensitivity as seen in plethysmography and trachea contractility. In both cases, CDDO was able to reduce that hyperresponsiveness. Indicators of allergic inflammation were present in the sensitized mice, such as enhanced antigen-specific T cell proliferation, increased presence of inflammatory cells, and antigen-specific IgE expression. In all cases treatment with CDDO reduced the inflammatory effect. Additionally, antioxidant capacity was increased with treatment of CDDO and a shift towards antioxidant expression was displayed in the OVA sensitized mice and was further increased with CDDO. These data indicate that oxidative imbalance plays a major role in allergic airway inflammation processes and that balance can be restored with an Nrf2 pathway initiator.

Taken together these studies confirm our initial hypothesis that exogenous environmental pollutants can initiate or enhance an allergic inflammatory process. This process seems to be IgE independent, but may rely on more chronic inflammation processes such as inflammatory cell signaling and IgG. Oxidative stress plays a vital role in allergic sensitization and is enhanced by environmental insult. Treatment with anti-oxidants can ameliorate the effect of the pollutant, however it seems the oxidative balance is delicate and can actually be overwhelmed by an overabundance of antioxidants, enhancing inflammation. By increasing the antioxidant response pathway the effects of allergic sensitization can be blocked and may represent an effective treatment in the future. Mechanistic examination of how this pathway is initiated is and how to determine the appropriate balance in the pro-oxidant/anti-oxidant is material for future studies.

## Reference List

- [1] Cho SH, Park HW, Rosenberg DM: The current status of asthma in Korea. *J Korean Med Sci* 2006;21:181-187.
- [2] Kawano T, Matsuse H, Kondo Y, Machida I, Saeki S, Tomari S, Mitsuta K, Obase Y, Fukushima C, Shimoda T, Kohno S: Acetaldehyde induces histamine release from human airway mast cells to cause bronchoconstriction. *Int Arch Allergy Immunol* 2004;134:233-239.
- [3] Brightling CE, Bradding P, Pavord ID, Wardlaw AJ: New insights into the role of the mast cell in asthma. *Clin Exp Allergy* 2003;33:550-556.
- [4] Fireman P: Understanding asthma pathophysiology. *Allergy Asthma Proc* 2003;24:79-83.
- [5] Holgate ST: The role of mast cells and basophils in inflammation. *Clin Exp Allergy* 2000;30 Suppl 1:28-32.
- [6] Holgate ST: Pathogenesis of asthma. *Clin Exp Allergy* 2008;38:872-897.
- [7] Ghio AJ, Smith CB, Madden MC: Diesel exhaust particles and airway inflammation. *Curr Opin Pulm Med* 2012;18:144-150.
- [8] Kjellstrom T, Friel S, Dixon J, Corvalan C, Rehfuess E, Campbell-Lendrum D, Gore F, Bartram J: Urban environmental health hazards and health equity. *J Urban Health* 2007;84:i86-i97.
- [9] Akinbami LJ, Lynch CD, Parker JD, Woodruff TJ: The association between childhood asthma prevalence and monitored air pollutants in metropolitan areas, United States, 2001-2004. *Environ Res* 2010;110:294-301.
- [10] Annesi-Maesano I, Dab W: [Air pollution and the lung: epidemiological approach]. *Med Sci (Paris)* 2006;22:589-594.
- [11] Leung TF, Ko FW, Wong GW: Roles of pollution in the prevalence and exacerbations of allergic diseases in Asia. *J Allergy Clin Immunol* 2012;129:42-47.
- [12] Lin RS, Sung FC, Huang SL, Gou YL, Ko YC, Gou HW, Shaw CK: Role of urbanization and air pollution in adolescent asthma: a mass screening in Taiwan. *J Formos Med Assoc* 2001;100:649-655.
- [13] Martins LC, Latorre MR, Saldiva PH, Braga AL: Air pollution and emergency room visits due to chronic lower respiratory diseases in the elderly: an ecological time-series study in Sao Paulo, Brazil. *J Occup Environ Med* 2002;44:622-627.

- [14] McMichael AJ: The urban environment and health in a world of increasing globalization: issues for developing countries. *Bull World Health Organ* 2000;78:1117-1126.
- [15] Nordling E, Berglind N, Melen E, Emenius G, Hallberg J, Nyberg F, Pershagen G, Svartengren M, Wickman M, Bellander T: Traffic-related air pollution and childhood respiratory symptoms, function and allergies. *Epidemiology* 2008;19:401-408.
- [16] Parker JD, Akinbami LJ, Woodruff TJ: Air pollution and childhood respiratory allergies in the United States. *Environ Health Perspect* 2009;117:140-147.
- [17] Peel JL, Tolbert PE, Klein M, Metzger KB, Flanders WD, Todd K, Mulholland JA, Ryan PB, Frumkin H: Ambient air pollution and respiratory emergency department visits. *Epidemiology* 2005;16:164-174.
- [18] Tramuto F, Cusimano R, Cerame G, Vultaggio M, Calamusa G, Maida CM, Vitale F: Urban air pollution and emergency room admissions for respiratory symptoms: a case-crossover study in Palermo, Italy. *Environ Health* 2011;10:31.
- [19] D'Amato G, Cecchi L, D'Amato M, Liccardi G: Urban air pollution and climate change as environmental risk factors of respiratory allergy: an update. *J Investig Allergol Clin Immunol* 2010;20:95-102.
- [20] D'Amato G: Effects of climatic changes and urban air pollution on the rising trends of respiratory allergy and asthma. *Multidiscip Respir Med* 2011;6:28-37.
- [21] D'Amato G: Urban air pollution and respiratory allergy. *Monaldi Arch Chest Dis* 2002;57:136-140.
- [22] D'Amato G: Environmental urban factors (air pollution and allergens) and the rising trends in allergic respiratory diseases. *Allergy* 2002;57 Suppl 72:30-33.
- [23] D'Amato G, Liccardi G, D'Amato M, Cazzola M: The role of outdoor air pollution and climatic changes on the rising trends in respiratory allergy. *Respir Med* 2001;95:606-611.
- [24] Haryanto B, Franklin P: Air pollution: a tale of two countries. *Rev Environ Health* 2011;26:53-59.
- [25] Lippmann M, Ito K, Nadas A, Burnett RT: Association of particulate matter components with daily mortality and morbidity in urban populations. *Res Rep Health Eff Inst* 2000;5-72, discussion.
- [26] Schwarze PE, Ovrevik J, Hetland RB, Becher R, Cassee FR, Lag M, Lovik M, Dybing E, Refsnes M: Importance of size and composition of particles for effects on cells in vitro. *Inhal Toxicol* 2007;19 Suppl 1:17-22.

- [27] Calcabrini A, Meschini S, Marra M, Falzano L, Colone M, De BB, Paoletti L, Arancia G, Fiorentini C: Fine environmental particulate engenders alterations in human lung epithelial A549 cells. *Environ Res* 2004;95:82-91.
- [28] Ebtekar M: Air pollution induced asthma and alterations in cytokine patterns. *Iran J Allergy Asthma Immunol* 2006;5:47-56.
- [29] Miyata R, van Eeden SF: The innate and adaptive immune response induced by alveolar macrophages exposed to ambient particulate matter. *Toxicol Appl Pharmacol* 12-1-2011;257:209-226.
- [30] Siegel PD, Saxena RK, Saxena QB, Ma JK, Ma JY, Yin XJ, Castranova V, Al-Humadi N, Lewis DM: Effect of diesel exhaust particulate (DEP) on immune responses: contributions of particulate versus organic soluble components. *J Toxicol Environ Health A* 2-13-2004;67:221-231.
- [31] Dergham M, Lepers C, Verdin A, Billet S, Cazier F, Courcot D, Shirali P, Garcon G: Prooxidant and proinflammatory potency of air pollution particulate matter (PM<sub>2.5</sub>) produced in rural, urban, or industrial surroundings in human bronchial epithelial cells (BEAS-2B). *Chem Res Toxicol* 4-16-2012;25:904-919.
- [32] Ghio AJ, Carraway MS, Madden MC: Composition of air pollution particles and oxidative stress in cells, tissues, and living systems. *J Toxicol Environ Health B Crit Rev* 2012;15:1-21.
- [33] Jeng HA: Chemical composition of ambient particulate matter and redox activity. *Environ Monit Assess* 2010;169:597-606.
- [34] Shiraiwa M, Selzle K, Poschl U: Hazardous components and health effects of atmospheric aerosol particles: reactive oxygen species, soot, polycyclic aromatic compounds and allergenic proteins. *Free Radic Res* 2012;46:927-939.
- [35] Davis JA, Meng Q, Sacks JD, Dutton SJ, Wilson WE, Pinto JP: Regional variations in particulate matter composition and the ability of monitoring data to represent population exposures. *Sci Total Environ* 11-1-2011;409:5129-5135.
- [36] Han I, Mihalic JN, Ramos-Bonilla JP, Rule AM, Polyak LM, Peng RD, Geyh AS, Breysse PN: Assessment of heterogeneity of metal composition of fine particulate matter collected from eight U.S. counties using principal component analysis. *J Air Waste Manag Assoc* 2012;62:773-782.
- [37] Osornio-Vargas AR, Bonner JC, Alfaro-Moreno E, Martinez L, Garcia-Cuellar C, Ponce-de-Leon RS, Miranda J, Rosas I: Proinflammatory and cytotoxic effects of Mexico City air pollution particulate matter in vitro are dependent on particle size and composition. *Environ Health Perspect* 2003;111:1289-1293.
- [38] Strak M, Janssen NA, Godri KJ, Gosens I, Mudway IS, Cassee FR, Lebret E, Kelly FJ, Harrison RM, Brunekreef B, Steenhof M, Hoek G: Respiratory Health Effects of

Airborne Particulate Matter: The Role of Particle Size, Composition, and Oxidative Potential-The RAPTES Project. *Environ Health Perspect* 2012;120:1183-1189.

- [39] Tsai JH, Chang LT, Huang YS, Chiang HL: Particulate composition characteristics under different ambient air quality conditions. *J Air Waste Manag Assoc* 2011;61:796-805.
- [40] Valavanidis A, Fiotakis K, Vlachogianni T: Airborne particulate matter and human health: toxicological assessment and importance of size and composition of particles for oxidative damage and carcinogenic mechanisms. *J Environ Sci Health C Environ Carcinog Ecotoxicol Rev* 2008;26:339-362.
- [41] Faroon O, Roney N, Taylor J, Ashizawa A, Lumpkin MH, Plewak DJ: Acrolein environmental levels and potential for human exposure. *Toxicol Ind Health* 2008;24:543-564.
- [42] Ghilarducci DP, Tjeerdema RS: Fate and effects of acrolein. *Rev Environ Contam Toxicol* 1995;144:95-146.:95-146.
- [43] Liu W, Zhang J, Kwon J, Weisel C, Turpin B, Zhang L, Korn L, Morandi M, Stock T, Colome S: Concentrations and source characteristics of airborne carbonyl compounds measured outside urban residences. *J Air Waste Manag Assoc* 2006;56:1196-1204.
- [44] Spada N, Fujii E, Cahill TM: Diurnal cycles of acrolein and other small aldehydes in regions impacted by vehicle emissions. *Environ Sci Technol* 10-1-2008;42:7084-7090.
- [45] Stevens JF, Maier CS: Acrolein: sources, metabolism, and biomolecular interactions relevant to human health and disease. *Mol Nutr Food Res* 2008;52:7-25.
- [46] Chen B, Kan H: Air pollution and population health: a global challenge. *Environ Health Prev Med* 2008;13:94-101.
- [47] Ito K, Mathes R, Ross Z, Nadas A, Thurston G, Matte T: Fine particulate matter constituents associated with cardiovascular hospitalizations and mortality in New York City. *Environ Health Perspect* 2011;119:467-473.
- [48] Wang B, Peng Z, Zhang X, Xu Y, Wang H, Allen G, Wang L, Xu X: Particulate matter, sulfur dioxide, and pulmonary function in never-smoking adults in Chongqing, China. *Int J Occup Environ Health* 1999;5:14-19.
- [49] Collaco CR, Hochman DJ, Goldblum RM, Brooks EG: Effect of sodium sulfite on mast cell degranulation and oxidant stress. *Ann Allergy Asthma Immunol* 2006;96:550-556.
- [50] Levetin E, Van de Water P: Environmental contributions to allergic disease. *Curr Allergy Asthma Rep* 2001;1:506-514.
- [51] Ohyama K, Ito T, Kanisawa M: The roles of diesel exhaust particle extracts and the promotive effects of NO<sub>2</sub> and/or SO<sub>2</sub> exposure on rat lung tumorigenesis. *Cancer Lett* 5-24-1999;139:189-197.



- [52] Duran A, Carmona M, Ballesteros R: Competitive diesel engine emissions of sulphur and nitrogen species. *Chemosphere* 2003;52:1819-1823.
- [53] Burra TA, Moineddin R, Agha MM, Glazier RH: Social disadvantage, air pollution, and asthma physician visits in Toronto, Canada. *Environ Res* 2009;109:567-574.
- [54] Clark NA, Demers PA, Karr CJ, Koehoorn M, Lencar C, Tamburic L, Brauer M: Effect of early life exposure to air pollution on development of childhood asthma. *Environ Health Perspect* 2010;118:284-290.
- [55] Dong GH, Zhang P, Sun B, Zhang L, Chen X, Ma N, Yu F, Guo H, Huang H, Lee YL, Tang N, Chen J: Long-term exposure to ambient air pollution and respiratory disease mortality in shenyang, china: a 12-year population-based retrospective cohort study. *Respiration* 2012;84:360-368.
- [56] Forbes LJ, Kapetanakis V, Rudnicka AR, Cook DG, Bush T, Stedman JR, Whincup PH, Strachan DP, Anderson HR: Chronic exposure to outdoor air pollution and lung function in adults. *Thorax* 2009;64:657-663.
- [57] Liu L, Poon R, Chen L, Frescura AM, Montuschi P, Ciabattini G, Wheeler A, Dales R: Acute effects of air pollution on pulmonary function, airway inflammation, and oxidative stress in asthmatic children. *Environ Health Perspect* 2009;117:668-674.
- [58] Luttinger D, Wilson L: A study of air pollutants and acute asthma exacerbations in urban areas: status report. *Environ Pollut* 2003;123:399-402.
- [59] Diaz-Sanchez D, Garcia MP, Wang M, Jyrala M, Saxon A: Nasal challenge with diesel exhaust particles can induce sensitization to a neoallergen in the human mucosa. *J Allergy Clin Immunol* 1999;104:1183-1188.
- [60] Diaz-Sanchez D, Penichet-Garcia M, Saxon A: Diesel exhaust particles directly induce activated mast cells to degranulate and increase histamine levels and symptom severity. *J Allergy Clin Immunol* 2000;106:1140-1146.
- [61] Aguilera-Aguirre L, Bacsı A, Saavedra-Molina A, Kurosky A, Sur S, Boldogh I: Mitochondrial dysfunction increases allergic airway inflammation. *J Immunol* 10-15-2009;183:5379-5387.
- [62] Csillag A, Boldogh I, Pazmandi K, Magyarics Z, Gogolak P, Sur S, Rajnavolgyi E, Bacsı A: Pollen-induced oxidative stress influences both innate and adaptive immune responses via altering dendritic cell functions. *J Immunol* 3-1-2010;184:2377-2385.
- [63] Dharajiya N, Boldogh I, Cardenas V, Sur S: Role of pollen NAD(P)H oxidase in allergic inflammation. *Curr Opin Allergy Clin Immunol* 2008;8:57-62.
- [64] Dharajiya N, Choudhury BK, Bacsı A, Boldogh I, Alam R, Sur S: Inhibiting pollen reduced nicotinamide adenine dinucleotide phosphate oxidase-induced signal by intrapulmonary administration of antioxidants blocks allergic airway inflammation. *J Allergy Clin Immunol* 2007;119:646-653.

- [65] Endo S, Hochman DJ, Midoro-Horiuti T, Goldblum RM, Brooks EG: Mountain cedar pollen induces IgE-independent mast cell degranulation, IL-4 production, and intracellular reactive oxygen species generation. *Cell Immunol* 2011;271:488-495.
- [66] Speranza A, Scoccianti V: New insights into an old story: Pollen ROS also play a role in hay fever. *Plant Signal Behav* 8-1-2012;7:994-998.
- [67] Hosakote YM, Komaravelli N, Mautemps N, Liu T, Garofalo RP, Casola A: ANTIOXIDANT MIMETICS MODULATE OXIDATIVE STRESS AND CELLULAR SIGNALING IN AIRWAY EPITHELIAL CELLS INFECTED WITH RESPIRATORY SYNCYTIAL VIRUS. *Am J Physiol Lung Cell Mol Physiol* 9-28-2012.
- [68] Hosakote YM, Liu T, Castro SM, Garofalo RP, Casola A: Respiratory syncytial virus induces oxidative stress by modulating antioxidant enzymes. *Am J Respir Cell Mol Biol* 2009;41:348-357.
- [69] Taylor MR, Rubin ES, Hounshell DA: Effect of government actions on technological innovation for SO<sub>2</sub> control. *Environ Sci Technol* 10-15-2003;37:4527-4534.
- [70] Motallebi N, Taylor CA, Jr., Croes BE: Particulate matter in California: part 2--Spatial, temporal, and compositional patterns of PM<sub>2.5</sub>, PM<sub>10-2.5</sub>, and PM<sub>10</sub>. *J Air Waste Manag Assoc* 2003;53:1517-1530.
- [71] Pandya RJ, Solomon G, Kinner A, Balmes JR: Diesel exhaust and asthma: hypotheses and molecular mechanisms of action. *Environ Health Perspect* 2002;110 Suppl 1:103-112.
- [72] Chow JC, Watson JG, Mauderly JL, Costa DL, Wyzga RE, Vedal S, Hidy GM, Altshuler SL, Marrack D, Heuss JM, Wolff GT, Pope CA, III, Dockery DW: Health effects of fine particulate air pollution: lines that connect. *J Air Waste Manag Assoc* 2006;56:1368-1380.
- [73] SKALPE IO: LONG-TERM EFFECTS OF SULPHUR DIOXIDE EXPOSURE IN PULP MILLS. *Br J Ind Med* 1964;21:69-73.
- [74] Atkinson DA, Sim TC, Grant JA: Sodium metabisulfite and SO<sub>2</sub> release: an under-recognized hazard among shrimp fishermen. *Ann Allergy* 1993;71:563-566.
- [75] Gong H, Jr., Linn WS, Terrell SL, Anderson KR, Clark KW: Anti-inflammatory and lung function effects of montelukast in asthmatic volunteers exposed to sulfur dioxide. *Chest* 2001;119:402-408.
- [76] Lazarus SC, Wong HH, Watts MJ, Boushey HA, Lavins BJ, Minkwitz MC: The leukotriene receptor antagonist zafirlukast inhibits sulfur dioxide-induced bronchoconstriction in patients with asthma. *Am J Respir Crit Care Med* 1997;156:1725-1730.
- [77] Balasubramanian N, Ramakrishna TV: Spectrophotometric determination of sulphite. *Z Gesamte Hyg* 1986;32:154-155.

- [78] Meng Z, Zhang B: Polymerase chain reaction-based deletion screening of bisulfite (sulfur dioxide)-enhanced gpt-mutants in CHO-AS52 cells. *Mutat Res* 3-10-1999;425:81-85.
- [79] Beck-Speier I, Lenz AG, Godleski JJ: Responses of human neutrophils to sulfite. *J Toxicol Environ Health* 1994;41:285-297.
- [80] Labbe P, Pelletier M, Omara FO, Girard D: Functional responses of human neutrophils to sodium sulfite (Na<sub>2</sub>SO<sub>3</sub>) in vitro. *Hum Exp Toxicol* 1998;17:600-605.
- [81] Kawabata TT, Babcock LS: Measurement of murine ovalbumin-specific IgE by a rat basophil leukemia cell serotonin release assay. Comparison to the rat passive cutaneous anaphylaxis assay. *J Immunol Methods* 6-4-1993;162:9-15.
- [82] Oka T, Sato K, Hori M, Ozaki H, Karaki H: FcepsilonRI cross-linking-induced actin assembly mediates calcium signalling in RBL-2H3 mast cells. *Br J Pharmacol* 2002;136:837-846.
- [83] Lee RJ, Oliver JM: Roles for Ca<sup>2+</sup> stores release and two Ca<sup>2+</sup> influx pathways in the Fc epsilon R1-activated Ca<sup>2+</sup> responses of RBL-2H3 mast cells. *Mol Biol Cell* 1995;6:825-839.
- [84] Chamulitrat W: Activation of the superoxide-generating NADPH oxidase of intestinal lymphocytes produces highly reactive free radicals from sulfite. *Free Radic Biol Med* 1999;27:411-421.
- [85] Seale JP, Temple DM, Tennant CM: Bronchoconstriction by nebulized metabisulfite solutions (SO<sub>2</sub>) and its modification by ipratropium bromide. *Ann Allergy* 1988;61:209-213.
- [86] Clark RA: The human neutrophil respiratory burst oxidase. *J Infect Dis* 1990;161:1140-1147.
- [87] Clark RA, Volpp BD, Leidal KG, Nauseef WM: Two cytosolic components of the human neutrophil respiratory burst oxidase translocate to the plasma membrane during cell activation. *J Clin Invest* 1990;85:714-721.
- [88] Hunt JF, Erwin E, Palmer L, Vaughan J, Malhotra N, Platts-Mills TA, Gaston B: Expression and activity of pH-regulatory glutaminase in the human airway epithelium. *Am J Respir Crit Care Med* 1-1-2002;165:101-107.
- [89] Nel AE, Diaz-Sanchez D, Ng D, Hiura T, Saxon A: Enhancement of allergic inflammation by the interaction between diesel exhaust particles and the immune system. *J Allergy Clin Immunol* 1998;102:539-554.
- [90] Diaz-Sanchez D, Tsien A, Fleming J, Saxon A: Combined diesel exhaust particulate and ragweed allergen challenge markedly enhances human in vivo nasal ragweed-specific IgE and skews cytokine production to a T helper cell 2-type pattern. *J Immunol* 3-1-1997;158:2406-2413.

- [91] Li N, Hao M, Phalen RF, Hinds WC, Nel AE: Particulate air pollutants and asthma. A paradigm for the role of oxidative stress in PM-induced adverse health effects. *Clin Immunol* 2003;109:250-265.
- [92] Collaco CR, Hochman DJ, Goldblum RM, Brooks EG: Effect of sodium sulfite on mast cell degranulation and oxidant stress. *Ann Allergy Asthma Immunol* 2006;96:550-556.
- [93] Vagaggini B, Bartoli ML, Cianchetti S, Costa F, Bacci E, Dente FL, Di FA, Malagrino L, Paggiaro P: Increase in markers of airway inflammation after ozone exposure can be observed also in stable treated asthmatics with minimal functional response to ozone. *Respir Res* 2010;Jan 19;11:5.:5.
- [94] Liu XY, Zhu MX, Xie JP: Mutagenicity of acrolein and acrolein-induced DNA adducts. *Toxicol Mech Methods* 2010;20:36-44.
- [95] Rashid A, Sadroddiny E, Ye HT, Vratimos A, Sabban S, Carey E, Helm B: Review: Diagnostic and therapeutic applications of rat basophilic leukemia cells. *Mol Immunol* 2012;52:224-228.
- [96] Matzinger P: The JAM test. A simple assay for DNA fragmentation and cell death. *J Immunol Methods* 12-15-1991;145:185-192.
- [97] Kim KH, Pal R: Determination of acetaldehyde in ambient air: comparison of thermal desorption-GC/FID method with the standard DNPH-HPLC method. *Environ Monit Assess* 2010;161:295-299.
- [98] Jain S, Khare M: Urban air quality in mega cities: a case study of Delhi City using vulnerability analysis. *Environ Monit Assess* 2008;136:257-265.
- [99] Salaspuro M: Acetaldehyde: a cumulative carcinogen in humans. *Addiction* 2009;104:551-553.
- [100] Boorman G, Crabbs TA, Kolenda-Roberts H, Latimer K, Miller AD, Muravnick KB, Nyska A, Ochoa R, Pardo ID, Ramot Y, Rao DB, Schuh J, Suttie A, Travlos GS, Ward JM, Wolf JC, Elmore SA: Proceedings of the 2011 National Toxicology Program Satellite Symposium. *Toxicol Pathol* 2012;40:321-344.
- [101] Formaldehyde. *Rep Carcinog* 2011;12:195-205.
- [102] Oka T, Sato K, Hori M, Ozaki H, Karaki H: FcepsilonRI cross-linking-induced actin assembly mediates calcium signalling in RBL-2H3 mast cells. *Br J Pharmacol* 2002;136:837-846.
- [103] Lee RJ, Oliver JM: Roles for Ca<sup>2+</sup> stores release and two Ca<sup>2+</sup> influx pathways in the Fc epsilon R1-activated Ca<sup>2+</sup> responses of RBL-2H3 mast cells. *Mol Biol Cell* 1995;6:825-839.

- [104] Theoharides TC, Kempuraj D, Tagen M, Conti P, Kalogeromitros D: Differential release of mast cell mediators and the pathogenesis of inflammation. *Immunol Rev* 2007;217:65-78..65-78.
- [105] Shaughnessy RJ, Mcdaniels TJ, Weschler CJ: Indoor chemistry: ozone and volatile organic compounds found in tobacco smoke. *Environ Sci Technol* 7-1-2001;35:2758-2764.
- [106] Howard PH: Acrolein; in *Handbook of environmental fate and exposure data for organic chemicals*, Volume 1: Boca Raton, Florida, Lewis Publishers, 89 A.D., pp 5-12.
- [107] Borchers MT, Wert SE, Leikauf GD: Acrolein-induced MUC5ac expression in rat airways. *Am J Physiol* 1998;274:L573-L581.
- [108] Wang HT, Zhang S, Hu Y, Tang MS: Mutagenicity and sequence specificity of acrolein-DNA adducts. *Chem Res Toxicol* 3-16-2009;22:511-517.
- [109] Zhang S, Balbo S, Wang M, Hecht SS: Analysis of acrolein-derived 1,N2-propanodeoxyguanosine adducts in human leukocyte DNA from smokers and nonsmokers. *Chem Res Toxicol* 1-14-2011;24:119-124.
- [110] Roux E, Hyvelin JM, Savineau JP, Marthan R: Human isolated airway contraction: interaction between air pollutants and passive sensitization. *Am J Respir Crit Care Med* 1999;160:439-445.
- [111] Caldwell JC, Woodruff TJ, Morello-Frosch R, Axelrad DA: Application of health information to hazardous air pollutants modeled in EPA's Cumulative Exposure Project. *Toxicol Ind Health* 1998;14:429-454.
- [112] Tam BN, Neumann CM: A human health assessment of hazardous air pollutants in Portland, OR. *J Environ Manage* 2004;73:131-145.
- [113] Woodruff TJ, Axelrad DA, Caldwell J, Morello-Frosch R, Rosenbaum A: Public health implications of 1990 air toxics concentrations across the United States. *Environ Health Perspect* 1998;106:245-251.
- [114] Rahman I, MacNee W: Regulation of redox glutathione levels and gene transcription in lung inflammation: therapeutic approaches. *Free Radic Biol Med* 5-1-2000;28:1405-1420.
- [115] Ranganna K, Yousefipour Z, Nasif R, Yatsu FM, Milton SG, Hayes BE: Acrolein activates mitogen-activated protein kinase signal transduction pathways in rat vascular smooth muscle cells. *Mol Cell Biochem* 2002;240:83-98.
- [116] Kozekov ID, Turesky RJ, Alas GR, Harris CM, Harris TM, Rizzo CJ: Formation of deoxyguanosine cross-links from calf thymus DNA treated with acrolein and 4-hydroxy-2-nonenal. *Chem Res Toxicol* 11-15-2010;23:1701-1713.
- [117] Kehrer JP, Biswal SS: The molecular effects of acrolein. *Toxicol Sci* 2000;57:6-15.

- [118] Luo J, Shi R: Acrolein induces oxidative stress in brain mitochondria. *Neurochem Int* 2005;46:243-252.
- [119] Strider JW, Masterson CG, Durham PL: Treatment of mast cells with carbon dioxide suppresses degranulation via a novel mechanism involving repression of increased intracellular calcium levels. *Allergy* 2011;66:341-350.
- [120] Misonou Y, Takahashi M, Park YS, Asahi M, Miyamoto Y, Sakiyama H, Cheng X, Taniguchi N: Acrolein induces Hsp72 via both PKCdelta/JNK and calcium signaling pathways in human umbilical vein endothelial cells. *Free Radic Res* 2005;39:507-512.
- [121] Woods JS, Ellis ME, Dieguez-Acuna FJ, Corral J: Activation of NF-kappaB in normal rat kidney epithelial (NRK52E) cells is mediated via a redox-insensitive, calcium-dependent pathway. *Toxicol Appl Pharmacol* 2-1-1999;154:219-227.
- [122] Muijsers RB, van A, I, Folkerts G, Koster AS, van Oosterhout AJ, Postma DS, Nijkamp FP: Apocynin and 1400 W prevents airway hyperresponsiveness during allergic reactions in mice. *Br J Pharmacol* 2001;134:434-440.
- [123] Swindle EJ, Metcalfe DD: The role of reactive oxygen species and nitric oxide in mast cell-dependent inflammatory processes. *Immunol Rev* 2007;217:186-205.
- [124] Masini E, Bani D, Vannacci A, Pierpaoli S, Mannaioni PF, Comhair SA, Xu W, Muscoli C, Erzurum SC, Salvemini D: Reduction of antigen-induced respiratory abnormalities and airway inflammation in sensitized guinea pigs by a superoxide dismutase mimetic. *Free Radic Biol Med* 8-15-2005;39:520-531.
- [125] Rangasamy T, Guo J, Mitzner WA, Roman J, Singh A, Fryer AD, Yamamoto M, Kensler TW, Tuder RM, Georas SN, Biswal S: Disruption of Nrf2 enhances susceptibility to severe airway inflammation and asthma in mice. *J Exp Med* 7-4-2005;202:47-59.
- [126] Lin W, Xu X, Ma Z, Zhao H, Liu X, Wang Y: Characteristics and recent trends of sulfur dioxide at urban, rural, and background sites in north China: effectiveness of control measures. *J Environ Sci (China)* 2012;24:34-49.
- [127] Liu D, Jin H, Tang C, Du J: Sulfur dioxide: a novel gaseous signal in the regulation of cardiovascular functions. *Mini Rev Med Chem* 2010;10:1039-1045.
- [128] Taube C, Wei X, Swasey CH, Joetham A, Zarini S, Lively T, Takeda K, Loader J, Miyahara N, Kodama T, Shultz LD, Donaldson DD, Hamelmann EH, Dakhama A, Gelfand EW: Mast cells, Fc epsilon RI, and IL-13 are required for development of airway hyperresponsiveness after aerosolized allergen exposure in the absence of adjuvant. *J Immunol* 5-15-2004;172:6398-6406.
- [129] Goyal SK: Use of rosaniline hydrochloride dye for atmospheric SO2 determination and method sensitivity analysis. *J Environ Monit* 2001;3:666-670.

- [130] Ameredes BT, Otterbein LE, Kohut LK, Gligonic AL, Calhoun WJ, Choi AMK: Low-dose carbon monoxide reduces airway hyperresponsiveness in mice. *Am J Physiol Lung Cell Mol Physiol* 12-1-2003;285:L1270-L1276.
- [131] Hamelmann E, Schwarse J, Takeda K, OSHIBA A, Larsen G, Irvin C, Gelfand E: Noninvasive Measurement of Airway Responsiveness in Allergic Mice Using Barometric Plethysmography. *Am J Respir Crit Care Med* 9-1-1997;156:766-775.
- [132] de Jager W, te Velthuis H, Prakken BJ, Kuis W, Rijkers GT: Simultaneous Detection of 15 Human Cytokines in a Single Sample of Stimulated Peripheral Blood Mononuclear Cells. *Clin Diagn Lab Immunol* 1-1-2003;10:133-139.
- [133] Ameredes BT, Sethi JM, Liu HL, Choi AM, Calhoun WJ: Enhanced nitric oxide production associated with airway hyporesponsiveness in the absence of IL-10. *Am J Physiol Lung Cell Mol Physiol* 2005;288:L868-L873.
- [134] Cho HL, Ho PP, Mihelich ED, Snyder DW: Relative potencies of 5-lipoxygenase inhibitors on antigen-induced contractions of guinea pig tracheal strips. *J Pharmacol Methods* 1991;26:277-287.
- [135] Kruisbeek AM, Shevach E, Thornton AM: Proliferative assays for T cell function. *Curr Protoc Immunol* 2004;Chapter 3:Unit.
- [136] Boyle JJ: Macrophage activation in atherosclerosis: pathogenesis and pharmacology of plaque rupture. *Curr Vasc Pharmacol* 2005;3:63-68.
- [137] Makay B, Makay O, Yenisey C, Icoz G, Ozgen G, Unsal E, Akyildiz M, Yetkin E: The interaction of oxidative stress response with cytokines in the thyrotoxic rat: is there a link? *Mediators Inflamm* 2009;2009:391682.
- [138] Vlahopoulos S, Boldogh I, Casola A, Brasier AR: Nuclear factor-kappaB-dependent induction of interleukin-8 gene expression by tumor necrosis factor alpha: evidence for an antioxidant sensitive activating pathway distinct from nuclear translocation. *Blood* 9-15-1999;94:1878-1889.
- [139] Slebos DJ, Ryter SW, Choi AM: Heme oxygenase-1 and carbon monoxide in pulmonary medicine. *Respir Res* 2003;4:7.
- [140] Tsikas D: Methods of quantitative analysis of the nitric oxide metabolites nitrite and nitrate in human biological fluids. *Free Radic Res* 2005;39:797-815.
- [141] Marletta MA, Yoon PS, Iyengar R, Leaf CD, Wishnok JS: Macrophage oxidation of L-arginine to nitrite and nitrate: nitric oxide is an intermediate. *Biochemistry* 11-29-1988;27:8706-8711.
- [142] Moncada S, Palmer RM, Higgs EA: Biosynthesis of nitric oxide from L-arginine. A pathway for the regulation of cell function and communication. *Biochem Pharmacol* 6-1-1989;38:1709-1715.

- [143] Palmer RM, Ashton DS, Moncada S: Vascular endothelial cells synthesize nitric oxide from L-arginine. *Nature* 6-16-1988;333:664-666.
- [144] Palmer RM, Rees DD, Ashton DS, Moncada S: L-arginine is the physiological precursor for the formation of nitric oxide in endothelium-dependent relaxation. *Biochem Biophys Res Commun* 6-30-1988;153:1251-1256.
- [145] Alderton WK, Cooper CE, Knowles RG: Nitric oxide synthases: structure, function and inhibition. *Biochem J* 8-1-2001;357:593-615.
- [146] Bogdan C: Nitric oxide and the immune response. *Nat Immunol* 2001;2:907-916.
- [147] Bowler RP: Oxidative stress in the pathogenesis of asthma. *Curr Allergy Asthma Rep* 2004;4:116-122.
- [148] Li N, Hao M, Phalen RF, Hinds WC, Nel AE: Particulate air pollutants and asthma. A paradigm for the role of oxidative stress in PM-induced adverse health effects. *Clin Immunol* 2003;109:250-265.
- [149] Risom L, Moller P, Loft S: Oxidative stress-induced DNA damage by particulate air pollution. *Mutat Res* 12-30-2005;592:119-137.
- [150] Tao F, Gonzalez-Flecha B, Kobzik L: Reactive oxygen species in pulmonary inflammation by ambient particulates. *Free Radic Biol Med* 8-15-2003;35:327-340.
- [151] Xu Z, Xu X, Zhong M, Hotchkiss IP, Lewandowski RP, Wagner JG, Bramble LA, Yang Y, Wang A, Harkema JR, Lippmann M, Rajagopalan S, Chen LC, Sun Q: Ambient particulate air pollution induces oxidative stress and alterations of mitochondria and gene expression in brown and white adipose tissues. *Part Fibre Toxicol* 2011;8:20.
- [152] Ichikawa T, Li J, Meyer CJ, Janicki JS, Hannink M, Cui T: Dihydro-CDDO-trifluoroethyl amide (dh404), a novel Nrf2 activator, suppresses oxidative stress in cardiomyocytes. *PLoS One* 2009;4:e8391.
- [153] Ikeda T, Sporn M, Honda T, Gribble GW, Kufe D: The novel triterpenoid CDDO and its derivatives induce apoptosis by disruption of intracellular redox balance. *Cancer Res* 9-1-2003;63:5551-5558.
- [154] Nichols DP, Ziady AG, Shank SL, Eastman JF, Davis PB: The triterpenoid CDDO limits inflammation in preclinical models of cystic fibrosis lung disease. *Am J Physiol Lung Cell Mol Physiol* 2009;297:L828-L836.
- [155] Place AE, Suh N, Williams CR, Risingsong R, Honda T, Honda Y, Gribble GW, Leesnitzer LM, Stimmel JB, Willson TM, Rosen E, Sporn MB: The novel synthetic triterpenoid, CDDO-imidazolide, inhibits inflammatory response and tumor growth in vivo. *Clin Cancer Res* 2003;9:2798-2806.
- [156] Thimmulappa RK, Scollick C, Traore K, Yates M, Trush MA, Liby KT, Sporn MB, Yamamoto M, Kensler TW, Biswal S: Nrf2-dependent protection from LPS induced



inflammatory response and mortality by CDDO-Imidazolidine. *Biochem Biophys Res Commun* 12-29-2006;351:883-889.

- [157] Honda T, Padegimas EM, David E, Sundararajan C, Liby KT, Williams C, Sporn MB, Visnick M: 2-Cyano-3,10-dioxooleana-1,9(11)-dien-28-oic acid anhydride. A novel and highly potent anti-inflammatory and cytoprotective agent. *Bioorg Med Chem Lett* 4-1-2010;20:2275-2278.

## Vita

Daniel Hochman was born in New York City, January 4, 1971 to Dr. Robert and Laurie Hochman. Daniel has a long academic background obtaining degrees and certifications from several institutes of higher education. Daniel attended: UNIVERSITY OF TEXAS MEDICAL BRANCH, Galveston, TX (2005-2012) PhD Candidate , Experimental Pathology / Environmental Toxicology; UNIVERSITY OF HOUSTON – CLEAR LAKE, Webster, TX (1999-2002) Master's Degree in (Secondary Science Education); UNIVERSITY OF MARYLAND, College Park, MD (1995-2001, Master of Science in Marine Estuarine and Environmental Sciences, concentration in Ecology; GEORGE MASON UNIVERSITY, Fairfax, VA (1994-1995), Post-Baccalaureate (Pre-Medical Bachelor of Science); NORTHERN VIRGINIA COMMUNITY COLLEGE, Arlington, VA (1992-1993), Emergency Medical Technician Certification ; JAMES MADISON UNIVERSITY, Harrisonburg, VA (1988-1992), Bachelor of Business Administration in International Business/Japanese, magna cum laude. Daniel has extensive teaching and laboratory experience.

In the scientific field Daniel has worked in the following positions: TOXICOLOGY CONSULTING, Galveston, TX (2008-Present ) Private Consultant; UNIVERSITY OF TEXAS MEDICAL BRANCH, Galveston, TX • (2002-2008), Research Associate; TEXAS A&M UNIVERSITY, Galveston, TX (1999; Summers 2000-2002) , Research Associate – Seafood Microbiology Lab; GALVESTON COUNTY HEALTH DISTRICT, LaMarque, TX (1998-1999), Environmental Health Specialist II; UNIVERSITY OF MARYLAND, College Park, MD (1996-1998), Graduate Research Assistant II – College of Life Sciences, Department of Biology.

In the field of education Daniel has held several positions at every level including: SAN JACINTO COLLEGE, Houston, TX (2008-2011) , Adjunct Professor of Biology; UNIVERSITY OF TEXAS MEDICAL BRANCH, Galveston, TX (2003-Present), Mentor, Summer Undergraduate Research Program and Bromberg Scholars Bench tutorial mentor; TEXAS A&M UNIVERSITY, Galveston, TX (2006-2008), Instructor; GALVESTON ISD – BALL HIGH SCHOOL, Galveston, TX (1999-2002) Chemistry Teacher; UNIVERSITY OF MARYLAND, College Park, MD (1997-1998), Teaching Assistant II – College of Life Sciences, Department of Biology.

Daniel has several publications in the varying fields of his study. Daniel's publications include: **1)** Hochman, D, Collaco, C., Brooks, E. "Acrolein induction of oxidative stress and degranulation in mast cells" *Environmental Toxicology*, 2012; **2)** Collaco, C., D.H. Hochman, R.M. Goldblum, and E.G. Brooks. "Sodium sulfite activates basophils through induction of oxidative stress," *Annals of Allergy, Asthma and Immunology*, 96:550-556, 2006; **3)** Thaller, E., S. Petronella, D. Hochman, S. Howard, R. Chhikara, E. Brooks. "Moderate increases in ambient PM2.5 and ozone are associated with lung function decreases in healthy athletes." *Journal of Occupational and*

*Environmental Medicine*, 2008 Feb;50(2):202-11; **4)** Endo, S., Hochman, D., Midoro-Horiuti, T., Boldogh, I., Goldblum, RM., and Brooks, E. "Cedar Pollen Induces IgE-independent Mast Cell Degranulation and IL-4 Production through the Generation of Reactive Oxygen Intermediates." *Cellular Immunology*, 2011;271(2):488-95; **5)** Robles, Luisa and Hochman, Daniel J. "Model of a Forested Riparian Buffer Zone with Emphasis on *Asimina triloba*. Journal of Ecological Modeling." Special Issue. Forward by Dr. Robert Costanza; **6)** Hochman, Daniel J., et al. Handbook of Exotic and Invasive Species of the Eastern United States. Gypsy Moths. Wild Ponies of Assateague, Virginia. University of Maryland, College Park, Maryland. Pending Publication. Edited by Dr. Patrick Kangas; **7)** Hochman, Daniel J. "An Ecological Study of Pine Invasion on a Maryland Serpentine Grass Prairie," Master's Thesis, University of Maryland, May 2001; **8)** Hochman, Daniel J. et al. "International Marketing and Management Plan: The Sports Authority in Mexico City," Senior Thesis, James Mason University, September 1988.

Permanent address: 1610 Postoffice St. #2 Galveston, TX 77550

This dissertation was typed by: Daniel Jason Hochman